Fall 2015

Release behavior of alkyl-p-aminobenzoate ester–PVP solid dispersions

Yi Wu
University of Iowa

RELEASE BEHAVIOR OF ALKYL-p-AMINOBENZOATE ESTER–PVP SOLID DISPERSIONS

By

Yi Wu

A thesis submitted in partial fulfillment
of the requirements for the Doctor of
Philosophy degree in Pharmacy
in the Graduate College of
The University of Iowa

December 2015

Thesis Supervisor: Professor Emeritus Douglas R. Flanagan

Graduate College
The University of Iowa
Iowa City, Iowa

CERTIFICATE OF APPROVAL

_____

PH.D. THESIS

_____

This is to certify that the Ph.D. thesis of

Yi Wu

has been approved by the Examining Committee for
the thesis requirement for the Doctor of Philosophy degree
in Pharmacy at the December 2015 graduation.

Thesis Committee:_____
Douglas R. Flanagan, Thesis Supervisor

_____
Aliasger K. Salem

_____
Dale E. Wurster

_____
Maureen D. Donovan

_____
Lewis L. Steven

To my parents, my sister and Derek

ACKNOWLEDGMENTS

Foremost, I would like to express my greatest gratitude toward my advisor, Professor Douglas R. Flanagan for all of his intellectual guidance, patience, unconditional support during my graduate school life.

Secondly, I would like to thank all of the faculties, especially for the committee members in my comprehensive exam and dissertation defense, Dr. Aliasger K. Salem, Dr. Maureen D. Donovan, Dr. Dale E. Wurster and Dr. Lewis L. Stevens for their helpful discussions and challenging perspectives on my research.

Additionally, I want to thank all my lab mates: Frank, Yang and Hui, for their scientific discussions and friendship.

Lastly, I would like to thank my parents and my sister for their continued encouragement, patience, and endless love; Derek for his friendship, support, happiness, encouragement and his help with the multicomponent analysis.

ABSTRACT

Solid polymer-drug dispersions are used to prepare and stabilize amorphous forms of poorly soluble drugs as a means of improving drug solubility, dissolution and bioavailability. Despite many reports on this subject, solid dispersion dissolution mechanisms have not been well understood. An early study was reported by Simonelli, Mehta and Higuchi (SMH) in 1969 and has served as a model for dispersion dissolution behavior. These authors proposed a dissolution model (SMH) which gave good agreement between their experimental results and model predictions for one drug and one type of PVP.

Few researchers have applied this traditional approach (SMH) in a systematic fashion to solid dispersion systems. One difficulty is obtaining parameters needed for predictions such as polymer diffusion coefficient, diffusion layer thickness or other pertinent parameters. In this work, a general model has been developed based on the concepts in the traditional approach (SMH) and simulations with this model were performed to show how dispersion dissolution rates change with system variables. Such simulations showed underestimation of dissolution rates resulted when compounds had low solubility.

In this work, solid dispersion dissolution behavior was studied systematically with a homologous compound series (alkyl-p-aminobenzoate esters, or PABA esters) and three polyvinylpyrrolidone (PVP) molecular weights (K15, K30 and K90). The PABA esters with varying solubility used in this study were methyl PABA (MePABA), ethyl PABA (EtPABA), propyl PABA (PrPABA) and butyl PABA (BuPABA). Six solid dispersions for each PABA ester and PVP (weight ratios of PVP:PABA ester 20:1, 10:1, 6:1, 3:1, 4:1 and 2:1) were prepared by a solvent evaporation method. Solid dispersions were obtained and their amorphous character confirmed by powder X-ray diffraction (PXRD) and differential scanning calorimetry (DSC).

Intrinsic dissolution rates for these dispersions were obtained in water with a rotating disc dissolution system. Both dissolution rate of drug (PABA ester) and carrier (PVP) were measured to obtain more information on which to evaluate the release behavior. Measuring the dissolution of the polymer (dispersion agent) and drug is unique in this work and has not been done in most other reported studies.

For the more soluble PABA esters (i.e., MePABA, EtPABA and PrPABA), as drug loading increased, PABA ester dissolution rates first increased and then decreased to that of the pure drug for PVP K15 and K30 dispersions. For K90 systems, drug dissolution rates were below pure drug rates and increased steadily as drug loading increased, eventually reaching that of the pure drug. On the other hand, PVP dissolution rates decreased constantly as drug content increased for all three PVP grades. However, the decrease in polymer dissolution was more pronounced for the lower molecular weight PVPs (K15 and K30) than the higher molecular weight PVP (K90). Comparison of drug and polymer dissolution behavior indicated that congruent release of both components occurred when drug loading was low (< 15%). As drug loading increased, more deviation from congruent release behavior was observed. For BuPABA, the least soluble PABA ester, precipitated BuPABA solid accumulated on the disc surface during dissolution.

PABA ester relative dissolution rates were calculated and compared with the predictions from the developed general model (based on assumptions in the traditional approach). Such predictions correlated well with experimental results at high drug loadings (i.e., >25%) but at low drug loadings (i.e., <25%) there was inconsistent correlation between experimental and predicted results. A new model was developed in which dispersion systems were generally classified into two regions: a carrier-controlled region and a drug-controlled region. Congruent release was

predominated in the carrier-control region and pure drug release occurred in the drug-controlled region. The results showed the new model offered better agreement with experimental results.

PUBLIC ABSTRACT

Solid drug-polymer dispersions are used to prepare and stabilize amorphous forms of poorly soluble compounds. These dispersions have attracted considerable interest as a means of improving drug solubility, dissolution and bioavailability. Despite many reports on solid dispersions, the drug release mechanism from dispersion systems has not been well understood.

In this study, a systemic approach was employed to better elucidate solid dispersion dissolution mechanism(s). A homologous compound series (alkyl-p-aminobenzoate esters, or PABA esters) was used together with three different molecular weights of polyvinylpyrrolidone (PVP K15, K30 and K90). Intrinsic dissolution studies were performed on the PABA ester-PVP dispersions. Both drug and carrier dissolution were followed simultaneously which is a unique aspect of this study; in most other such studies, only drug dissolution was monitored.

The results showed that the PABA ester-PVP solid dispersion intrinsic dissolution could be generally categorized into two regions: a polymer-controlled region and a drug-controlled region, which depends on drug loading, drug solubility or PVP used in the dispersion. In the polymer-controlled region, drug dissolution was mainly influenced by drug loading as well as polymer dissolution which depended on the PVP grade used. In the drug-controlled region, drug dissolution was largely independent of carrier and was equivalent to that of the pure drug. The model developed in this study described the dissolution behavior of these dispersions fairly well.

TABLE OF CONTENTS

LIST OF TABLES

LIST OF FIGURES

CHAPTER 1 INTRODUCTION

One of the challenges in pharmaceutical research is the poor solubility and slow dissolution rate of active pharmaceutical ingredients (APIs).[1] This problem becomes more common among new drug candidates due to the high throughput screening process in drug discovery.[2,3] Many of these drug candidates belong to the Biopharmaceutical Classification System II (BCS II), which are poorly soluble and highly permeable.[3,4] In general these drugs present low oral bioavailability despite their high intestinal permeability. The reason that this problem occurs is because of their slow and limited dissolution in gastrointestinal (GI) fluids. Thus, an important aspect in pharmaceutical research is to improve the dissolution and potentially the bioavailability of such drugs.

Many strategies have been applied to increase drug solubility/dissolution rate. These approaches include salt formation,[5] prodrug formation,[6] solubilization/complextion,[7] polymorph modification,[8] particle size reduction[9] and solid dispersions.[3,10-14] Among them, solid dispersion is considered as one of the most versatile methods to increase drug solubility/dissolution rate.[15]

1.1 Solid dispersions

The concept of solid dispersions was first introduced by Sekiguchi and Obi in 1961.[16] In their pioneering study, a eutectic mixture of sulfathiazole and urea was formed by melting followed by rapid solidification. The authors showed that this eutectic mixture possessed higher absorption than sulfathiazole alone after oral administration. Later, the term solid dispersion was given to this type of system which include other methods combining drug with soluble carriers. To date, numerous publications have been published on this subject.[3,10-14,17] The classical definition of solid dispersion has evolved from “the dispersion of one or more active ingredients in an inert carrier matrix in the

solid-state by melting (fusion), solvent or melting-solvent methods" to "the product formed by converting a fluid drug-carrier combination to the solid state".[10,12]

1.2 Method preparation solid dispersions

There are three major ways to prepare solid dispersions which includes melt, solvent evaporation and melt-solvent method.[12] For the melt method, drug and carrier are first melted together and then fast cooled. The obtained solid is crushed, pulverized and sieved. An important requirement to use the melt method is API miscibility with the carrier in the molten state. Thus, in general, a suitable carrier shares similar physicochemical properties with drugs. The main advantage of this direct melt method is that it does not require any solvent. However, this method is not suitable for thermally labile compounds. Another disadvantage of this method is that it can only be used if the drug and carrier are compatible and miscible when they are melted. Incompatibility can cause phase separation. High viscosity of a melted polymeric carrier in the molten stage can cause mixing difficulties. Both can lead to an inhomogeneous solid dispersion, which severely impact its ability to increase bioavailability. Inhomogeneous solid dispersions may have poor physical stability, as well.

For the solvent method, drug and carrier are first dissolved in a common solvent and then solvent is evaporated and the two components are co-precipitated. The solvent evaporation method avoids thermal decomposition of drugs because of the relative low temperature used in organic solvent removal. Some polymers that cannot be used in a melt method due to their high melting temperature can be used in the solvent method. However, both drug and carrier need to be dissolved in a common solvent. Sometimes it is difficult to find a common solvent to dissolve hydrophobic drugs and hydrophilic carriers. Also, sufficient solubility in the solvent is needed for this method to operate.

One of the problems associated with this preparation method is that complete solvent removal is difficult. Residual solvent in solid dispersions can cause toxicity issues. Another disadvantage is that the residual solvent can act as a plasticizer, which could lead to phase separation due to increased mobility of the components.

The melt-solvent method is a combination of the melt method and the solvent method. In this type of preparation, drugs are first dissolved in a solvent and then mixed with the molten carrier. Sold dispersions are obtained after solvent removal and solidification. The advantage of this method is that the temperature is lower than the melt method. Also, the mixing time is often reduced too. Both these differences can reduce thermal degradation. Moreover, the carrier in the molten state is easier to dissolve and disperse in the solvent in comparison than just the solvent method.

A summary of all the techniques used for solid dispersion preparations is shown in Figure 1-1. The optimized method for preparation is determined by the physicochemical properties of drug and carrier. In general, hot melt extrusion and spray drying are widely used due to their high scalability and general applicability.

1.3 Carriers used for solid dispersion

Early solid dispersions were prepared with crystalline carriers. Urea[16] and sugars[18] such as sorbitol and mannitol are examples of such crystalline carriers. Sekiguchi and Obi prepared the first solid dispersion for pharmaceutical application.[16] In their pioneer work, they used urea as a carrier to form solid dispersion with sulfathiazole. These crystalline carriers usually have high melting points which make them unsuitable for the melt method. Urea has high solubility in water and many organic solvents which makes it a good carrier candidate for preparing solid dispersions

by the solvent method. On the other hand, sugars have poor solubility in most organic solvents. Therefore, sugars are less commonly used in solid dispersion preparations.

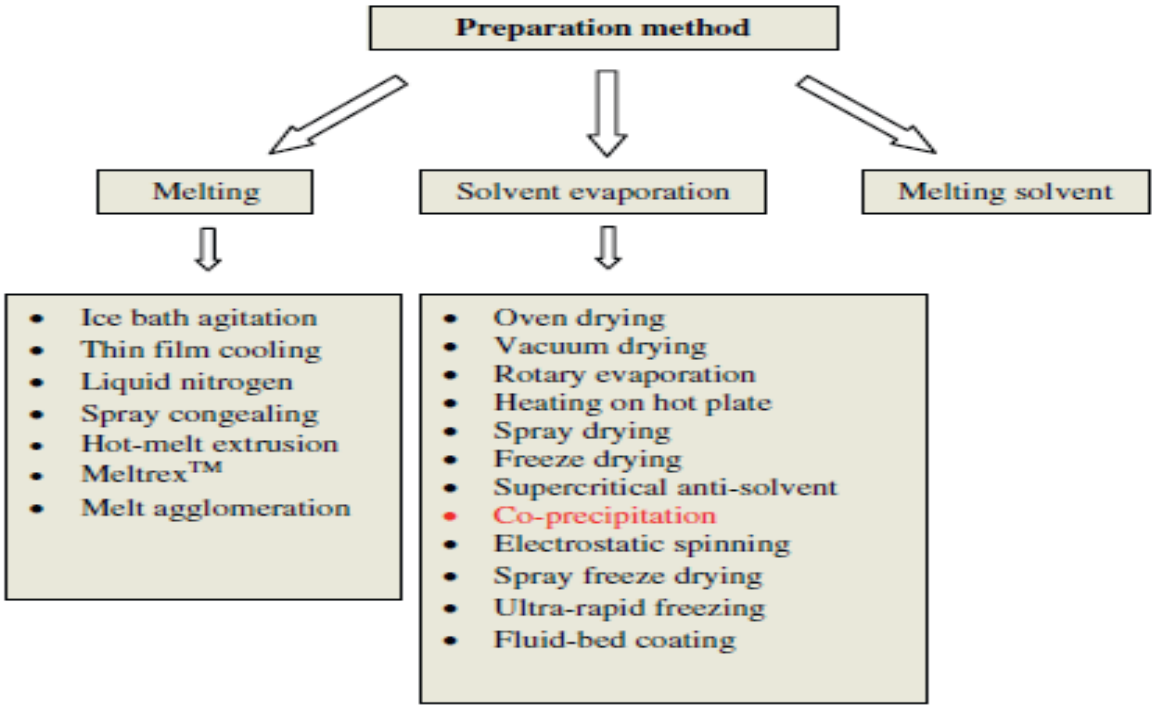

Figure 1-1: Techniques used for solid dispersion preparation.[3]

Later, solid dispersions were prepared with amorphous carriers which are mostly polymers. Those polymers can be totally synthetic polymers or modified natural polymers. Among them, polyethylene glycol (PEG)[19], polyvinylpyrrolidone (PVP)[20] and hydroxylpropylmethyl-cellulose (HPMC)[21] are the most commonly used polymers. PEG has a very low melting point (< 65 ºC) regardless of molecular weight. This feature makes it very suitable for preparing solid dispersions by the melt method. On the other hand, PVP has a high glass transition temperature (> 150 ºC)

which makes it rarely used in the melt method. However, PVP has high solubility in many organic solvents which makes it a good carrier choice for the solvent method. Like PVP, HPMC also has good solubility in many organic solvents and has been widely used in the solvent method.

Although solid dispersions can enhance drug dissolution rate, the subsequent drug supersaturation may cause precipitation which potentially decreases drug bioavailability. Therefore, surface active agents have been introduced as carriers or additives and to produce significant improvement in overcoming the precipitations and recrystallization problems. Surfactants with amphiphilic structure can enhance the miscibility of drug and carrier and reduce drug recrystallization. They also can prevent drug precipitation by adsorbing to the surface of drug particles or forming micelles to encapsulate drug.[3] Thus, the introduction of surfactants or emulsifiers in solid dispersions improves not only the dissolution profile but also the physical and chemical stability of solid dispersions. Some examples of the surfactants include sodium lauryl sulfate (SLS)[22], Tween 80[23], d-alpha tocopheryl polyethylene glycol 1000 succinate (TPGS 1000) etc.[22]

More recently controlled release solid dispersions have been reported.[24] In these formulations, the dispersed drug exhibits improved solubility while the water-insoluble polymer or swellable polymer retards drug release. The polymers used in controlled release dispersions have included ethyl cellulose (EC)[25], hydroxylpropylcellulose (HPC)[26], Eudragit RS/RL[27,28] and carboxyvinylpolymer (Carbopol).[29]

1.4 Solid dispersion structures

Solid dispersions are complex systems and structurally there are many varieties. Depending on how many phases are present in solid dispersions, solid dispersions can be divided into one-phase

or two-phase systems. If the drug molecules are homogeneously dispersed as separate molecules in the carrier, these are categorized as one-phase systems. On the other hand, if the drug is dispersed in the carrier as amorphous or crystalline solids, they are two-phase systems.

One phase systems can either be crystalline solid solutions or amorphous solutions (glassy solutions) depending on whether the carrier is crystalline material or amorphous polymer. For crystalline solid solutions, when the size of the drug molecules are comparable to the size of carrier molecules they can replace the carrier molecules in the crystalline lattice. This type of solid solution is called a substitutional crystalline solid solution (Figure 1-2). If the drug molecules are small compared to the carrier molecules, they can fit into the interstitial spaces between the carrier molecules. This type of solid solutions is called an interstitial crystalline solid solution (Figure 1-3). On the other hand, when the carrier is an amorphous polymer, they are called amorphous solid solutions (Figure 1-4). To obtain a one-phase system, drug loading in solid dispersions needs to be below its solubility in the carrier. One-phase systems represent thermodynamically stable systems. Recently studies have reported values for the true equilibrium solubility of selected crystalline APIs in polymers.[30,31] These values are quite low at temperatures near or below the glass transition temperature (T_g). In general, it is believed that drug loading less than 2% w/w is needed to achieve a one-phase system.[32]

Due to the low solubility of APIs in carriers, the majority of the solid dispersions are two-phase systems. For a two-phase system, drug can exist as molecular aggregates, amorphous solids or crystalline solids. Just like one-phase systems, carriers can be either crystalline materials or amorphous polymers. In two-phase systems, drug loadings have exceeded their solubilities in the carrier and drugs are in supersaturated states. Thermodynamically, two-phase systems are not stable systems. Over time, phase separation can occur due to the molecular mobility of the API.

One example of the two–phase systems is a eutectic mixture.[16] A simple eutectic mixture consists of two compounds which are completely miscible in the liquid state but only miscible to a very limited extent in the solid state. At the eutectic composition, the two components co-crystallize at the eutectic temperature. At any other compositions, one of the two components will start crystallizing before the eutectic temperature is reached. Eutectic systems are two-phase systems with both drug and carriers as crystalline materials. In a eutectic system, both drug and carrier are in a well dispersed state and as fine particles. The enhanced release characteristics of eutectic systems are mainly due to the dispersion of the drug as fine particles.

1.5 Methods to characterize solid dispersions

There are many methods to characterize solid dispersions.[3] Among these, the most important methods are thermoanalytical techniques such as differential scanning calorimetry (DSC) and modulated differential scanning calorimetry (MDSC), powder X-ray diffraction (PXRD) and Fourier transformed infrared spectroscopy (FTIR) and dissolution behavior.

Differential scanning calorimetry (DSC) is a thermal analysis technique that measures heat flow associated with physical transitions as a function of temperature. In a typical DSC measurement, the test sample and the reference are heated such that the temperature of the two is maintained identical. If an energy associated with phase transition (i.e. endothermic and exothermic) occurs in the test sample, the heat difference applied between the test sample and reference is recorded and used to quantify the energy of the phase transition.

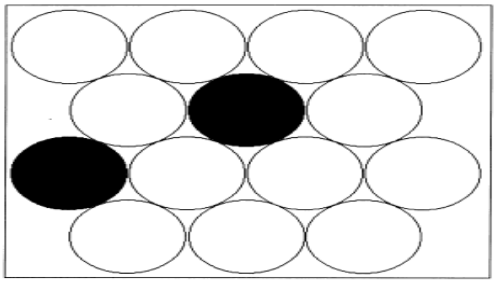

Figure 1-2: Substitutional crystalline solid solution.[17]

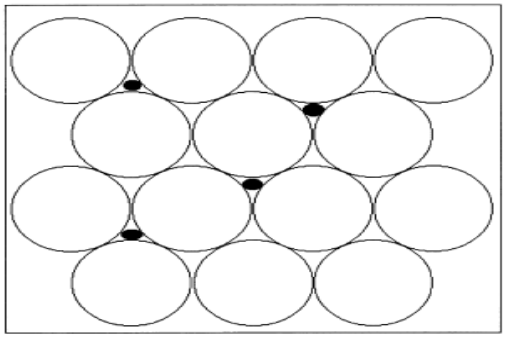

Figure 1-3: Interstitial crystalline solid solution.[17]

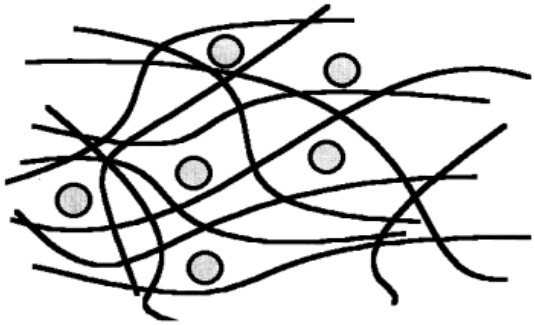

Figure 1-4: Amorphous solid solution.[17]

DSC measurements provide both qualitative and quantitative information about physical and chemical changes in the heating or cooling process. Information can be extracted from DSC data include melting point, glass transition temperature as well as heats of transition associated with the phase transitions (crystallization and fusion process).[33] The lack of a drug melting peak in a solid dispersion thermogram indicates that the drug probably exists as an amorphous form. The degree of crystallinity can also be calculated for systems in which drug is partly amorphous and partly crystalline.[34]

MDSC is an advanced thermal technique that can deconvolute different thermal events in DSC thermograms.[34] In MDSC, a sinusoidal wave modulation is superimposed on the conventional linear temperature heating or cooling programs. By doing that, total heat flow can be separated into reversing and non-reversing thermal transitions. Thermal events such as enthalpic relaxation, evaporation, crystallization and thermal decomposition are considered as non-reversing thermal transitions. Reversing thermal events include melting and glass transitions. The application of MDSC to solid dispersion characterization can offer better sensitivity and resolution of events compared to the traditional DSC. It can also help analyze complex overlapping transitions and detect weak glass transitions.[34]

PXRD is a widely used method to identify and characterize the crystallinity of drugs in solid dispersions.[35] X-ray diffraction is based on constructive interference of monochromatic X-rays and a crystalline sample. The interaction of the incident rays with the sample produces constructive interference and diffracted rays when conditions satisfy Bragg's Law. These diffracted X-rays are then detected, processed and counted. By scanning the sample through a range of 2θangles, all possible diffraction directions of the lattice should be attained due to the random orientation of the powdered material. This method can detect material with long-range order and offer sharp peaks

indicating crystallinity. Crystallinity in the sample is reflected by a characteristic fingerprint region in the X-ray diffraction pattern. The specificity of the fingerprint region can be used to identify and differentiate the amorphous and crystalline state of drugs in solid dispersions. Disappearance of peaks in an X-ray diffraction graph usually indicates the amorphous state of the drug in solid dispersions. However, crystallinity under 5-10% cannot be detected by PXRD.[34] With moisture and temperature programming, PXRD can also be used to study phase transitions kinetics.

Structural changes and lack of a crystallinity can lead to changes in bonding between functional groups in drugs which can be detected by Fourier transformed infrared spectroscopy (FTIR).[3] FTIR can also be used to investigate the intermolecular interactions between drug and carrier. For example, hydrogen bonding, which is an important interaction between drug and carrier in solid dispersions, can be identified by FTIR. Taylor et al. studied solid dispersions of indomethacin and polyvinylpyrrolidone (PVP) with FTIR.[36] Their results showed that indomethacin interacts with PVP in solid dispersions through hydrogen bonding between drug hydroxyl groups and polymer carbonyl groups. This interaction influences crystallization kinetics by preventing the self-association of indomethacin molecules.

When the goal of preparing solid dispersions is to improve dissolution rate, it is important to assess the success of this approach.[32] Dissolution testing will show whether drug dissolution has been enhanced by a solid dispersion. Comparison of the dispersion dissolution results with those of pure drug and physical mixtures of drug and carrier can help indicate the mechanism by which the dissolution is improved. However, in *vitro* dissolution testing can be significantly affected by many factors such as: dissolution test methods, content and amount of dissolution media, sink or non-sink conditions, agitation rates, media pH, dispersion particle size, etc.[32]

1.6 Solid dispersion dissolution

The most important advantage of a solid dispersion is its ability in improving dissolution rates for poorly water soluble drugs, which can potentially increase drug bioavailability. Considerable dissolution rate increases have been reported for many solid dispersions.[32] In many cases, improved bioavailability has been observed as well.[32] It is, therefore, surprising that drug release mechanisms from solid dispersions are not well understood.[37,38] Possible mechanisms include particle increased surface area, reduced agglomeration, increased wetting, amorphous or polymorph crystal forms and complexations.[37]

Both size reduction and reduced particle agglomeration can be considered as means to increase surface area. Size reduction has been classically considered the result of eutectic or solid solution formation. It has also been suggested that the release of separate particles into the dissolution medium reduces aggregation and therefore increases effective dissolution surface area. In both cases, the exposed surface of drug is increased, which leads to a dissolution rate increase. Many carriers used in solid dispersions have the ability to improve wetting. Wetting can lead to particle agglomeration reduction. As a consequence of wetting, drug surface area is increased and dissolution rate is improved.[37] Carriers used in solid dispersions have also been shown to increase drug solubility. Solubility increase leads to dissolution improvement. Similarly, carrier and drug may form a soluble complex, which increases solubility and dissolution. Complex formation has been evidenced for cyclodextrins.[3,37] Finally, change of drug physical state (polymorph or decreased crystallinity or amorphous) may also improve drug solubility and contribute to increase in drug dissolution.[37]

One approach for studying solid dispersion dissolution mechanisms is to analyze release data with dissolution kinetic models. In this approach, constant surface area dissolution (i.e. intrinsic

dissolution) process is considered into more details. Intrinsic dissolution is considered to be a valuable tool to investigate in solid dispersion studies because it belies particle size effects, maintains a constant surface area and constant hydrodynamics at the dissolving surface. Kinetically modelling on intrinsic dissolution has not been widely incorporated into the study of solid dispersions despite its mechanistic interpretation possibilities. The only modelling attempt to study solid dispersion intrinsic dissolution to date was conducted by Simonelli et al.[20] In this study, the authors investigated both intrinsic dissolution rates of sulfathiazole and PVP from solid dispersions. The intrinsic dissolution test was carried out with a Simonelli dissolution apparatus.[20] They proposed that the dissolution of sulfathiazole and PVP from solid dispersions could be explained by a physical model. In this dissertation, this model is referred as the traditional approach (or SMH for Simonelli, Mehta and Higuchi).

Schematically the proposed SMH model is shown in Figure 1-5. In this model, it is proposed that a number of phases are present in the solid dispersion. These possibilities include unbound and bound PVP, unbound and bound sulfathiazole in any of its known forms. Initially, a tablet has all phases homogeneously dispersed throughout. As dissolution proceeds, the tablets can develop segregation of these phases at or near the surface region of the tablet due to preferential dissolution rate of one phase over the others. Furthermore, this segregation can produce layers of one or more phases. When this happens, the outermost layer (layer containing component whose boundary moves slowest) will have the greatest influence on the dissolution process. This is particularly true if the next layer has sufficiently receded from the tablet surface to prevent it from having any significant contributions to the overall dissolution rate.

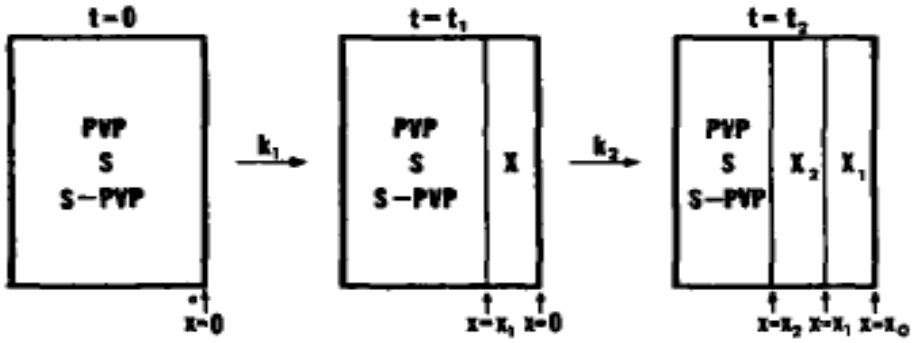

Figure 1-5: SMH model that describes the release of PVP, sulfathiazole and their complex as a function of time.[20] Initial condition is shown in t = 0. A primary layer, X_1, is formed at $t = t_1$. A second layer, X_2, is formed at $t = t_2$.

As it shows in Figure 1-5, changes can occur at the tablet surface as dissolution proceeds. Initially at time zero, the tablet contains unbound PVP, unbound sulfathiazole and the PVP-sulfathiazole complex. As time progresses to a finite time, t_1, a layer develops which has a different composition than the original tablet composition. However, the inner region maintains its original composition unchanged. The formation of this layer can be the result of one or more components of the original composition being preferentially released due to a more favorable combination of factors, such as solubility, diffusion coefficients, degree of dissociation, etc. Another possibility for this layer is the result of new formation at the tablet surface. The thickness of this layer will continue to grow. Consequently, the release rates of other components will decrease. In the end, the thickness of the new phase layer is large enough to sufficiently slow the release of other components to that of congruent release (i.e. each component release according to its tablet composition). At this point, steady-state is reached and the layer thickness remains constant. As time further progresses, the possibility of a second a layer appears. This is illustrated by the system

at time, t_2. The new layer formation can be explained by the same mechanism of the first layer. Regardless of number of phases present, only the outer layer controls the release rate of all components at the steady-state (i.e. congruent release rates will be observed with the outer layer setting the absolute rate).

In the SMH study, the authors not only measured the release rate of sulfathiazole and but also the release of PVP. They calculated expected drug release with the SMH model. A good correlation between theoretical predictions and experimental results were achieved as shown in Figure 1-6. In the SMH model, it was proposed that the system was in carrier control at higher PVP contents. Sulfathiazole dissolved rapidly as PVP dissolved in this region. Both PVP and sulfathiazole were released simultaneously. At lower PVP contents, sulfathiazole (various forms) formed an external controlling layer. This theoretical analysis also highlighted that potentially considerable enhancement in dissolution rate can be obtained at a critical mixture ratio when the formation of "high energy" drug (i.e. amorphous) is coupled with complexation.

Chiou and Riegelman analyzed the original data in the SMH model and showed that the relative boundary movement for both PVP and sulfathiazole were close to unity in 20:1, 10: 1 and 5:1 PVP- sulfathiazole systems. The authors interpreted this finding as molecular and/or colloidal dispersion of drug in the polymer.[10]

After the SMH study, a few researchers attempted to measure both the intrinsic dissolution rates of drug and carrier simultaneously.[19,39-41] Corrigan et al. was one of them.[19] In one of his studies, the authors measured the intrinsic dissolution rates of both bendrofluazide or hydroflumethiazide and PEG 4000 in solid dispersions using a modified beaker method.[19] They found that the dissolution of drug and polymer occurred congruently at both 20:1 and 10:1 weight ratios (PEG: drug), leading to the conclusion that the dissolution of drug was controlled by the

PEG carrier. These authors also found that drug release was the highest from 10:1 solid dispersions. The dissolution rate was increased 180-fold higher than the pure drug in the case of hydroflumethiazide while it was increased 13-fold for bendrofluazide. Despite the large differences in the relative dissolution rate enhancements, the absolute dissolution rate are of the same order of magnitude. These authors interpreted this as PEG dissolution was in control.

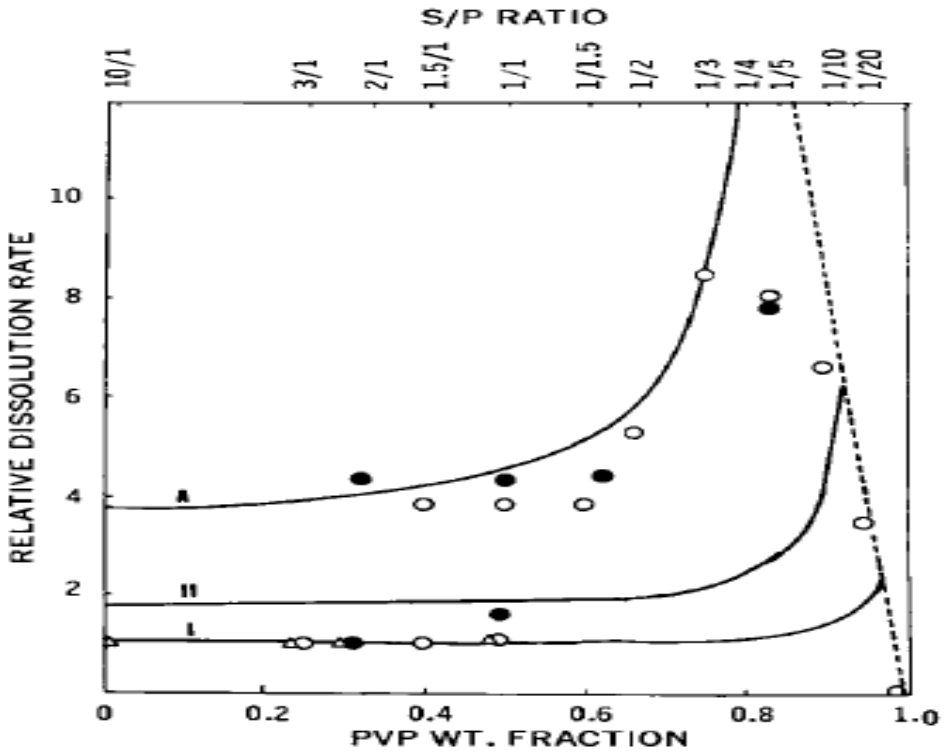

Figure 1-6: Comparison of the theoretical and experimental relative release rate of sulfathiazole to sulfathiazole form I as a function of PVP weight fraction in tablet. Experimental points: open circle, 95% alcohol coprecipitated mixtures; dot, aqueous coprecipitated mixtures; triangle, mechanic mixtures. Theoretical curves for controlling layers: I, sulfathiazole form I. II, sulfathiazole form II. A, amorphous sulfathiazole.[20]

In another intrinsic dissolution study conducted by Corrigan et al., the authors examined PEG 4000 and barbituric acid or phenobarbital dispersions.[39] For 20:1 and 10: 1 PEG:barbituric acid and 50:1 and 30:1 PEG:phenobarbital systems, comparison of the relative movement of the solid-liquid boundary of each component indicated that both components were released simultaneously from the intrinsic dissolution tablet surface. The authors concluded that these solid dispersions were carrier-controlled systems. As PEG dissolved, the drugs dissolved at the same rate after correction of the weight ratio. Thus, drug release was controlled by the dissolution rate of polymer and drug: polymer ratio in the dispersions.

Zhou et al. prepared cyclosporine A and TPGS (d-alpha tocopheryl polyethylene glycol 1000 succinate) dispersions and conducted constant surface area dissolution tests.[41] They found that both components displayed linear dissolution profiles. Moreover, the two normalized dissolution profiles matched closely, demonstrating that drug and carrier dissolved concurrently from these solid dispersions. These findings were consistent for dispersions with up to 15% cyclosporine A (i.e., 85:15 carrier: drug ratio). At higher drug contents, drug precipitated during dissolution and the dissolution rate fell to that of the pure drug.

The above results were supported by the work of Dubois et al.[42] In this study, the intrinsic dissolution rate of ten different drugs in PEG 6000 were examined using a rotating disc method. The authors did not analyze the PEG release. Instead, only drug release was monitored. However, the results were close to the findings described earlier in which drug release rates were linearly related to drug content (% drug) in the dispersions. However the range over which this linearity displayed varied significantly, e.g. 0-2% for phenylbutazone and 0-15% for paracetamol. The linear release ranges were not related to drug solubility. The authors also discovered that

statistically the linear dissolution slopes were the same for nine of the ten drugs studied. The only exception was griseofulvin, which did not form a solid dispersion with PEG 6000.

Craig et al. used a homologous series of drugs (methyl, ethyl, and propyl and butyl *p*-aminobenzoate or PABA esters) and studied their release from PEG 6000 solid dispersions using a constant surface area dissolution.[43] For solid dispersions containing the PABA esters, dissolution was most rapid from the systems containing 10% w/w drug, while higher drug content (20% w/w and 50% w/w) and pure drug gave similar initial dissolution rates (Figure 1-7). The authors speculated that at relatively low drug concentrations (< 10% w/w), the drug was released into the medium as individual particles, hence providing a large surface area for dissolution. At higher concentrations, the results were consistent with the concept that the drug forms a continuous layer across the dissolving surface, thus producing a dissolution rate controlling barrier. The authors argued that PABA ester dissolution rate would be independent of which PABA ester was used in the dispersions if the system was carrier-controlled and drug loading was the same. In other words, the drug dissolution rate should be identical for all the PABA esters if the dispersions were carrier-controlled. This was contradictory to the results. The authors proposed that in addition to the carrier-controlled dissolution mechanisms and precipitation suggested by the SMH, there was a third mechanism which involved the release of intact particles, from which dissolution occurred over the large surface area produced.

The intrinsic dissolution characteristics of nortriptyline HCl dispersions in a range of different molecular weight PEG carriers has also been investigated by Craig et al.[44] This study indicated that the rate of drug dissolution from the solid dispersions was affected by the PEG release rate. A decrease in dissolution rate was seen with increasing PEG molecular weight for the 10% drug loading dispersions. A linear relationship was found between drug dissolution rates and

concentration in PEG 20,000 up to 25% w/w drug. These findings supported the idea that the controlling step to drug release was the recession of the PEG solid-liquid interface and drug/carrier ratio. The authors also showed that nortriptyline HCl (10% w/w in PEG 20,000 solid dispersions) dissolution rate increased with rotation speed. However the results obtained were not consistent with the rotating disc relationship proposed by Levich (i.e. a non-linear relationship was obtained between the drug dissolution rate from solid dispersions and the square root of the rotation speed).[45]

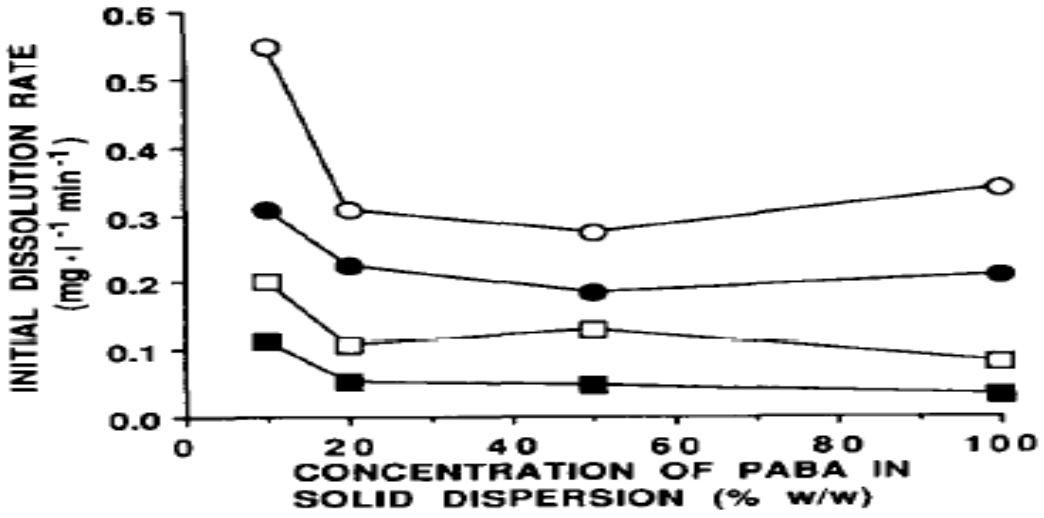

Figure 1-7: Relationship between intrinsic dissolution rate and PABA ester content in PEG 6000 solid dispersions. (open circle: methyl PABA. filled circle: ethyl PABA; open square: propyl PABA; filled square: butyl PABA).[43]

Solid dispersions of CI-987 (5-{[3,5-bis(l,l-dimethylethyl)-4-hydroxyphcnyl]-methylene)-2,4-thiazolidinedione) with varying concentrations of polyvinylpyrrolidone (PVP K30) were prepared and intrinsic dissolution studies were performed in an attempt to understand the dissolution mechanism.[46] The dissolution rate profile (Figure 1-8) showed three distinct phases: (1) At low PVP weight fractions (< ~0.2), the dissolution rate was controlled by and approximates pure crystalline CI-987. This occurs because as PVP was released and its boundary receded into the tablet, the surface of the disc became drug-enriched; (2) At intermediate PVP weight fractions (~0.2-0.81), the dissolution rate of CI-987 increased as the fraction of PVP increased. This trend was consistent with a change in the physical state of CI-987. X-ray diffraction data revealed that the degree of crystallinity of CI-987 within the dispersion decreased as the fraction of PVP increased in this weight fraction region. This was further supported by the finding that the maximum dissolution rate occurred with the dispersion where CI-987 appeared to exist in a totally amorphous state (i.e., a PVP weight fraction of 0.81). At this PVP weight fraction, the maximum dissolution of drug occurred and both the drug and PVP boundaries receded at similar rates; (3) At high PVP weight fractions (> 0.81) the dissolution rate decreased as the PVP fraction increased. This trend was consistent with a change in the rate-controlling component. In this region, the PVP boundary receded slower than the drug boundary and the dissolution rate was controlled by PVP and the polymer: drug weight ratio.

The intrinsic dissolution rates and profiles of a furosemide-polyvinylpyrrolidone (PVP) mix and solid dispersion systems (l0-100% w/w furosemide) were examined by York and co-authors.[47] Solid dispersion systems exhibited higher dissolution rates than corresponding physical mixtures with PVP and untreated furosemide (Figure 1-9). The peak intrinsic dissolution rate, found for both mixture and dispersion systems containing 40% w/w furosemide, was attributed to a balance

of two opposing factors. In physical mixtures, a dissolution-promoting effect of soluble complex formation with PVP was counterbalanced by a viscosity-related retardation effect with increasing PVP content in the diffusion layer. In solid dispersions, a large dissolution-promoting effect of the amorphous drug state produced a highly supersaturated diffusion layer demonstrated in time/solubility profiles which was also counterbalanced by the increasing PVP content in the diffusion layer. The authors also presented scanning electron photomicrographs (SEMs) to show the dissolution surfaces of compressed discs before and after dissolution. They found that when the drug level was 40% w/w or less a PVP layer covered the dissolving face and when drug level was 40% w/w or more a drug layer covered the dissolving face. The author argued that the change from a crystalline drug-controlled dissolution mechanism to a polymer controlled system occurred at 40% w/w furosemide.

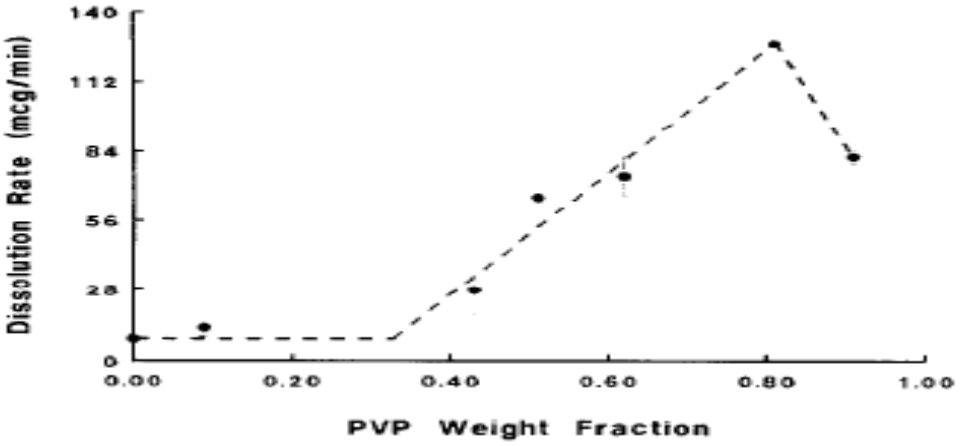

Figure 1-8: The effect of varying weight fraction of PVP on the dissolution rate of CI-987 from solid dispersions at 37 ºC and in 10% w/v polysorbate 80 in water.[46]

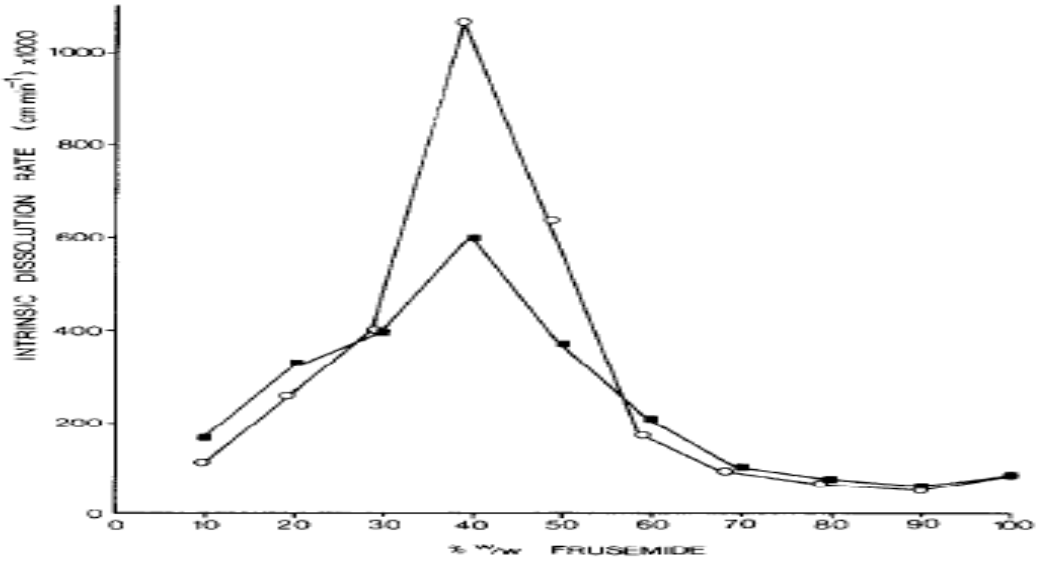

Figure 1-9: Intrinsic dissolution rates of furosemide-PVP mixture in pH 4.95 acetate buffer. Open circle: solid dispersions; solid squares: physical mixture (note: furosemide is also known as frusemide).[47]

In a study by Collett and Kesteven, intrinsic dissolution rates of allopurinol-PVP solid dispersions were examined.[48] At drug loading was > 40% w/w, drug release from the dispersions was close to that of the pure drug. At drug loading was < 60% w/w, an increase in drug dissolution was observed. The highest drug dissolution rate was achieved for solid dispersions containing 90% PVP and 10% allopurinol (9:1 weight ratios).

An interesting study was conducted by Dave at Long Island University.[49] They prepared solid dispersions of sulfathiazole and various molecular weight PVPs and conducted intrinsic dissolution (Simonelli apparatus) studies. It was unique that they used various molecular weights of the same carrier. Most previous studies focused on just one carrier and one or several drugs. Their work showed that with increasing sulfathiazole content in the dispersions, the drug intrinsic dissolution rate was first increased and then decreased, eventually down to reach that of the pure

drug. However, the maximum release rate occurred at different drug/carrier ratios for different PVP molecular weight. For example, the highest release rate occurred at a 1:5 ratio (sulfathiazole:PVP) for PVPs of molecular weight 10,000 and 40,000. On the other hand, for higher molecular weight PVPs (90,000 and 130,000) the highest release rate was obtained at a 1:1 ratio (sulfathiazole:PVP). These authors also correlated the intrinsic dissolution rate of sulfathiazole to its chemical potential in the solid dispersions. All solid dispersions prepared were assumed to form solid solutions. With this assumption, the authors used the Flory-Huggins equation to calculate the chemical potential of the dispersion systems. Reasonable correlations between the calculated chemical potential and intrinsic dissolution rate were achieved. However, large deviations occurred for solid dispersions prepared with high PVP content. This seems to be contradictory to the solid solution assumption. In solid dispersions with high PVP content, lower drug/carrier ratios exist and the formation of a solid solution should be more likely. This region should be the region with little or no deviations from their chemical potential model. The author also extended this study to ibuprofen and indomethacin dispersions with various molecular weight PVPS with limited success due to possible precipitation.[49]

This correlation between chemical potential and intrinsic dissolution rate was extended to ternary systems consisting of one drug and a carrier consisting of one or two polymers, or a polymer plus a surfactant.[50] The carriers were either PVP alone or PVP in combination with other hydrophilic polymers (copovidone, poloxamer) and the surfactant Tween® 20. The drugs used were ethinyl estradiol and levonorgestrel. Again, solid solution was assumed in order to calculate chemical potential and relate it to intrinsic dissolution rate. Limited success in this correlation was achieved.

Recently, Ji et al. proposed a novel approach to elucidate solid dispersion dissolution mechanism.[51] In this study, the authors considered solid dispersion dissolution as two steps: a surface reaction process which involves dissolution of API or polymer from solid phase into solid-liquid interface and diffusion process which involves transportation of both components from solid-liquid phase to solution bulk phase. This is different than previous studies where diffusion is considered the rate-limiting process (i.e. surface reaction is considered instantaneously established). A chemical-potential-gradient model combined with the thermodynamic model PC-SAFT (Perturbed Chain Statistical Associating Fluid Theory, a thermodynamic model to predict solubility of amorphous API under various conditions) was developed to investigate the dissolution mechanism of indomethacin and naproxen from their solid dispersions at different conditions and to predict the dissolution profiles of these APIs. The dissolution profiles of APIs and carrier (PVP K25) from solid dispersions were measured using a rotating-disk system. Their results showed that API and PVP K25 co-dissolved according to the API loading. Moreover, the dissolution rate of indomethacin and naproxen was increased as the API loading increased while the dissolution of PVP was decreased as API loading increased. Lastly, the dissolution of indomethacin and naproxen was mainly controlled by the surface reaction.

CHAPTER 2 STATEMENT OF THE PROBLEM AND OBJECTIVES

Solid dispersions have been widely investigated as an approach to enhance the solubility, dissolution and bioavailability of poorly soluble drugs. This approach has been utilized for many poorly soluble drugs with success. However the drug release mechanism from solid dispersions is not well understood despite the great success of this formulation technique. Such understanding is critical because the prediction of dissolution behavior is one of the key factors in designing a successful dosage form. One reason for the lack of a more basic understanding of solid dispersion dissolution behavior is the lack of basic studies directed to understanding the operative release mechanism(s).

A seminal study was conducted by Simonelli, Mehta and Higuchi in 1969. In this pioneering study, the authors studied the solid dispersion intrinsic dissolution kinetics in more depth. One of the unique aspects in this study was that the authors not only measured drug release but also measured carrier release. By combining the two release results, the authors proposed a physical model (SMH) to explain the intrinsic dissolution kinetics with good predictability. However, few researchers have attempted to further investigate this traditional dissolution model or develop alternate models. For the few studies where both the drug and carrier release were monitored, the results correlated well with the traditional dissolution model predictions. However, such studies had been limited to low drug loading dispersions (i.e. drug loading < 10% w/w). Where only the drug intrinsic dissolution was followed, the release profiles qualitatively matched the traditional dissolution model predictions: in general, as drug content in solid dispersion increased, the drug intrinsic dissolution rate first increased then decreased and eventually fell to that of the pure drug. The shape of the drug dissolution rate vs dispersion content plots seemed to be related to both the

properties of the drug and the carrier, which was in agreement with the traditional dissolution model.

Though, the traditional dissolution model offered a great potential for dissolution predictability with solid dispersions, limited efforts have been expanded in understanding the mathematical or the physical principles underlying the traditional dissolution model. No one has developed a generalized formula for the traditional dissolution model to demonstrate how physicochemical parameters affect predicted dissolution behavior. No one has attempted to extend the SMH work to various drugs and carriers. Thus, the main focus of this research involves:

- Developing a model based on the concepts in the traditional approach to predict drug intrinsic dissolution by varying different physicochemical parameters;
- Systematically studying drug and carrier intrinsic dissolution rate by varying drug and/or carrier properties and solid dispersion compositions;
- Correlating model predictions and experimental results to modify the traditional dissolution model if needed.

The specific aims of this dissertation are:

- To understand the physical principles underlying the traditional dissolution approach concept and develop a mathematical model to predict drug intrinsic dissolution by varying different physicochemical parameters.
- To study a homologous series of drugs and a carrier with varying molecular weights to investigate release properties in a systematic fashion.
- To develop analytical procedure to measure both drug and carrier release in dissolution studies.

- To formulate solid dispersions with selected carriers and model drugs of varying compositions. Also, to characterize the solid dispersions with thermal and X-ray diffraction methods and perform intrinsic dissolution studies on them to understand the dissolution mechanism.
- To correlate the traditional dissolution model predictions with experimental results and modify the model or propose a new model, if needed.

CHAPTER 3 MODEL DEVELOPMENT FOR SOLID DISPERSIONS RELEASE

3.1 Two-component dissolution models

In practice, solid dispersions consist of more than one component and the drug release involves the simultaneous dissolution of more than one phase. Physical models have been developed and tested rigorously to describe the simultaneous diffusion and fast equilibria for two- and three-component systems.[52-56] These models serve as the basic foundation for the traditional approach (SMH) for drug release from solid dispersions. In these models, the dissolution of each component is assumed to be a diffusion controlled process and the dissolution surface is assumed as non-disintegrating. Upon exposure to the solvent, the dissolution of each component is proportional to its solubility (C_s) and diffusion coefficient (D) in the dissolving medium, as predicted for single component systems by the well-known Noyes–Whitney equation. However, these models predict that the interfacial layer between the tablet dissolving front and the solvent will become depleted in the more rapidly dissolving component, leading to the creation of a surface layer rich in one-component through which the others must diffuse prior to release into the bulk solvent phase. For a two-component system, three different situations are possible at the dissolving surface (Figure 3-1). Exactly which one exists depends on the solubility, diffusional coefficient and amount of each component in the system.

In a two-component system (A and B):

a. G_A and G_B are the dissolution rates of A and B;

b. N_A and N_B are the weights of A and B in the mixture;

c. D_A and D_B are the diffusion coefficients of A and B;

d. C_A^0 and C_B^0 are the solubility of pure A and B;

e. The diffusion layer thickness is h.

The dissolution profile of each component is linear under the sink conditions. At a critical mixture ratio (expressed in Equation 3-), both components A and B coexist at the solid-liquid interface (Figure 3-1).

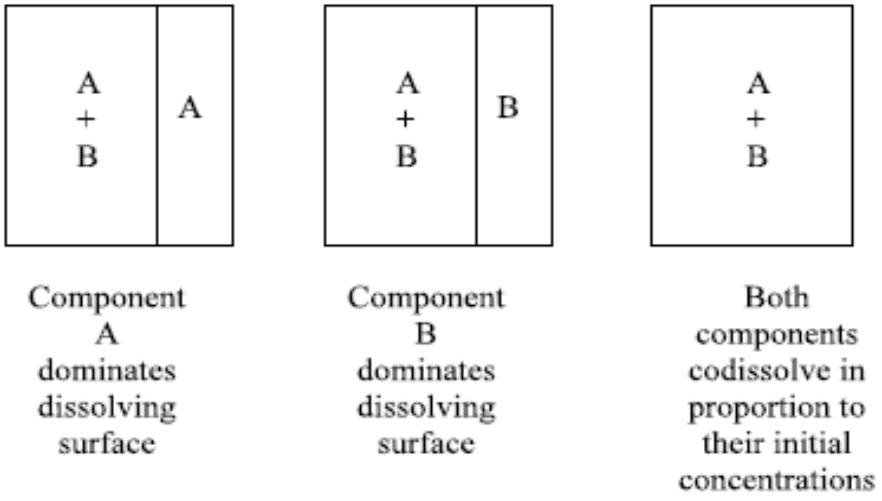

Figure 3-1: Schematic representation for the dissolution model for a two component system.[52]

$$G_B = \frac{N_B}{N_A} G_A \qquad \text{Equation 3-1}$$

At all other weight ratios (i.e., not critical ratio) one or the other component forms a porous layer at the front surface which acts as an additional diffusional barrier retarding the receding component dissolution (Figure 3-1). If that is the case, the receding component will have a non-linear dissolution profile before steady-state is reached. At steady-state, the faster receding component will have a linear release profile. At that time, the dissolution rate of both components

(A or B) can be calculated. If A forms a porous layer and B is the receding component, G_A can be calculated using Equation 3-2 and G_B can be calculated from G_A using Equation 3-1.

$$G_A = \frac{D_A C_A^0}{h} \qquad \text{Equation 3-2}$$

Similarly, if B forms a porous layer and A is the receding component, G_A can be calculated using Equation 3-3 and G_A can be calculated from G_B using Equation 3-1.

$$G_B = \frac{D_B C_B^0}{h} \qquad \text{Equation 3-3}$$

The above discussion is limited to non-interacting systems, only. If A and B form a soluble complex (AB) in the dissolution medium, the system becomes more complex and the model is to modified to account for this interaction.[52] In this case, new terms are introduced: G_A^T and G_B^T are the total dissolution rates of A and B in all forms; G_{AB} is the dissolution rate of soluble AB complex; D_{AB} is the diffusion coefficient of the AB complex and K_{ass}) is the association constant between A and B. G_A^T and G_B^T are expressed by Equation 3-4:

$$G_A^T = G_A + G_{AB} \qquad \text{Equation 3-4}$$

and Equation 3-5:

$$G_B^T = G_B + G_{AB} \qquad \text{Equation 3-5}$$

Like non-interacting systems, three different situations may occur (Figure 3-1). The critical mixture is determined by Equation 3-6.

$$G_B{}^T = \frac{N_B}{N_A}\, G_A{}^T \qquad \text{Equation 3-6}$$

At other ratios, when A forms a porous layer and B is the receding component, $G_A{}^T$ can be calculated using Equation 3-7:

$$G_A{}^T h = \frac{D_A C_A{}^0}{1 - \frac{N_B D_{AB} K_{ass} C_A{}^0}{N_A (D_B + D_{AB} K C_A{}^0)}} \qquad \text{Equation 3-7}$$

Similarly, when B forms a porous layer and A is the receding component, $G_B{}^T$ can be calculated using Equation 3-8:

$$G_B{}^T h = \frac{D_B C_B{}^0}{1 - \frac{N_A D_{AB} K_{ass} C_B{}^0}{N_B (D_A + D_{AB} K C_B{}^0)}} \qquad \text{Equation 3-8}$$

Both the non-interacting and interacting system models have been tested in binary mixtures of small molecules.[52] As shown in Figure 3-2 and Figure 3-3, the experimental results showed reasonably good agreement with theoretical predictions for non-interacting and interacting components, respectively.

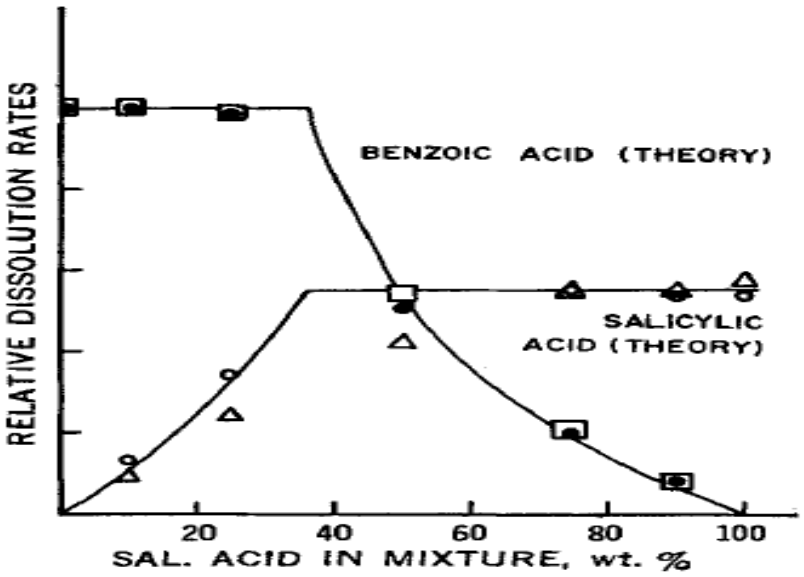

Figure 3-2: Dissolution rate comparison of experimental results with theoretical predictions for non-interacting salicylic acid-benzoic acid mixtures.[52] (open circles: melt mixtures-salicylic acid; square: melt mixtures-benzoic acid; triangles: physical mixtures-salicylic acid; closed circles: physical mixtures-benzoic acid; lines are predicted results).

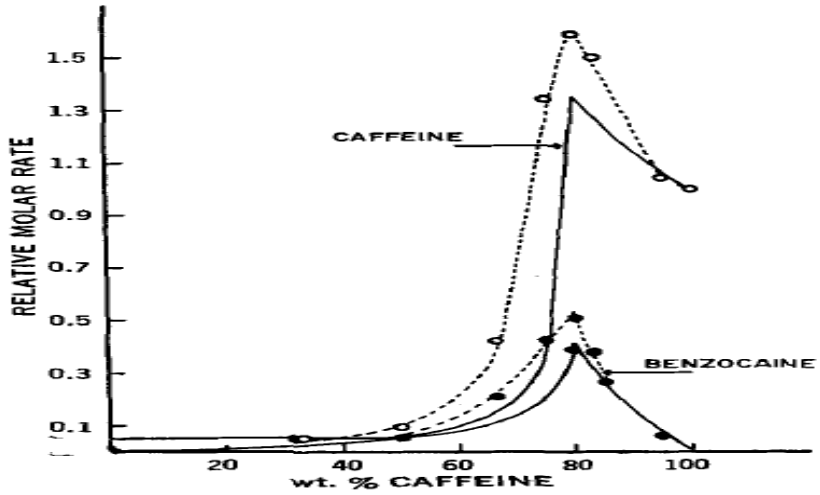

Figure 3-3: Comparison of experimental results with theoretical prediction for interacting caffeine-benzocaine mixtures.[52] (open circles: caffeine; closed circles: benzocaine; dash lines are experimental results and solid lines are predicted results).

3.2 Model development based on the traditional approach

In previous dispersion reviews[10,19,37,40], a detailed understanding of the traditional approach has been missing. It is important to develop a model in a mathematical form which will allow the traditional approach can be examined thoroughly. In order to develop this model, the first things to do are to understand the assumptions in the traditional approach. For the traditional approach, there are a few assumptions:

- Solid dispersion systems two-component systems: drug (sulfathiazole) and carrier (PVP).
- PVP form a soluble complex with sulfathiazole in solution.
- Experimental results showed that PVP and sulfathiazole released congruently according to their ratios in the solid dispersions when the system contained a high level of PVP in the dispersion.

In summary, the traditional approach is a combination of an interaction two-component model and an empirical approach. If A is the drug (a small molecule) and B is the carrier (polymer), X is the weight fraction of polymer in the dispersion described by:

$$X = \frac{N_B}{N_A + N_B} \qquad \text{Equation 3-9}$$

where, N_A and N_B are weights of drug and carrier respectively. Like the classic two-component model, three different scenarios were proposed in the traditional approach: 1) weight regions where polymer (B) is the front layer; 2) weight regions where drug (A) is the front layer; 3) a specific ratio where both the polymer and drug are together at the front (critical mixture ratio). When polymer (B) is the front layer, release is described empirically as congruent release. Under this condition, the simultaneous release of sulfathiazole and PVP according to their ratios in solid dispersions was observed. It is assumed that PVP release rates from solid dispersions was equivalent to that of the pure polymer when PVP is the front layer. Thus, the dissolution rate of polymer (G_B^T) is expressed by:

$$G_B^T = G_B^0 \qquad \text{Equation 3-10}$$

where, G_B^0 is the pure polymer dissolution rate. The dissolution rate of drug (A) can be calculated with Equation 3-6 and Equation 3-10 which is:

$$G_A^T = \frac{N_A}{N_B} G_B^0 = \frac{1-X}{X} G_B^0 \qquad 0 < X \leq 1 \qquad \text{Equation 3-11}$$

Two parameters (W_1 and $W_{2)}$ are introduced. W_1 is the initial dissolution rate ratio of the pure compounds (A and B) and is defined by:

$$W_1 = \frac{G_B^0}{G_A^0}$$ Equation 3-12

where, G_A^0 and G_B^0 are pure drug and carrier dissolution rates, respectively and W_1 is their ratio. R is the ratio of the drug dissolution rate (G_A^T) in the dispersion to that of the pure drug (G_A^0):

$$R = \frac{G_A^T}{G_A^0}$$ Equation 3-13

Equation 3-13 can be expressed as:

$$R = \frac{G_A^T}{G_A^0} = \frac{1-X}{X} G_B^0 / G_A^0 = \frac{1-X}{X} W_1 \qquad 0 < X \leq 1$$ Equation 3-14

In the regions when drug (A) is the front layer, the interacting two-component model (Equation 3-7) can be used to describe the obtained results. R can be expressed by:

$$R = \frac{1}{1 - \frac{XW_2}{(1-X)(1+W_2)}} \qquad 0 \leq X < 1$$ Equation 3-15

where, The second parameter W_2 is defined by:

$$W_2 = \frac{D_{AB}}{D_B} K_{ass} C_A^0$$ Equation 3-16

where, D_B and DA_B are diffusion coefficients of B and AB complex and C_A^0 is the drug solubility. Thus, W_2 describes a product of drug solubility and drug-polymer interaction.

Overall, the relative dissolution rate of drug (R) can be expressed by Equation 3-17. This equation is the general formulation developed based on the concepts in the tradition approach.

With this expression, various dissolution predictions can be made depending on the values of W_1, W_2 and X.

$$R(X) = \begin{cases} \dfrac{(X-1)(1+W_2)}{2W_2X + X - W_2 - 1}, 0 \le X \le W_1(W_2+1)/(2W_2W_1 + W_2 + W_1 + 1) \\ \dfrac{1-X}{X}\, W_1,\ W_1(W_2+1)/(2W_2W_1 + W_2 + W_1 + 1) \le X \le 1 \end{cases} \quad \text{Equation 3-17}$$

W_1 represents the initial dissolution rate ratio between carrier and drug. Carriers are usually fast dissolving in solid dispersions while drugs are poorly soluble and slow dissolving. Therefore, W_1 is usually quite large. W_2 is the product of drug solubility and drug-polymer interaction Since $C_A{}^0$ is a usually small for poorly soluble drugs and $KC_A{}^0$ may be also small and D_{AB} and D_B are comparable. Thus, W_2 is small.

Predictions with different values of W_1 (i.e., 10, 50, 100, 250, 500 and 1000) vs W_2 (i.e., 0.1, 0.01 and 0.001) are shown in Figure 3-4 to Figure 3-9. In each figure, the solid lines (various colors) represent the regions where drug is the front layer while the dashed line (red) represents the region where carrier is the front layer. As shown in these figures, the maximum relative dissolution rate (R) is obtained (~ 10% of W_1) when $W_2 = 0.1$. When W_2 is smaller (0.01 or 0.001), R=1 regardless how much carrier is present in solid dispersions (i.e., drug release rate is equivalent to that of the pure drug regardless of solid dispersion compositions).

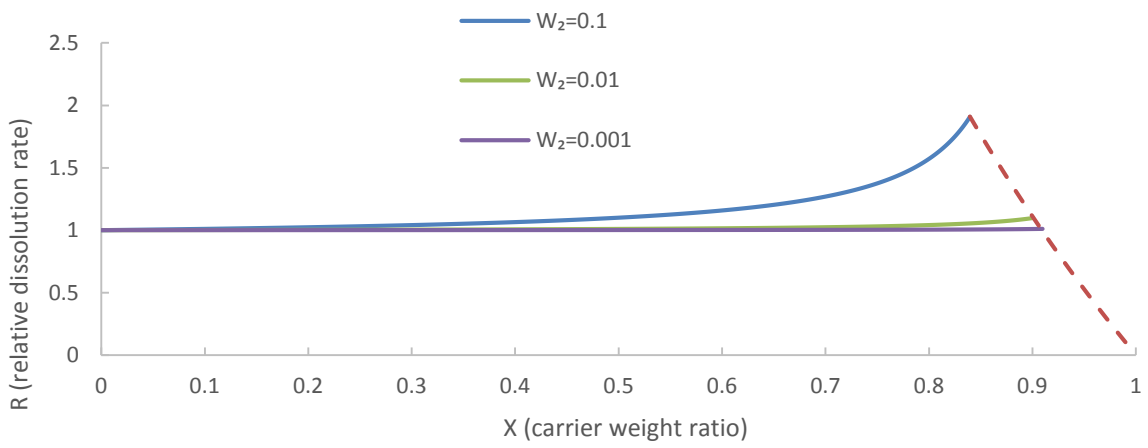

Figure 3-4: Model predictions with W_1=10 and W_2=0.1, 0.01 and 0.001.

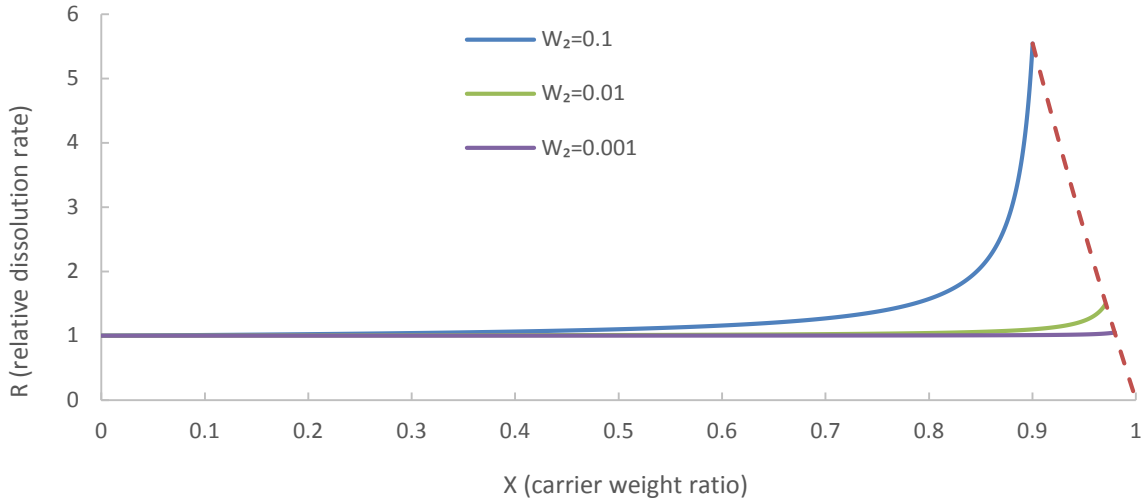

Figure 3-5: Model predictions with W_1=50 and W_2=0.1, 0.01 and 0.001.

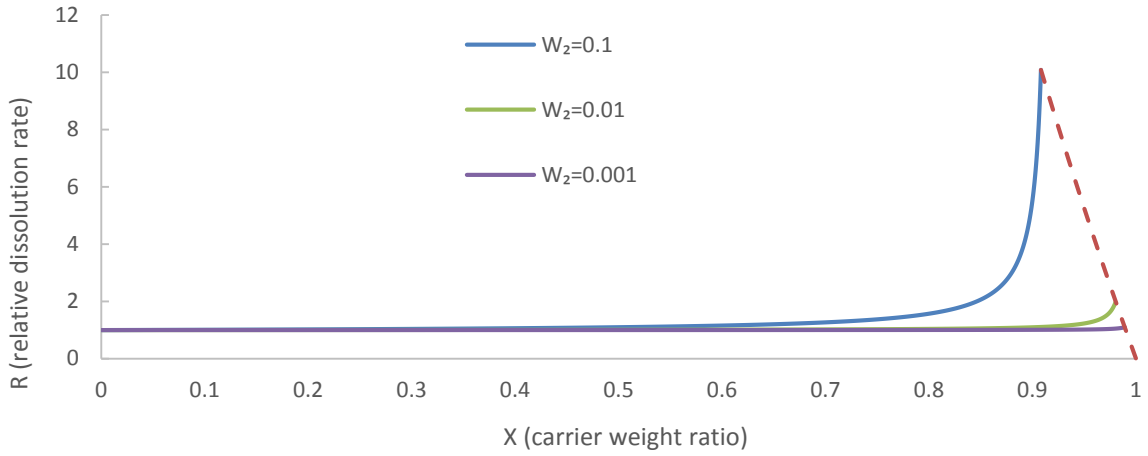

Figure 3-6: Model predictions with W_1=100 and W_2=0.1, 0.01 and 0.001.

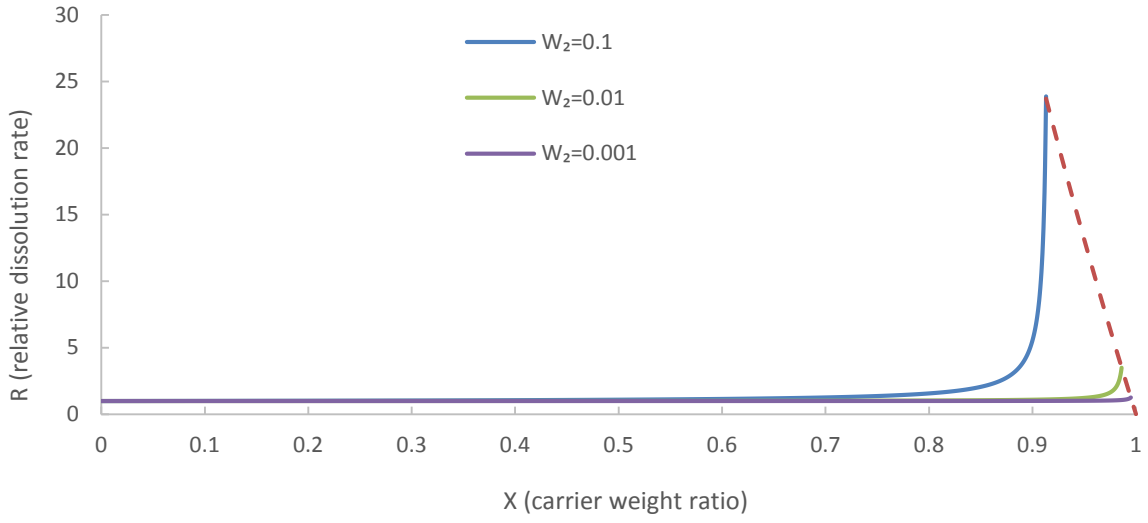

Figure 3-7: Model predictions with W_1=250 and W_2=0.1, 0.01 and 0.001.

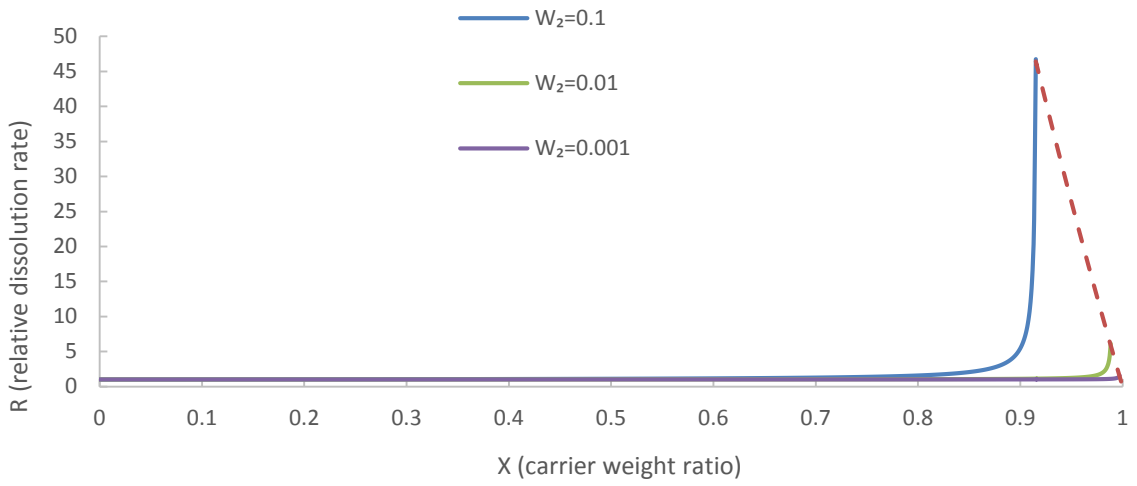

Figure 3-8: Model predictions with W_1=500 and W_2=0.1, 0.01 and 0.001.

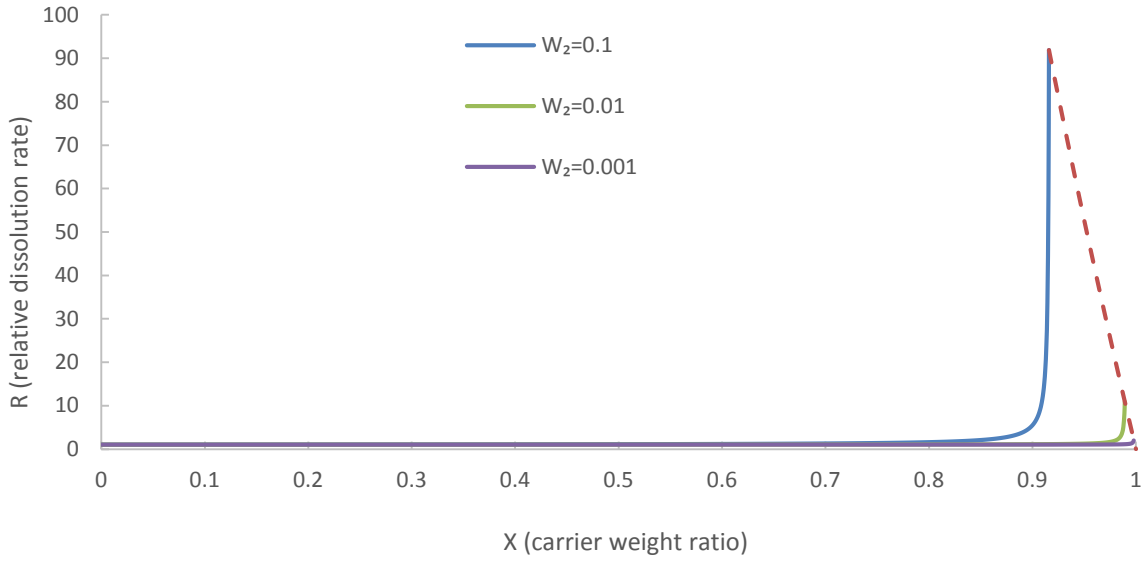

Figure 3-9: Model predictions with W_1=1000 and W_2=0.1, 0.01 and 0.001.

The model based on the concepts in the traditional approach predicts a general profile (drug release vs carrier content; like the one shown in Figure 1-8) which is observed in many dispersion studies: with increasing drug content, drug release rate first increases then decreases and eventually reaches to that of the pure drug. However, there are a few aspects that need to be discussed in more details. One of them is its predictions for low drug loaded dispersions when the drug is poorly soluble. For example, when W_2 is < 0.01 (reasonable for any poorly soluble drug), the predicted R values are ~ 1 (Table 3-1). Even at 20:1 and 10: 1 (carrier:drug) ratios, the predicted R values are ~ 1. These predictions are contrary to many reported results.[19,39,41,46,47] In such cited studies, large R-values were observed. For example, for a 10:1 PEG 4000:hydroflumethiazide dispersion, the drug release rate was 180-fold higher than that of the pure drug and for a 10:1 PEG 4000: bendrofluazide dispersion the drug release rate was 13-fold higher than that of the pure drug.[19] In the study of furosemide dispersion systems, a large R-value (~1000) was obtained for a 40% w/w solid dispersion prepared with PVP K25.[47]

Table 3-1: Predicted R-values when W_2 is small.

Polymer:drug	W_2=0.01	W_2=0.005	W_2=0.001	W_2=0.0005	W_2=0.0001
2:1	1.02	1.01	1.00	1.00	1.00
3:1	1.03	1.02	1.00	1.00	1.00
4:1	1.04	1.02	1.00	1.00	1.00
5:1	1.05	1.03	1.01	1.00	1.00
10:1	1.11	1.05	1.01	1.01	1.00
20:1	1.25	1.11	1.02	1.01	1.00

Another is duration of the carrier-controlled region which is the empirical region. This region arose from the observed congruent release of PVP and sulfathiazole. Few other studies have measured both drug and carrier release to demonstrate this carrier-controlled region. Corrigan et al. found that bendrofluazide or hydroflumethiazide and PEG 4000 released congruently at both 20:1 and 10:1 weight ratios (PEG:drug).[19] They also found similar behavior for 20:1 and 10:1 PEG 4000:barbituric acid dispersions and 50:1 and 30:1 PEG 4000:phenobarbital dispersions.[39] Similarly, Zhou et al. found that simultaneous release of cyclosporine A and TPGS occurred up to 15% drug content in a dispersion.[41] However, the weight ratio duration of this carrier-controlled region (defined by Equation 3-17) has been not been verified in these studies.

The third one is the region where the dissolution increase is a combination of drug solid-state changing and the drug-carrier interaction effect. This region is defined by the interacting two-component model and one of the assumptions of this region is the intact drug-front surface is maintained (i.e., no drug particles disintegrate from the surface). As seen in Figure 3-4 to Figure 3-9, the drug-front region starts at < 5% drug content in the dispersions. However, it is unrealistic to expect ~5% drug holding an intact solid surface together without particles falling from the surface and dissolving as they fall.

Overall, by using a relative dissolution (R), several parameters such as diffusion layer thickness and polymer diffusion coefficient can be eliminated and a general release formula presented based on the concepts in the traditional approach. This model shows that as drug loading increases, drug relative dissolution rate first increases then decreases to ~1. This type of profile qualitatively matches other literature results. However, simulation studies indicated that dissolution rate ratio underestimation could occur when drug solubility is low (i.e., W_2<0.01). Also, the drug front region predicted by the traditional approach starts at a very low drug loading in many cases. It is

unlikely that this can occur with so little drug present to maintain a solid intact drug surface. For the above reasons a new model needs to be developed to describe the dissolution behavior of a wider range of drug-carrier dispersions. This is one of the goals of this project.

CHAPTER 4 MATERIALS AND METHODS

4.1 Model compounds

A homologous series of small molecules (alkyl-p-aminobenzoate esters or PABA esters) were used as model compounds for this study. The PABA ester series has a general structure shown in Figure 4-1. These compounds were chosen because their physical properties have been studied extensively (i.e., solubility, partition coefficient, etc.).[43,57-59] They also are not known to form any hydrates or polymorphs which simplifies solid-state characterization and dissolution studies. Finally, they are very weak bases with pK_as of ~2.5. Because of the low pK_a for protonation of the amino group, they are uncharged in water (pH 5~7). Water was used as the dissolution medium; UV spectroscopy for analysis was used due to the low UV cutoff for water. Also, the ester group stability of the PABA esters was not a concern; it was sufficiently stable at the pH of water (pH 5~7) that hydrolysis was not observed over the time period of solubility and dissolution studies.

In this thesis, four PABA esters were used: methyl (C1), ethyl (C2), propyl (C3) and butyl (C4). For simplicity, methyl-p-aminobenzoate is abbreviated as MePABA, ethyl-p-aminobenzoate is EtPABA, propyl-p-aminobenzoate is PrPABA and butyl-p-aminobenzoate is BuPABA in this thesis. MePABA was obtained from Alfa Aesar (Ward Hill, MA). EtPABA and BuPABA were purchased from Sigma-Aldrich (St. Louis, MO). PrPABA was supplied by TCI America (Portland, OR).

4.2 Carriers

PVP (polyvinylpyrrolidone or polyvidone or povidone) was chosen as the polymeric carrier for dispersions. It is a polymer that is physiologically compatible, and is widely used as a pharmaceutical excipient.[60] Chemically, it is poly[1-(2-oxo-1-pyrrolidinyl)ethylene] and is a linear

polymer of 1-vinylpyrrolidin-2-one (Figure 4-2). PVP is a white, hygroscopic powder with a weak characteristic odor. In contrast to many other polymers, it is readily soluble in water and a large number of organic solvents, such as alcohols, amines, acids, chlorinated hydrocarbons, amides and lactams. This polymer is insoluble in the common liquid esters, ethers, hydrocarbons and ketones.[60] PVP is markedly hygroscopic. It has outstanding film formation properties, its concentrated solutions are tacky and adhere to different materials. PVP has a high capacity for complex formation, good stabilizing and solubilizing capacity and is insensitive to pH changes. All of these properties have made PVP one of the most frequently used polymers in drug formulations.[60]

PVP is synthesized by free-radical polymerization of N-vinylpyrrolidone in water or alcohols with a suitable initiator.[60] By selecting suitable polymerization conditions, a wide range of molecular weights can be obtained, extending from a few thousand Daltons to ~2.2 million Daltons. Traditionally, PVP is characterized by K-values which are essentially a function of its viscosity in aqueous solution. The K-values assigned to various grades of PVP represent a function of the average molecular weight, the degree of polymerization and the intrinsic viscosity. The K-values are derived from viscosity measurements and are calculated according to Fikentscher's formula.[60] The K-value is accepted by most pharmacopoeias and other authoritative bodies worldwide as a common descriptor.

PVP is one of the most investigated carriers for solid dispersions.[3,10,12,14,15] The reason for this are its water and organic solvent solubility and good biological compatibility. In this study, three different grades of PVP were used. They were K15, K30 and K90. Their properties are listed in Table 4-1. All three PVPs were obtained from Sigma-Aldrich (St. Louis, MO).

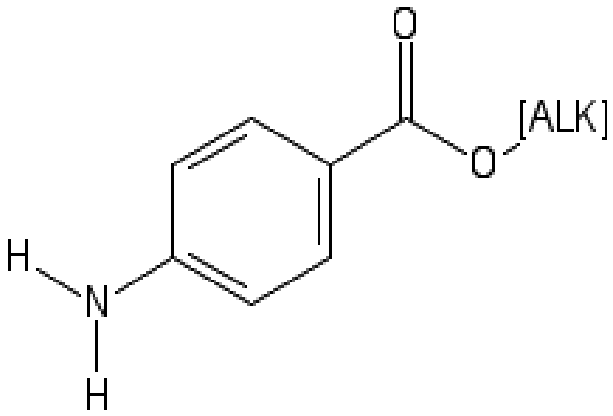

Figure 4-1: General structure of alkyl-p-aminobenzoate ester or PABA ester series.

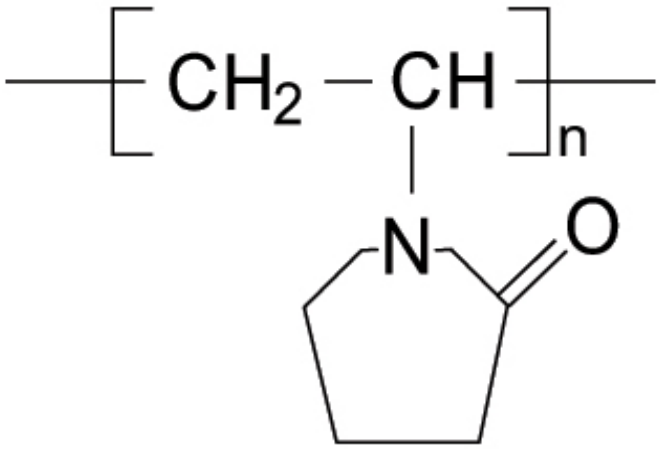

Figure 4-2: PVP structure.

Table 4-1: Characteristic PVP properties for grades used in this work.

PVP grade	MW	K range	T_g [a]
PVP K15	6,000-15,000	13-19	~130 ºC
PVP K30	40,000-80,000	26-35	~170 ºC
PVP K90	900,000-1,500,000	90-100	~176 ºC

[a.] T_g - glass transition temperature

4.3 Preparation of solid dispersions

The solvent evaporation method was utilized to prepare solid dispersions. For each dispersion, a solid mixture of PABA esters and PVP, in a selected weight ratio, was dissolved in a sufficient amount of methanol to dissolve both drug and polymer. Subsequently, the solvent was evaporated using a rotary evaporator to form a coprecipitate solid. The solid dispersion was dried overnight in a vacuum desiccator for at least 24 hours. The dried solid was ground with a mortar and pestle and passed through a 60 mesh sieve (Fisher Scientific). Dispersions were stored in a desiccator at room temperature until use.

4.4 Tablet preparation

Powdered materials (pure components or solid dispersion) were passed through a 60-mesh sieve. A weighted amount of solid (~250 mg) was compressed in a Varian® rotating disk intrinsic dissolution die (0.5 cm^2 area) with a Carver press (Model C, Carver, Inc., Wabash, IN) at 3000 pounds force for 30 seconds.

In preliminary studies, it was found that many air bubbles were generated at the tablet surface during the course of a dissolution study. However, this phenomenon only occurred in solid

dispersion formulations. These air bubbles caused significant variation in the dissolution results. It was discovered that there was space between the die and dissolution holder which held air. During dissolution, the dissolution holder was immersed in the dissolution medium at 37 ºC. When the air expanded, bubbles were continuously generated at the tablet surface. This did not occur with pure components because of their smaller particle size than the dispersions and no air passed through the less porous tablet during dissolution. To correct this problem, 500 gram of PVP (MW=3,500, Sigma-Aldrich, St. Louis, MO) was compressed behind the initial formulation (pure components or solid dispersions). This PVP layer served as a barrier to prevent the expanding air from moving out onto the tablet surface during dissolution. This amount and grade of PVP was chosen based on its successful air blocking and its ease for cleaning the holder and die after a completed dissolution run. Initial studies were also performed to make sure that enough formulation (~250 mg, pure components or solid dispersions) was compressed so that the pure PVP (MW=3,500) did not interfere with the dissolution or assay results.

4.5 Dissolution studies

Using a 6-station USP dissolution apparatus (VK700), the flat-faced tablet was mounted in the dissolution holder and rotated at 100 rpm in 500 mL of distilled water at 37 °C (n=3). At each time point, dissolution samples (5 mL) were taken and the volume was replaced with an equal volume of fresh medium (water).

4.6 UV assay

4.6.1 Single component assay

4.6.1.1 Single wavelength for pure PABA ester determinations

Samples were analyzed by UV spectrophotometry using a single wavelength to determine the concentration of PABA esters (at 285 nm). All analyses were performed with a diode-array ultraviolet (UV) spectrophotometer (HP 8453). A 1-cm cuvette was used for all the PABA esters determination. Appropriate dilutions were applied when needed to ensure an absorbance value within the calibration range. UV calibration curves for PABA esters are listed in APPENDIX A. The obtained calibration results are consistent with those found in the literature.[61]

4.6.1.2 Single component UV analysis for PVPs

Analytical methods for PVP include colorimetry, fluorimetry, HPLC, GPC and UV spectroscopy.[62-71] However, many of these methods have limited sensitivity. In preliminary studies, only UV spectroscopy showed sufficient sensitivity for dissolution sample analysis. Thus, UV spectroscopy was employed for all PVP analysis. A 2-mm cuvette was used for all PVP determinations. Appropriate dilutions were applied when needed to ensure absorbance within the calibration range. Samples were analyzed spectrophotometrically using a suitable wavelength range (195-225 nm) to determine the PVP concentration. This method is available in the HP 8453 software as a single component analysis algorithm. The UV spectra of PVPs are given in APPENDIX B.

4.6.2 Multicomponent assay

Samples containing both PVP and PABA ester were analyzed spectrophotometrically using a multi-component method (least squares algorithm) in the HP 8453 software over a wavelength

range of 195 to 325 nm to determine both the PVP and PABA ester content in mixture samples. A 2-mm cuvette was used for all determinations. Appropriate dilution was applied when needed to ensure absorbance values within the calibration range. Pure PVP or PABA ester solutions were utilized as standard solutions. Validation of this method was performed by preparing and analyzing known mixtures of the two components (PABA ester and PVP). The validation results are show in APPENDIX C.

4.7 Differential Scanning Calorimetry (DSC)

DSC thermograms were obtained using a Perkin-Elmer DSC 7. The DSC was calibrated using an indium standard. Samples (2 – 5 mg) which were crimped in aluminum pans were heated over a range of 30 to 65~120 °C at a constant heating rate (10 °C/min) under a nitrogen purge (30 – 40 mL/min). The temperature range was chosen based on the melting point of each PABA ester and was usually terminated 10-15 °C higher than its melting point. An empty pan was heated in the exactly the same way as the sample pans and used as a reference. Solid dispersions were prepared by the solvent evaporation method described above. For comparison, samples of the pure PABA ester or PVP were also dissolved in methanol and then precipitated after solvent removal. These treated samples served as pure compound references.

4.8 Powder X-ray diffraction (PXRD)

PXRD was performed on solid materials (pure component or dispersions) with a Siemens D-5000 diffractometer (Siemens Energy and Automation, Inc., Model D5000, Madison, WI). The instrument was controlled by a computer with Diffrac Plus® diffraction software for data processing

and presentation. The radiation used was generated by a copper K_α filter, with a wavelength 1.54A^o at 40 kV and 30 mA.

The procedure used to prepare samples for the X-ray analyses was as follows. Solid samples were placed on a sample holder that was approximately 2 cm × 2 cm × 2 mm. A spatula was used to put the powder in the holder and gently smoothed to produce a flat surface. The samples were then placed in the sample compartment. They were scanned over a range from 5^o to 45^o 2θ, using a scan rate of 2 degrees per minute. For comparison, treated samples of the pure PABA ester or PVP were also analyzed as references.

4.9 Solubility studies

4.9.1 Aqueous solubility

Excess powdered PABA ester solids were added to distilled water (10 mL) in a 20 mL screw-capped vial and rotated in a water bath at 37 °C for 72 hours (n=3). Each solid suspension was filtered (0.22 µm, MILLEX®-GS) and the filtrate was diluted with water. Diluted samples were analyzed by UV spectroscopy for PABA ester concentration.

4.9.2 Complexation studies

This study was similar to the solubility method described above except aqueous PVP solutions were used as the solvent instead of water. In this study, three different concentrations (1%, 5% and 10% w/v) were used for PVP K15 and PVP K30. For PVP K90, only 1% w/v was used because of its high viscosity at concentrations > 1% w/v. Because of no UV absorbance for PVP beyond 230 nm, the complexation study samples were analyzed using UV spectroscopy at a single wavelength of 285 nm as if they were pure PABA ester samples.

CHAPTER 5 RESULTS AND DISCUSSION

5.1 Physical characterization

PABA ester-PVP dispersions were prepared using various polymer:drug weight ratios (20:1, 10:1, 6:1, 4:1, 3:1 and 2:1) and three molecular weights of PVP (K15, K30 and K90). In order to first determine if amorphous solid dispersions were successfully prepared, DSC and powder X-ray diffraction (PXRD) were performed on the prepared samples. For the purpose of comparison, pure PABA esters and PVPs were also treated the same way as in solid dispersion preparation (i.e. pure PABA esters or PVPs were first dissolved in methanol and then the solvent removed by evaporation). The treated PABA esters and PVPs were used as reference materials for the solid dispersions.

5.1.1 DSC

DSC analysis was performed on pure PABA esters, treated PABA esters, pure PVPs, treated PVPs, and PABA-PVP solid dispersions, covering temperatures from almost room temperature to 10-15 °C higher than the melting point of each PABA ester. The DSC thermograms for pure PABA esters are shown in Figure 5-1. MePABA had a melting point of 110 °C; EtPABA had a melting point of 88 °C; PrPABA had a melting point of 72 °C; BuPABA had a melting point of 53 °C. These results are in good agreement with literature values.[43,72] The DSC thermograms for the treated PABA esters are shown in Figure 5-2. The treatment process did not change their melting behavior. Both the melting peak and ΔH (enthalpy of fusion) are very similar for each PABA ester with or without treatment (Figure 5-1 and Figure 5-2). As shown in Figure 5-3, the melting point of the PABA esters decreased as alkyl chain length increased which has been reported previously.[72]

The DSC thermograms for PVP are shown in Figure 5-4. PVPs, as amorphous polymers, did not have a melting point. Instead, they showed a broad relaxation phenomenon from 40-160 ^{o}C. The DSC thermograms for the treated PVPs are shown in Figure 5-5. The treatment did not affect the relaxation behavior of the polymers. For future discussions, only the DSC thermograms of the treated pure component (PABA esters or PVPs) will be discussed as reference.

The DSC thermograms for MePABA-PVP K15, MePABA-PVP K30 and MePABA-PVP K90 dispersions are shown in Figure 5-6 to Figure 5-8. Upon combining with PVP, the melting peak of MePABA at 110 ^{o}C disappeared at all polymer:drug ratios and for all PVP molecular weights (K15, K30 and K90), which indicates the lack of crystallinity in any of its solid dispersions. Similar thermal behaviors were observed for other PABA esters (EtPABA, PrPABA and BuPABA) and PVP (K15, K30 or K90) solid dispersions. Their thermograms are presented in APPENDIX D.

Table 5-1: DSC results for pure PABA esters.

PABA ester	Peak temperature (^{O}C)	ΔH (J/g)
MePABA	110	151.72
EtPABA	88	132.63
PrPABA	72	121.69
BuPABA	53	121.71

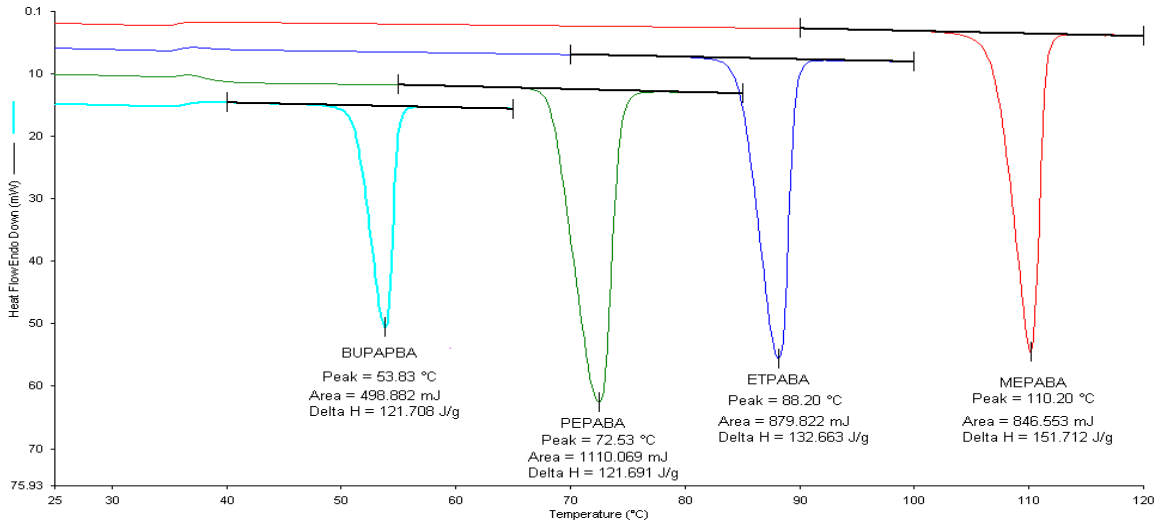

Figure 5-1: DSC thermograms of pure PABA esters. From right to left: MePABA (red), EtPABA (blue), PrPABA (green) and BuPABA (cyan).

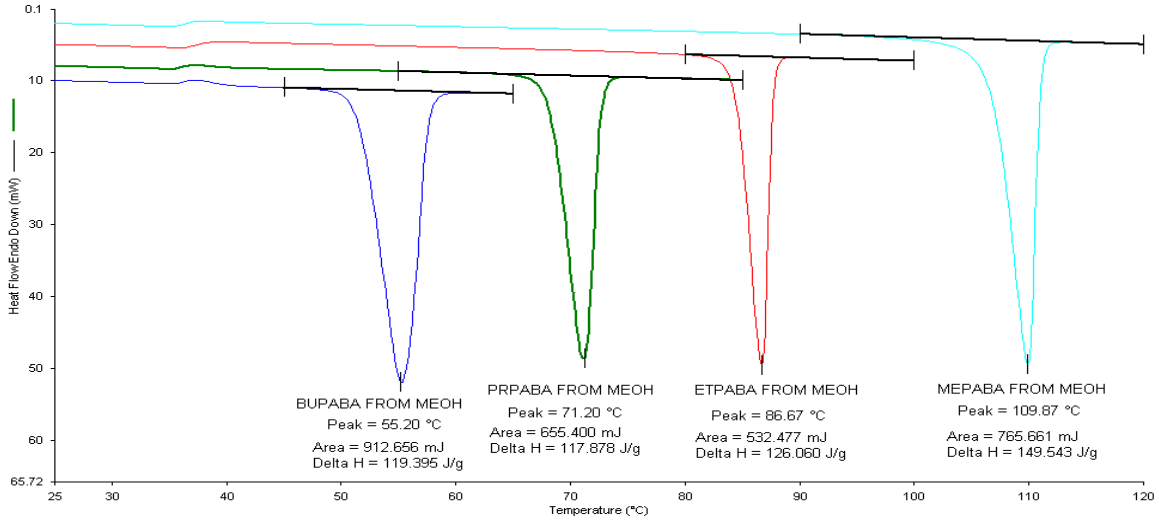

Figure 5-2: DSC thermograms of pure treated PABA esters (precipitated from methanol). From right to left: MePABA (cyan), EtPABA (red), PrPABA (green) and BuPABA (blue).

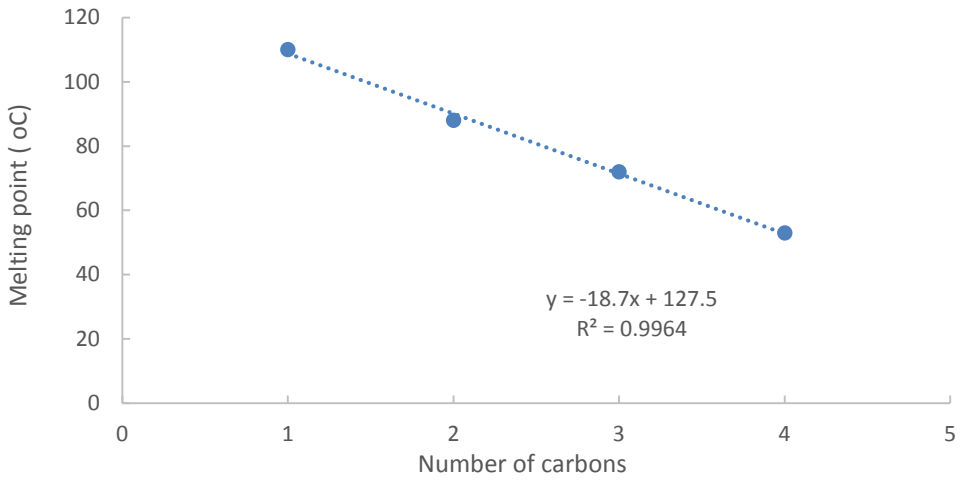

Figure 5-3: Melting points of PABA ester vs alkyl chain length.

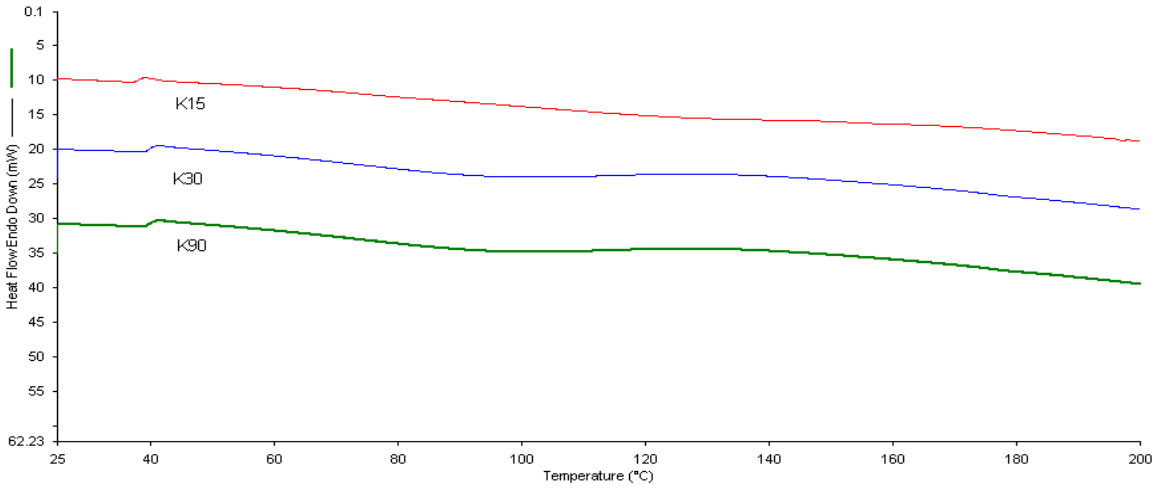

Figure 5-4: DSC thermograms of pure PVPs. From top to bottom: PVP K15 (red), PVP K30 (blue) and PVP K90 (green).

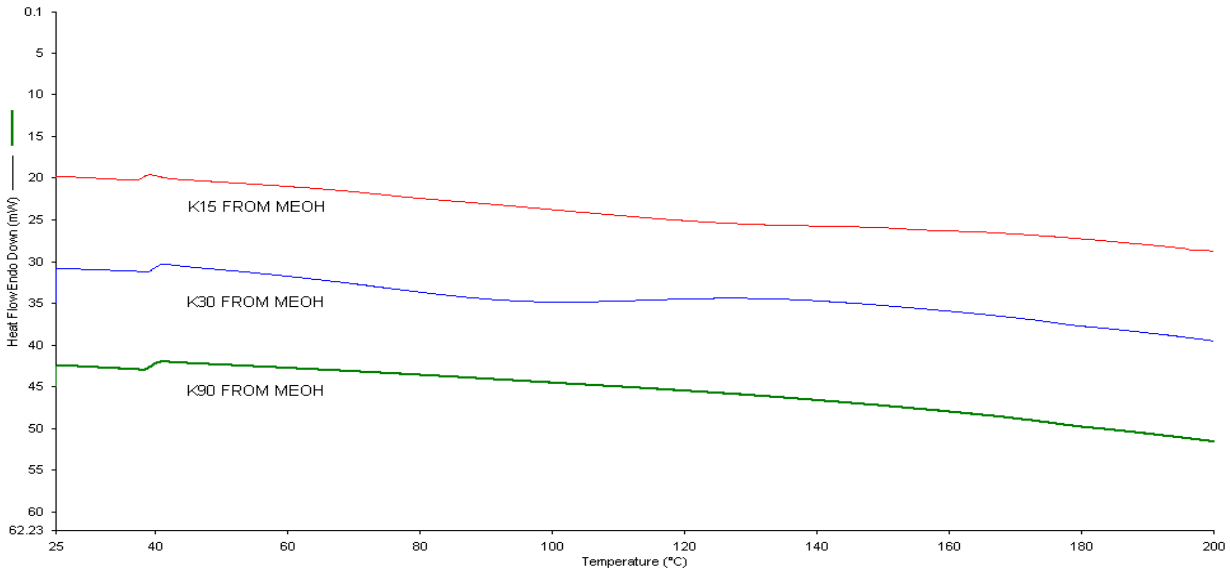

Figure 5-5: DSC thermograms of pure treated PVPs (precipitated from methanol). From top to bottom: PVP K15 (red), PVP K30 (blue) and PVP K90 (green).

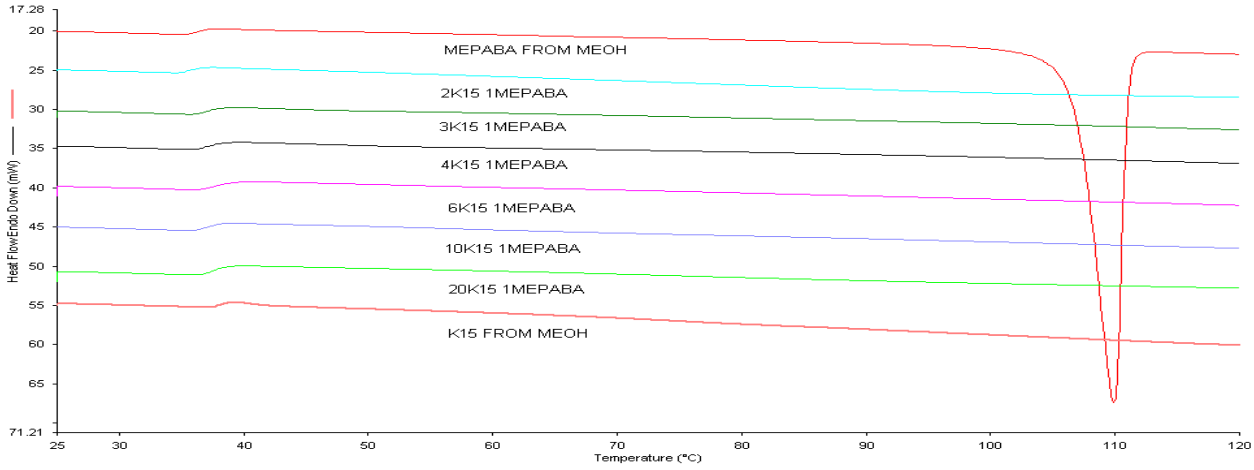

Figure 5-6: DSC thermograms of MePABA-K15 solid dispersions. From top to bottom: MePABA (treated), PVP K15: MePABA 2:1, PVP K15:MePABA 3:1, PVP K15:MePABA 4:1, PVP K15:MePABA 6:1, PVP K15:MePABA 10:1, PVP K15:MePABA 20:1 and PVP K15 (treated).

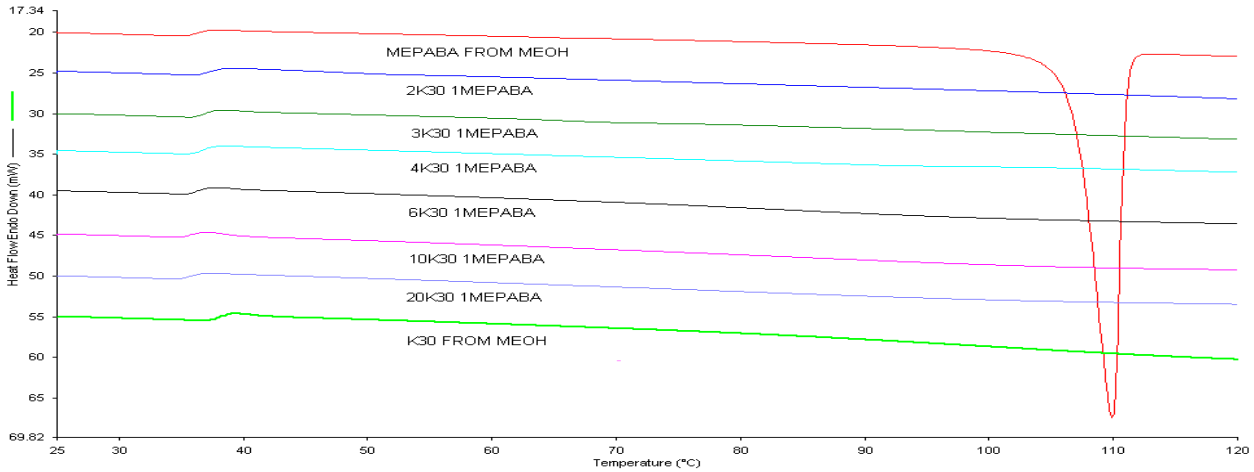

Figure 5-7: DSC thermograms of MePABA-K30 solid dispersions. From top to bottom: MePABA (treated), PVP K30:MePABA 2:1, PVP K30:MePABA 3:1, PVP K30:MePABA 4:1, PVP K30:MePABA 6:1, PVP K30:MePABA 10:1, PVP K30:MePABA 20:1 and PVP K30 (treated).

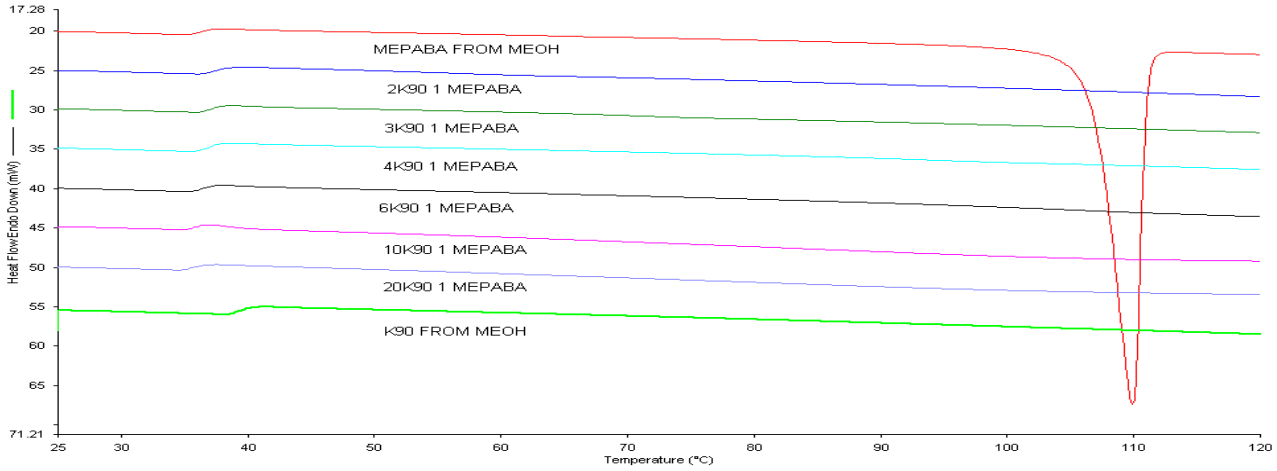

Figure 5-8: DSC thermograms of MePABA-K90 solid dispersions. From top to bottom: MePABA (treated), PVP K90:MePABA 2:1, PVP K90:MePABA 3:1, PVP K90:MePABA 4:1, PVP K90: MePABA 6:1, PVP K90:MePABA 10:1, PVP K90:MePABA 20:1 and PVP K90 (treated).

5.1.2 PXRD

Although DSC showed the apparent disappearance of crystallinity with dispersion of the PABA esters in PVPs, a second method was used to verify these results. For this purpose, powder X-ray diffraction (PXRD) analysis was also employed. As mentioned previously, X-ray diffraction would show any presence of solid crystallinity, and was performed on each dispersion sample to corroborate the DSC results. The diffractograms for PABA esters and treated PABA esters are shown in Figure 5-9 and Figure 5-10. PABA esters showed various diffraction peaks at different 2Θ angles, indicating the crystalline nature of these compounds; the treatment process did not change their crystallinity. The diffractograms for PVPs and treated PVPs are shown in Figure 5-11 and Figure 5-12. PVPs did not show any distinction peaks indicating their amorphous nature.

The PXRD diffractograms of the MePABA-PVP solid dispersions are shown in Figure 5-13 through Figure 5-15. MePABA crystallinity disappeared for all the polymer:drug ratios and PVP grades indicating that it was amorphously dispersed in the polymer as observed with the DSC analysis. Similar results were observed for other PABA esters (EtPABA, PrPABA and BuPABA) and PVP (K15, K30 or K90) solid dispersions. These PXRD diffractograms can be found in APPENDIX E.

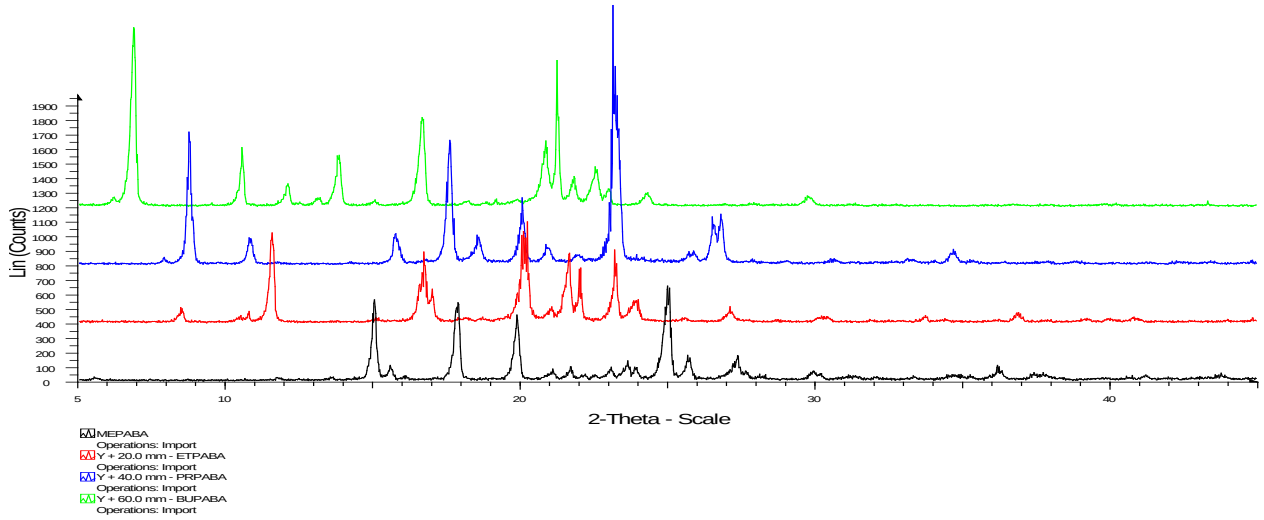

Figure 5-9: X-ray diffractograms of pure PABA esters. The curves represent the following compounds: MePABA (black), EtPABA (red), PrPABA (blue) and BuPABA (green).

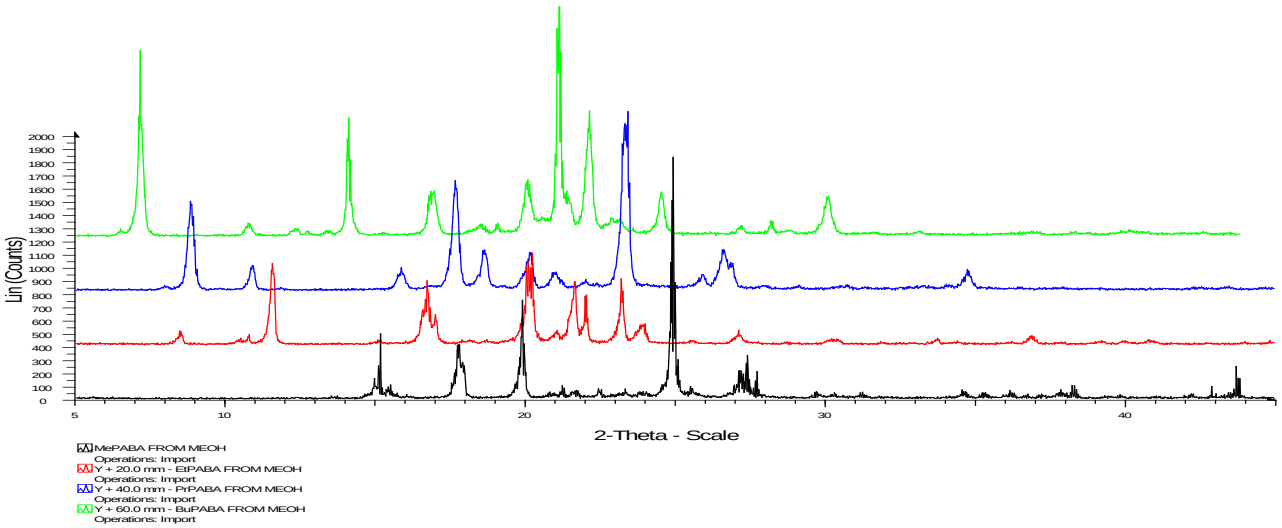

Figure 5-10: X-ray diffractograms of treated PABA esters. From top to bottom: treated MePABA (black), treated EtPABA (red), treated PrPABA (blue) and treated BuPABA (green).

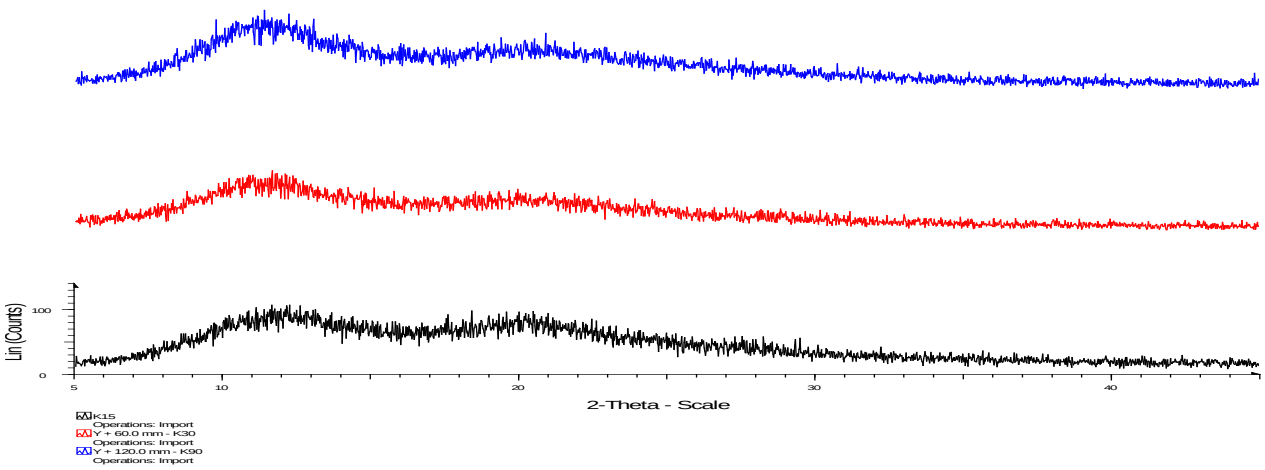

Figure 5-11: X-ray diffractograms of pure PVPs. From top to bottom: PVP K15 (black), PVP K30 (red) and PVP K90 (blue).

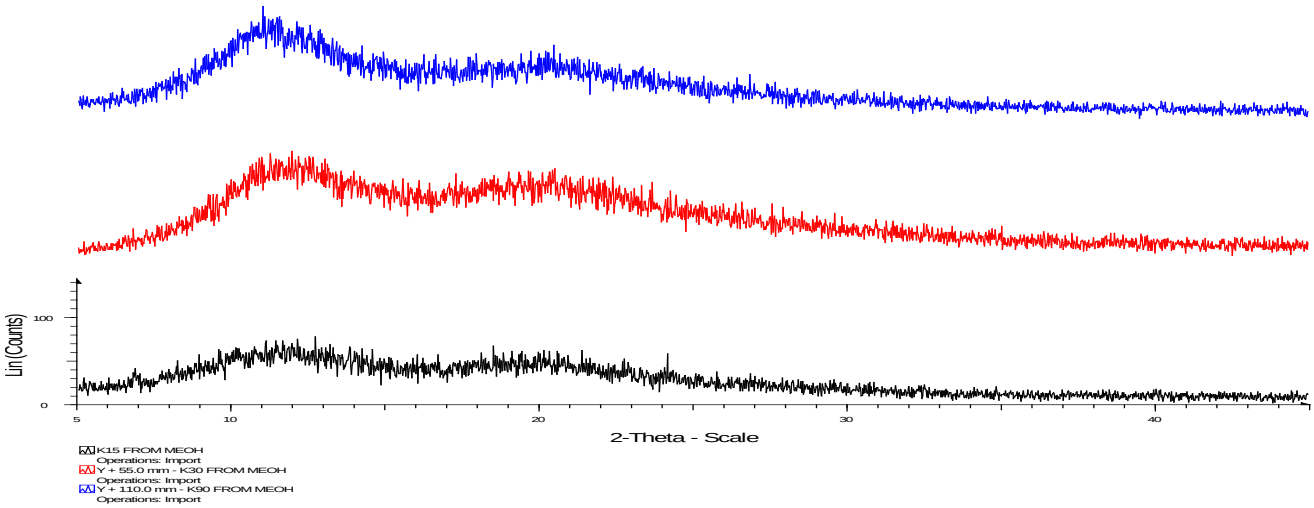

Figure 5-12: X-ray diffractograms of treated PVPs. From top to bottom: treated PVP K15 (black), treated PVP K30 (red) and treated PVP K90 (blue).

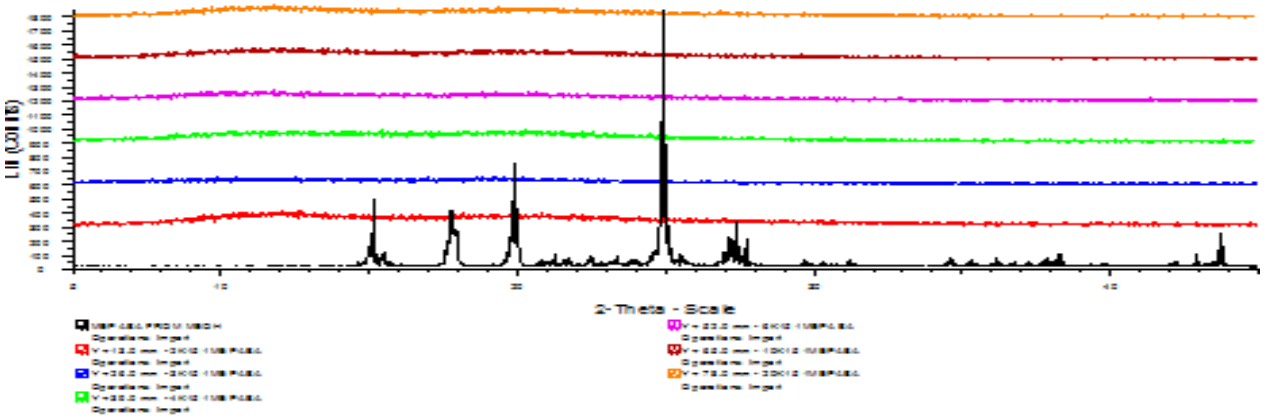

Figure 5-13: X-ray diffractograms of MePABA-K15 solid dispersions. From top to bottom: PVP K15:MePABA 20:1, PVP K15:MePABA 10:1, PVP K15:MePABA 6:1, PVP K15:MePABA 4:1, PVP K15:MePABA 3:1, PVP K15:MePABA 2:1 and MePABA (treated).

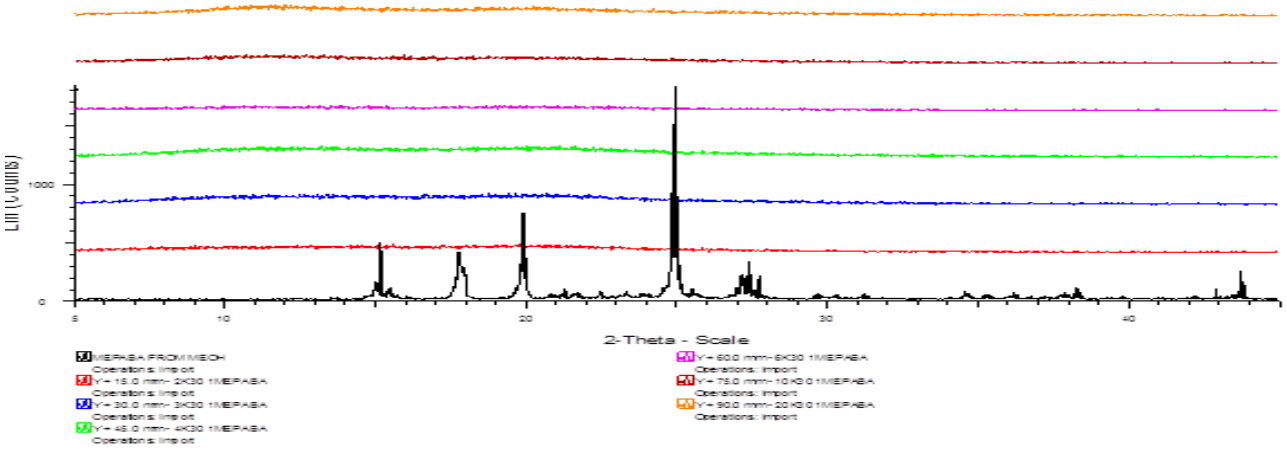

Figure 5-14: X-ray diffractograms of MePABA-K30 solid dispersions. From top to bottom: PVP K30:MePABA 20:1, PVP K30:MePABA 10:1, PVP K30:MePABA 6:1, PVP K30:MePABA 4:1, PVP K30:MePABA 3:1, PVP K30:MePABA 2:1 and MePABA (treated).

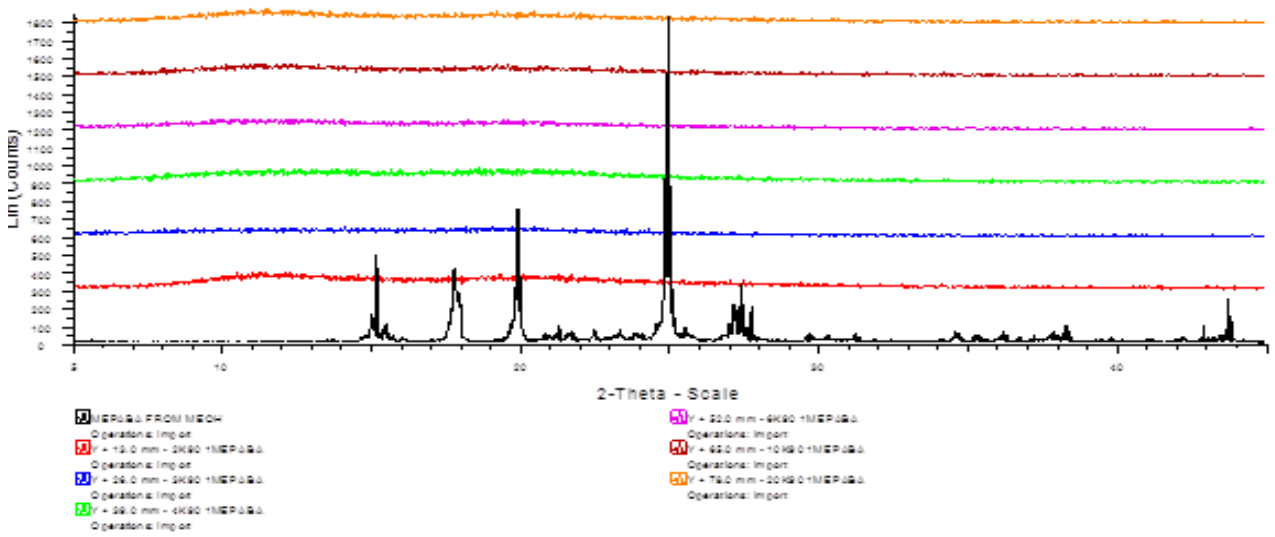

Figure 5-15: X-ray diffractograms of MePABA-K90 solid dispersions. From top to bottom: PVP K90:MePABA 20:1, PVP K90:MePABA 10:1, PVP K90:MePABA 6:1, PVP K90:MePABA 4:1, PVP K90:MePABA 3:1, PVP K90:MePABA 2:1 and MePABA (treated).

5.2 Solubility and complexation study

5.2.1 Solubility

The aqueous solubility of each PABA ester is presented in Table 5-2. These results agree well with literature results.[61,73] MePABA was the most soluble compound of all PABA esters investigated, having a solubility of ~ 2.3 mg/mL. BuPABA was the least soluble compound having a solubility of ~ 0.3 mg/mL.

Table 5-2: Aqueous solubility of PABA esters at 37 ºC.

PABA ester	Solubility[a] (mg/mL)
MePABA	2.30 ± 0.01
EtPABA	1.50 ± 0.03
PrPABA	0.72 ± 0.01
BuPABA	0.28 ± 0.03

[a.] N=3

5.2.2 Complexation studies

The goal of this study was to obtain the complexation constant (K_{ass}) between PABA esters and PVPs which is a key parameter in the model developed based on concepts in the traditional approach. The complexation study was similar to solubility determinations described above except that aqueous PVP solutions were used as the solvent instead of water. Complexation results are presented in Figure 5-16 to Figure 5-18.

To obtain K_{ass}, a 1:1 interaction between PABA ester and PVP monomer units was assumed. Thus, each PVP molecules was assumed to have a specific number of monomer units that each could interact independently with a PABA ester molecule. Complexation constants were calculated using Equation 5-1. For PVP K15 and PVP K30, K_{ass} was obtained by linear regression of all phase-solubility data. For PVP K90, K_{ass} was calculated based on one PVP K90 concentration. The calculated K_{ass} values are given in Table 5-3. The obtained K_{ass} values are generally the same for each PABA ester and PVPs even though the solubility profiles are quite differ going from C1 to C4 PABA ester; K_{ass} range slightly from 1.0-3.5. This is expected considering the structural similarities between the PABA esters. Higher K_{ass} values were observed

for lower MW PVP with a particular PABA ester. This is probably due to the lower MW polymer having less chain entanglement which leads to slightly stronger interaction with PABA esters or the monomer units of the lower MW PVP are more available for interaction. Also slightly higher K_{ass} values were obtained for longer chain PABA esters. This may be due to greater solubility enhancement for a longer chain PABA ester.

$$K_{ass} = \frac{(PABA - PVP)_{complex}}{PABA_{free} \times PVP_{free}} \qquad \text{Equation 5-1}$$

Table 5-3: Complexation constant (K_{ass}) for PABA esters and PVPs at 37 °C.

K_{ass}	PVP K15	PVP k30	PVP K90
MePABA	1.7	1.6	1.6
EtPABA	2.2	2.1	1.7
PrPABA	2.7	2.5	0.98
BuPABA	3.4	3.2	1.8

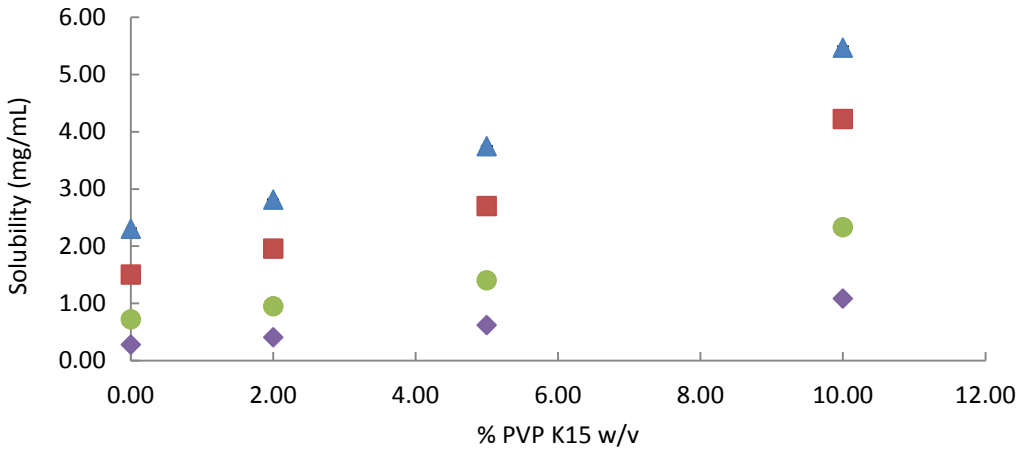

Figure 5-16: Phase-solubility data for PABA esters and PVP K15 (n=3) at 37 °C. The data points represent: blue triangle-MePABA, red square-EtPABA, green dot-PrPABA and purple diamond-BuPABA.

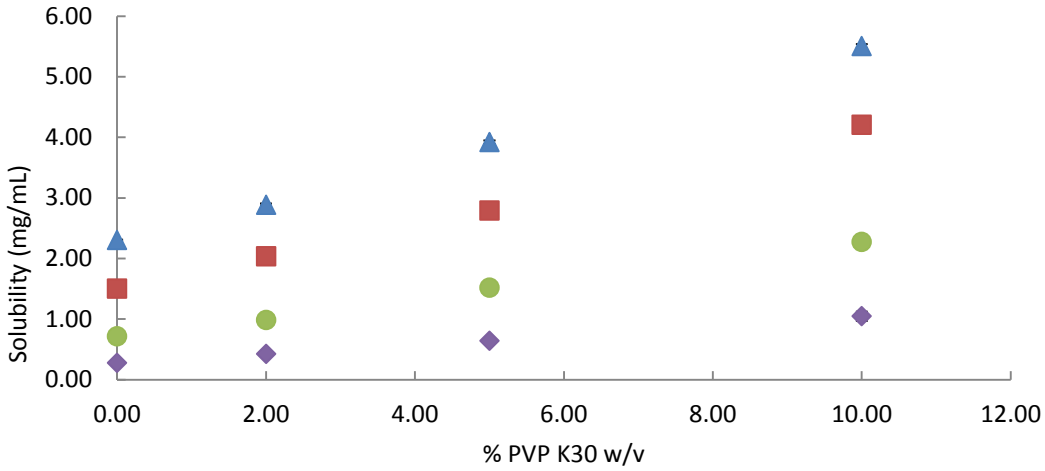

Figure 5-17: Phase-solubility data for PABA esters and PVP K30 (n=3) at 37 °C. The data points represent: blue triangle-MePABA, red square-EtPABA, green dot-PrPABA and purple diamond-BuPABA.

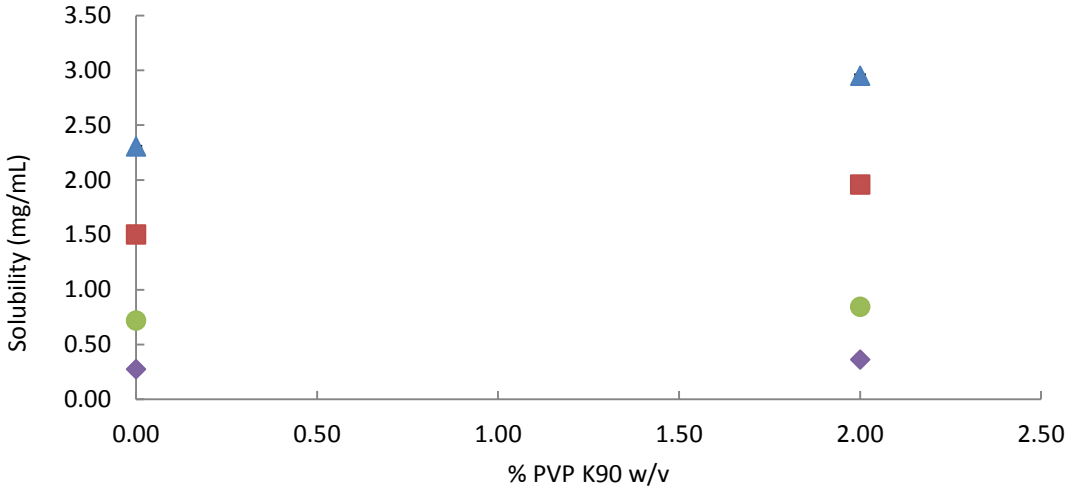

Figure 5-18: Phase-solubility data for PABA esters and PVP K90 (n=3) at 37 °C. The data points represent: blue triangle-MePABA, red square-EtPABA, green dot-PrPABA and purple diamond-BuPABA.

5.2.3 Pure PABA ester dissolution studies

The dissolution profiles of pure PABA esters are shown in Figure 5-19. A linear dissolution profile was obtained for all PABA esters under sink conditions at 37 °C. Linear regression was used to calculate the dissolution rates which are summarized in Table 5-4. In this thesis, the intrinsic dissolution rate are reported as the linear regression of the average dissolution data points (n=3). As expected, the PABA ester intrinsic dissolution rates were related to their solubilities. MePABA was the most soluble PABA ester. It also had the highest dissolution rate. Butyl PABA was the least soluble PABA ester. It had the lowest dissolution rate.

Similar to the DSC and PXRD results, the treatment process did not change the dissolution behavior of pure PABA ester. The dissolution profiles of the treated PABA esters are shown in APPENDIX F. The linear regression results are also present in APPENDIX F. Those results are comparable with the results presented in Figure 5-19 and Table 5-4.

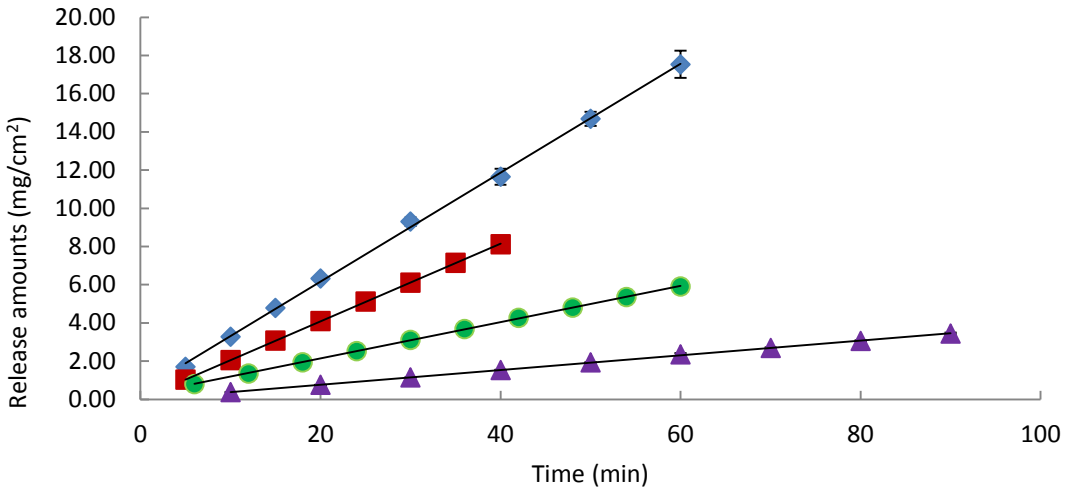

Figure 5-19: Rotating disk intrinsic release profiles of pure PABA esters (n=3) at 37 °C at 100 rpm. The data are represented as: blue diamond-MePABA, red square-EtPABA, green dot-PrPABA and purple triangle-BuPABA.

Table 5-4: Rotating disk intrinsic release rates of pure PABA esters (n=3) at 37 °C at 100 rpm.

	Slope (mg/cm^2·min)	Intercept (mg/cm^2)	R^2
MePABA	0.28	0.47	0.9991
EtPABA	0.20	0.026	0.9999
PrPABA	0.095	0.24	0.9998
BuPABA	0.038	0.0004	0.9997

5.2.4 Pure PVP dissolution studies

The intrinsic dissolution profiles of PVP are shown in Figure 5-20 and linear regression was used to calculate dissolution rates which are summarized in Table 5-5. Overall, PVPs had nearly linear dissolution profiles. A distinctly non-linear intrinsic dissolution profile of PVP was observed by Nagami et al.[74,75] However the dissolution was performed in a 4:1 acetone-water in their study. PVP is not soluble in acetone. The slow hydration of PVP in an acetone-water cosolvent might contribute to its non-linear dissolution behavior.

The dissolution rates of PVP are inversely related to their molecular weight. Similar phenomena was reported in other PVP studies and also for PEG.[19,74,75] PVP K15 has the lowest molecular weight and as expected its dissolution rate was the highest. PVP K90 has the highest molecular weight and its dissolution rate was the lowest. PVPs dissolved much faster than PABA esters. PVP K90, the slowest dissolving polymer of all three PVP grades, dissolved ~5-fold faster than MePABA which was the fastest dissolving PABA ester. PVP K15 dissolved 70-fold faster than MePABA and over 200-folder faster than BuPABA.

Like PABA esters, the treatment process did not change the dissolution behavior of PVP K15 and PVP K90. However, for PVP K30, the dissolution rate increased ~50% more than the untreated polymer which will be discussed in the discussion (page 101). The dissolution profiles of the treated PVPs and their dissolution rates are presented in APPENDIX F.

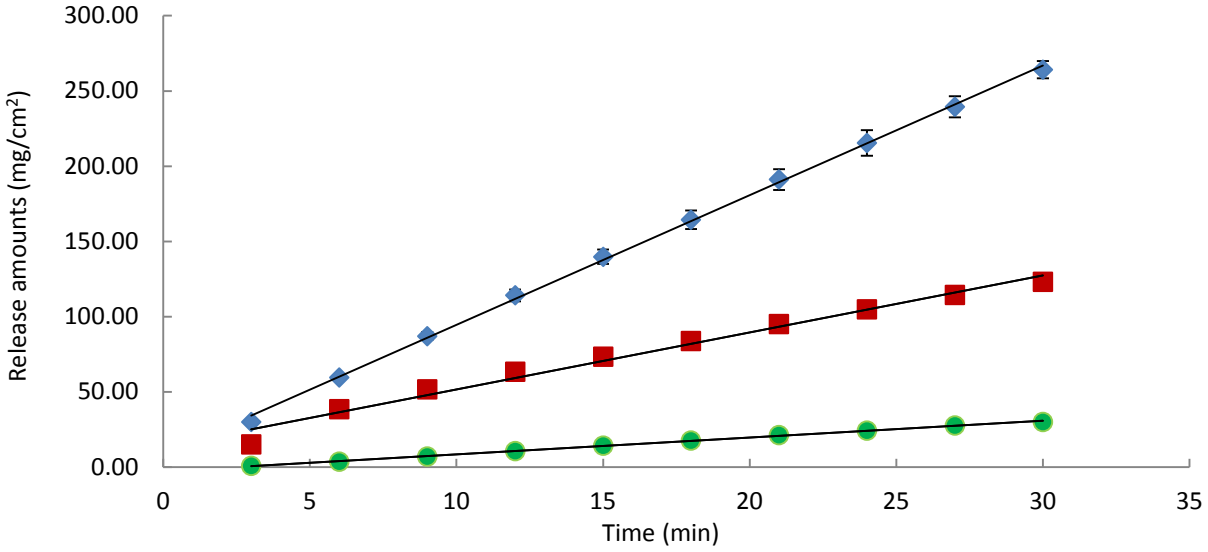

Figure 5-20: Rotating disk intrinsic release profiles of pure PVPs (n=3) at 37 °C at 100 rpm. The data are represented as: blue diamond-PVP K15, red square-PVP K30 and green dot-PVP K90.

Table 5-5: Rotating disk intrinsic release rates of pure PVPs (n=3) at 37 °C at 100 rpm.

	Slope (mg/cm^2·min)	Intercept (mg/cm^2)	R^2
PVP K15	8.6	8.4	0.9992
PVP K30	3.8	14	0.9839
PVP K90	1.1	-2.6	0.9984

5.3 Solid dispersion release studies

Solid dispersions were prepared by solvent evaporation to disperse PABA esters in PVPs at polymer:drug weight ratios of 20:1, 10:1, 6:1, 4:1, 3:1 and 2:1. The weight ratios in the prepared solid dispersions were confirmed by dissolving known amounts of the dispersions in water and analyzing for each component by UV multicomponent analysis.

5.3.1 MePABA-PVP solid dispersions

5.3.1.1 MePABA-PVP K15 solid dispersions

The release profiles of MePABA and PVP K15 from the MePABA-PVP K15 solid dispersions are shown in Figure 5-21 and Figure 5-22. For comparison, the treated pure MePABA and treated pure PVP K15 (i.e., dissolved in methanol and reprecipitated), are also shown in these figures. Overall, both MePABA and PVP K15 had nearly linear dissolution profiles for all solid dispersions. The MePABA release rate from dispersions first increased then decreased as the drug loading increased. This trend (i.e., release increasing then decreasing) has been reported in other similar studies.[20,46,47] A maximum MePABA release rate was observed at a 6:1 polymer:drug ratio. This is different than that are observed in the other studies. For example, a maximum dissolution rate was observed at a 3:1 PVP:sulfathiazole ratio and at 20% and 40% drug loadings for CI-987 and furosemide solid dispersions, respectively.[20,46,47] Where the maximum release rate occurs is related to drug properties.

Unlike MePABA, the dissolution rate for PVP K15 decreased continuously as drug content increased. Even at a 20:1(PVP:MePABA) ratio, K15's dissolution decreased compare to pure K15. Similar results were reported in studies by Corrigan et al. with PEG dispersion.[19,39] In one study with PEG 4000 and bendrofluazide and hydroflumethiazide solid dispersions, polymer intrinsic

dissolution rates decreased as drug loading increased. Also, a slight decrease in PEG 4000 dissolution was observed for a 20:1 polymer:drug solid dispersion.[19] In another of his studies, the authors investigated a 30:1 and 10:1 PEG 4000:barbituric acid and 30:1 and 50:1 PEG 4000:phenobarbitone solid dispersions. They found a polymer dissolution decrease which was clear at quite low drug loadings.[39] In a study by Ji et al., the authors monitored PVP release from PVP K25-indomethacin and PVP K25-naproxen dispersions.[51] They observed that PVP release rate from dispersions decreased compared to that of the pure polymer. Moreover, the reduction in PVP release was more pronounced when drug loading increased.

The MePABA and PVP release rates and ratios are tabulated in Table 5-6. In this table, the assayed ratio between PVP and PABA ester in the samples as well as the intrinsic release rates of polymer and drug are presented. Additionally, the ratio between the intrinsic release rates of PVP and PABA ester is calculated, as well. The term, "% Deviation", is included in this table which is the deviation calculated using Equation 5-2. In this equation, IDR refers to the intrinsic release rate (PVP or PABA ester) and N represents the weight of either of component in solid dispersions. The intrinsic release rates of PVP K15 are shown in the second column in Table 5-6. The intrinsic release rates of MePABA can be found in the third column in the table. Their ratios are calculated and presented in the fourth column. The weight ratios between polymer and drug in dispersions were assayed and shown in the fifth column in Table 5-6. Lastly, the "% Deviation" were calculated and summarized in the last column. Basically, the "% Deviation" shows how much deviation there was in the solid dispersion dissolution under the assumption of congruent release (i.e., dispersion dissolves according to its composition). Thus, the smaller the deviation, the closer system is closer to congruent release. When this deviation is close to zero, both components

(PABA ester and PVP) dissolves simultaneously from solid samples without an excess one component or the other remaining on the surface.

$$\%\ Deviation = \frac{Abs\left(\frac{IDR_{PVP}}{IDR_{PABA}} - \frac{N_{PVP}}{N_{PABA}}\right)}{\frac{N_{PVP}}{N_{PABA}}} \times 100 \qquad \text{Equation 5-2}$$

At the ratios of 20:1, 10:1 and even 6:1 PVP K15-MePABA solid dispersions, the polymer and drug dissolved congruently (i.e., release rate ratio equivalent to their composition ratios). This behavior is evidenced by the small % deviation values. Similar behavior was reported in other solid dispersion studies.[10,19,20,39-41,51] In the SMH study of sulfathiazole and PVP, the drug and polymer released congruently at 20:1, 10: 1 and 5:1 PVP-sulfathiazole ratios.[10,20] In a study of PEG 4000 and bendrofluazide or hydroflumethiazide solid dispersions, Corrigan et al. found that drug and polymer released simultaneously at 20:1 and 10: 1 ratios.[19] In other studies, these authors found congruently release for 30:1 and 50:1 PEG 4000:phenobarbitone solid dispersions.[39,40] Zhou et al. found that both cyclosporine A and TPGS displayed overlapping normalized dissolution profiles for the solid dispersions with up to 15% cyclosporine A loading when dispersed in TPGS.[41] More recently, Ji et al. showed that drug and carrier co-dissolved according their compositions in PVP K25-indomethacine and PVP K25-naproxen dispersions with up to 80% drug loading.[51] At other ratios, as drug loading increased, the % deviation increased. Finally, for a 2:1 dispersion, MePABA's dissolution rate (0.33 mg/cm^2·min) was close to that of pure MePABA (0.28 mg/cm^2·min) which indicates that the presence of PVP had little or no effect on drug release.

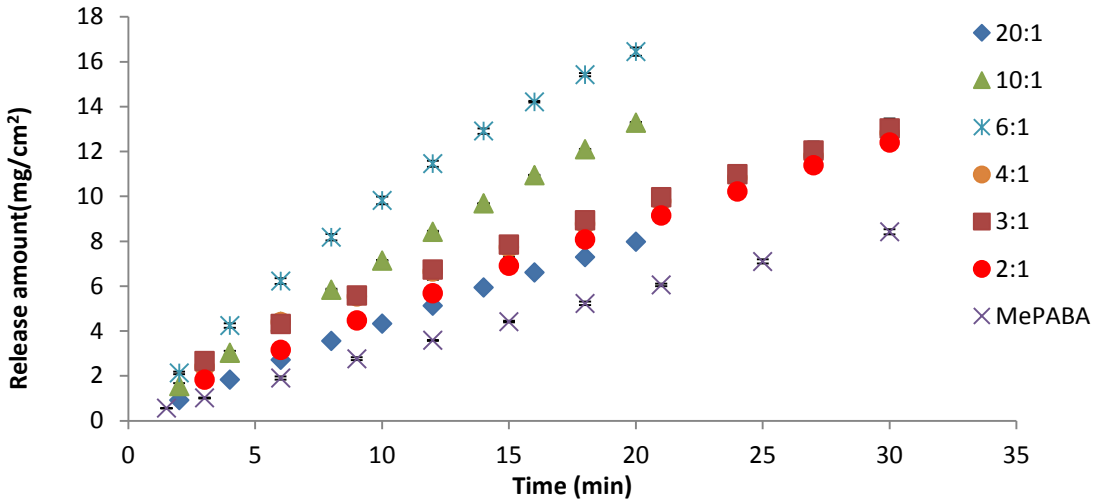

Figure 5-21: Rotating disk intrinsic release profiles of MePABA from PVP K15-MePABA dispersions at 37 ºC at 100 rpm (n=3).

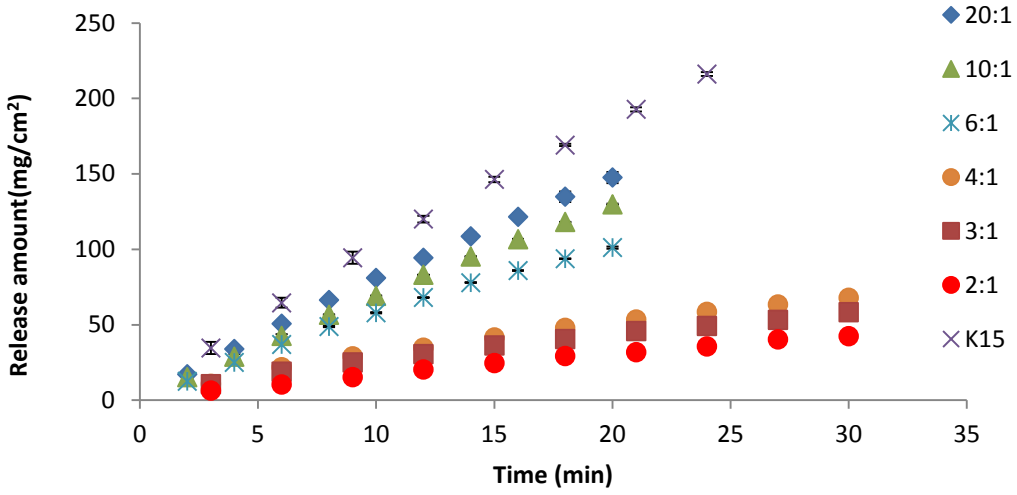

Figure 5-22: Rotating disk intrinsic release profiles of PVP K15 from PVP K15-MePABA dispersions at 37 ºC at 100 rpm (n=3).

Table 5-6: Rotating disk intrinsic release rates of PVP K15-MePABA dispersions at 37 ºC at 100 rpm.

Solid nominal ratio	PVP K15[a] release rate ($mg/cm^2 \cdot min$)	MePABA[a] release rate ($mg/cm^2 \cdot min$)	PVP:PABA ester release rate ratio	Solid dispersion assay ratio	% Deviation
20:1	7.19 (0.998)	0.39 (0.998)	18.4	18.5	0.2
10:1	6.38 (0.999)	0.65 (0.999)	9.80	9.80	0.0
6:1	4.91 (0.993)	0.80 (0.989)	6.1	5.9	4.2
4:1	2.05 (0.995)	0.37 (0.993)	5.5	3.9	41.3
3:1	1.70 (0.994)	0.37 (0.996)	4.6	2.9	60.7
2:1	1.36 (0.992)	0.37 (0.998)	3.7	2.1	72.6

[a.] in parentheses - R^2

5.3.1.2 MePABA-PVP K30 solid dispersions

The release profiles of MePABA and PVP K30 from MePABA-PVP K30 solid dispersions are shown in Figure 5-23 and Figure 5-24. In these figures, the intrinsic dissolution profiles of the treated MePABA and PVP are included as references. Just like the MePABA-PVP K15 dispersions, both the drug and polymer showed nearly linear dissolution profiles. Another similarity between the PVP K15 and PVP K30 dispersions was the polymer release rate vs the solid dispersion composition; a continuous decrease in polymer release as drug loading increased was observed. On the other hand, drug release differed somewhat between these two dispersions. Like PVP K15 dispersions, the drug release rate first increased then decreased as drug loading increased. However, a maximum drug release rate was observed at a 3:1 ratio for PVP K30-MePABA dispersion compared to a 6:1 ratio for PVP K15-MePABA.

The MePABA and PVP K30 release rates and release ratios are summarized in Table 5-7. For high polymer content dispersions (i.e., 20:1, 10:1 and 6:1 PVP:PABA ester), the drug dissolved congruently with the polymer dissolved as evidenced by the small deviation values observed. Unlike K15 dispersions, even for lower polymer content solid dispersions (i.e., 3:1 and 2:1 PVP K30:PABA ester), the % deviation value remained low (< 15%) for K30 dispersions compared to K15 dispersions (~70%). This indicated that PVP K30 and MePABA dissolved nearly congruently. This might be primarily because of the lower release rate of PVP K30 compared to K15. The % deviation did increase constantly as drug loading increased but not as much as with the K15 dispersion systems. Finally, the maximum drug release rate in K30 dispersions was smaller than that in the K15 dispersions. The maximum MePABA release rate in K30 dispersion systems was 0.57 $mg/cm^2 \cdot min$ while the maximum for K15 dispersion systems was 0.8 $mg/cm^2 \cdot min$. This shows that maximum drug release rate is affected by the carrier.

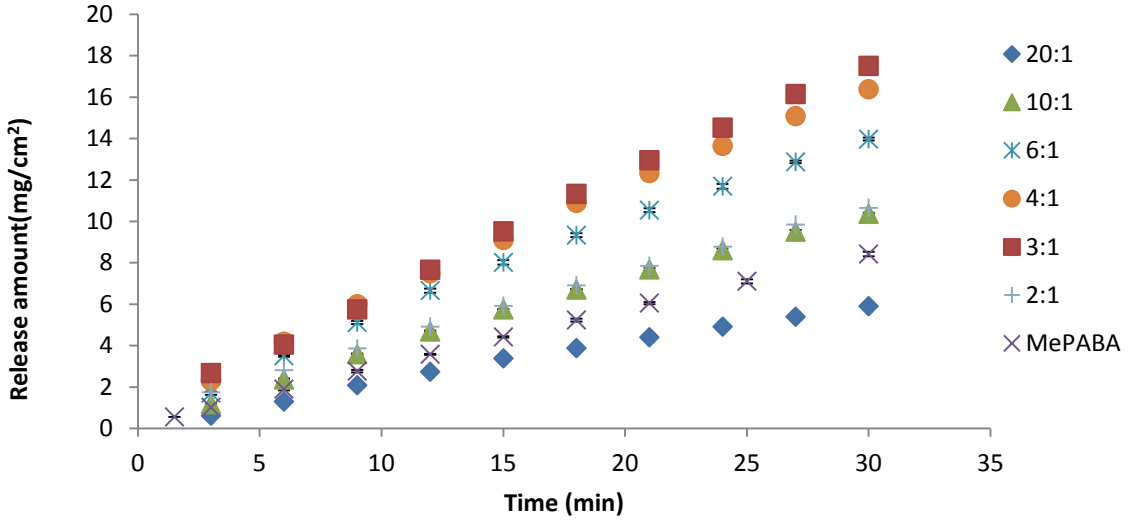

Figure 5-23: Rotating disk intrinsic release profiles of MePABA from PVP K30-MePABA dispersions at 37 ºC at 100rpm (n=3).

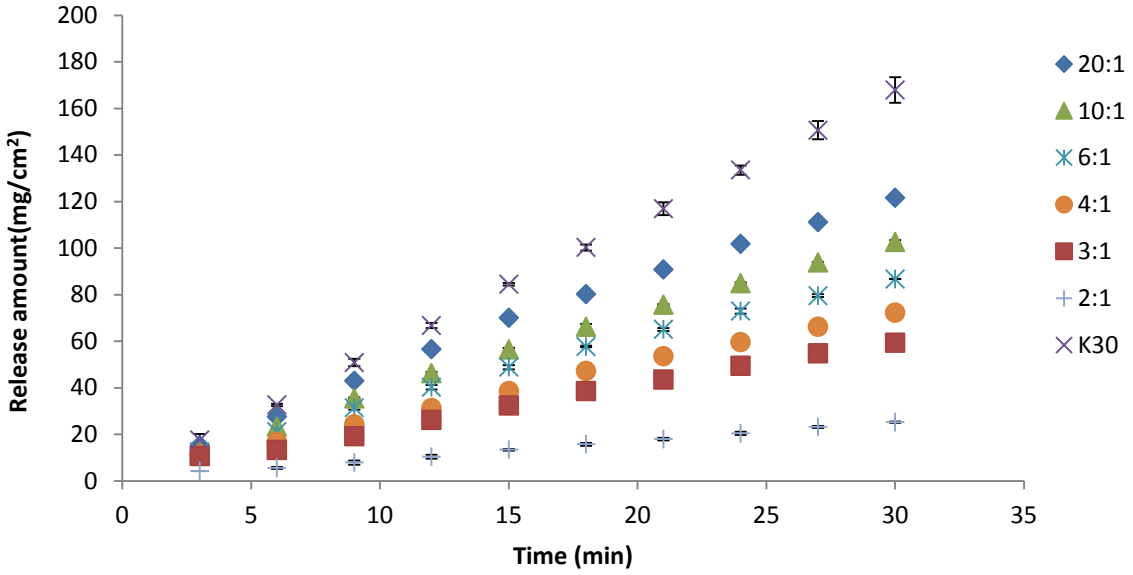

Figure 5-24: Rotating disk intrinsic release profiles of PVP K30 from PVP K30-MePABA dispersions at 37 ºC at 100 rpm (n=3).

Table 5-7: Rotating disk intrinsic release rates of PVP K30-MePABA dispersions at 37 ºC at 100 rpm.

Solid nominal ratio	PVP K30[a] release rate ($mg/cm^2 \cdot min$)	MePABA[a] release rate ($mg/cm^2 \cdot min$)	PVP:PABA ester release rate ratio	Solid dispersion assay ratio	% Deviation
20:1	3.94 (0.994)	0.19 (0.993)	20.7	20.5	1.3
10:1	3.32 (0.998)	0.34 (0.997)	9.8	9.8	0.0
6:1	2.76 (0.997)	0.45 (0.994)	6.1	5.9	4.1
4:1	2.32 (0.998)	0.52 (0.997)	4.5	3.9	14
3:1	1.89 (0.997)	0.57 (0.999)	3.3	2.9	16
2:1	0.81 (0.999)	0.33 (0.999)	2.5	2.1	15

[a.] in parentheses - R^2

5.3.1.3 MePABA-PVP K90 solid dispersions

The release profiles of MePABA and PVP K90 from MePABA-PVP K90 solid dispersions are shown in Figure 5-25 and Figure 5-26. The intrinsic dissolution profiles of treated MePABA and PVP K90 are included as references. There are some similarities but also differences between K90 dispersions and K15 and K30 dispersions. Firstly, both drug and polymer showed nearly linear release profiles for K90 dispersions which is similar to K15 and K30 dispersions. Another similarity is the polymer release rate vs the solid dispersion composition. Like K15 and K30 dispersions, a constant decrease in PVP K90 release was observed as drug loading increased. However, the decrease in polymer release for K90 dispersions was not as large as with the other two PVP dispersions. For example, K90's release rate dropped to ~ 50% of that of the pure polymer for a 2:1 solid dispersion; K15 and K30 release rate dropped to ~ 15% of that of the pure polymer

for the same ratio. Another difference is drug release rate vs the solid dispersion composition. In both K15 and the K30 dispersions, drug release rate first increased then decreased as drug loading increased. While for K90 dispersions, drug release rate increased constantly as drug loading increased. Thus, a maximum drug dissolution rate was observed at a 2:1 PVP K90-MePABA system. This was different than either the PVP K15 dispersion systems or the PVP K30 dispersion systems. This is probably because K90 retards drug release rather than increasing it due to its high viscosity and low dissolution rate.

MePABA and PVP K90 release rates and ratios are summarized in Table 5-8. Similar to K15 and K30 dispersions, drug dissolved congruently with polymer for 20:1, 10: 1 and 6:1 (polymer:drug) dispersions. % Deviation increased constantly as more drug was incorporated into the dispersions. A similar trend was also observed in PVP K15 and K30 dispersions. However the % deviation in K90 dispersions was not as large as in K15 dispersions; it was comparable to the K30 dispersions though. For example, the % deviation value was ~70% for a K15 dispersion, ~15% for a K30 dispersion and ~30% for a K90 dispersion at 2:1 PVP-MePABA ratio. This might be related to the fact that K30's and K90'slower dissolution rates and their higher viscosity compared to K15. Lastly, a maximum dissolution rate in the K90 dispersion was 0.20 mg/cm^2·min. which is lower than that in the K30 systems and in the K15 systems (0.57 mg/cm^2·min and 0.80 mg/cm^2·min, respectively). Another interesting observation is that the maximum drug release rate from any K90 dispersion was smaller than that of the pure drug. Thus, solid dispersion did not enhance drug intrinsic release rates with PVP K90. This is probably due to K90's higher viscosity and lower overall release rate compared to lower MW PVPs.

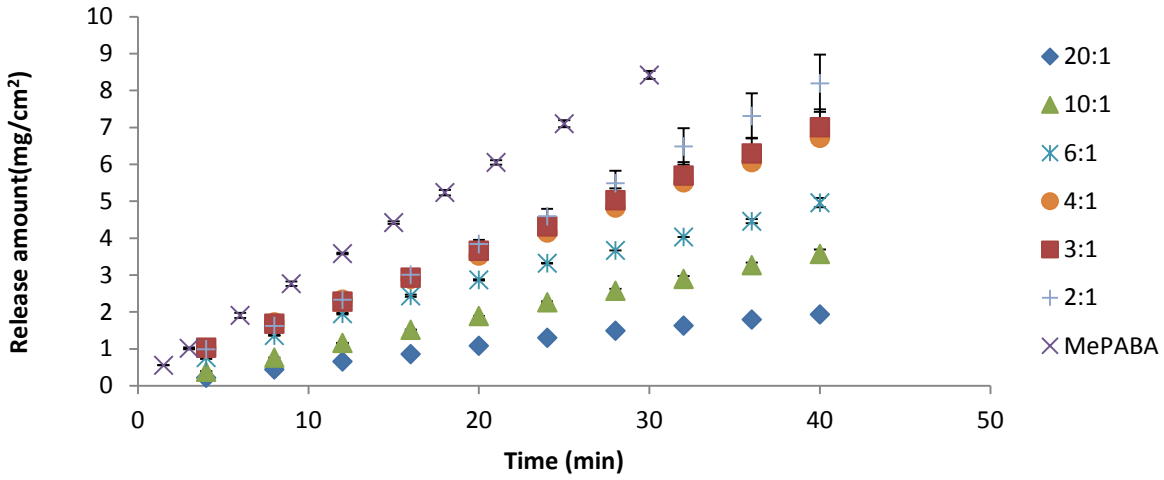

Figure 5-25: Rotating disk intrinsic release profiles of MePABA from PVP K90-MePABA dispersions at 37 ºC at 100 rpm (n=3).

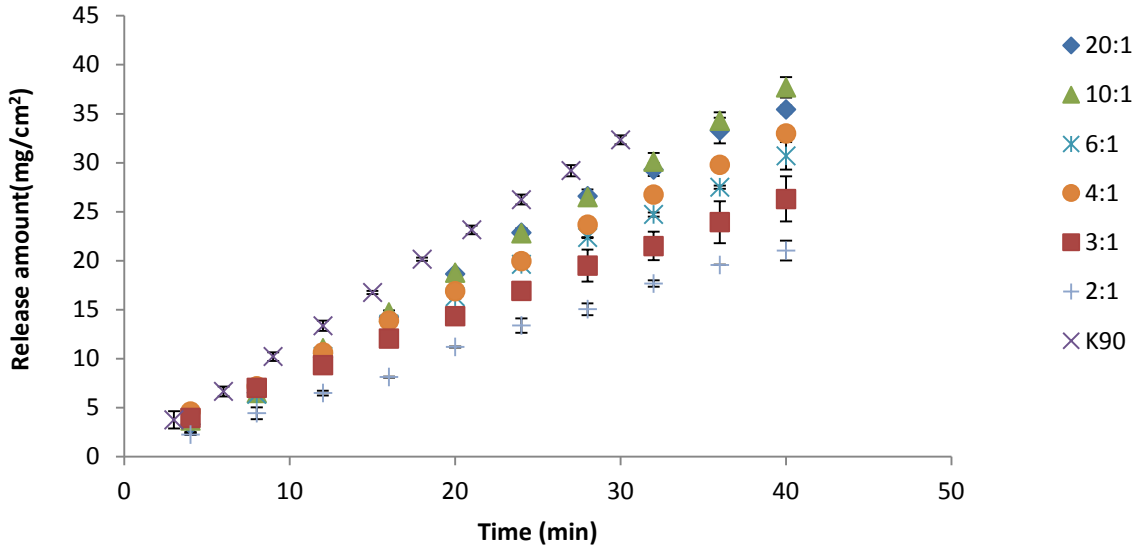

Figure 5-26: Rotating disk intrinsic release profiles of PVP K90 from PVP K90-MePABA dispersions at 37 ºC at 100 rpm (n=3).

Table 5-8: Rotating disk intrinsic release rates of PVP K90-MePABA dispersions at 37 ºC at 100 rpm.

Solid nominal ratio	PVP K90[a] release rate ($mg/cm^2 \cdot min$)	MePABA[a] release rate ($mg/cm^2 \cdot min$)	PVP:PABA ester release rate ratio	Solid dispersion assay ratio	% Deviation
20:1	0.93 (0.996)	0.048 (0.994)	19.4	20.6	5.8
10:1	0.96 (0.999)	0.088 (0.999)	10.9	10.3	6.0
6:1	0.74 (0.998)	0.11 (0.993)	6.7	6.3	6.1
4:1	0.80 (0.999)	0.16 (0.999)	5.0	4.1	22.3
3:1	0.61 (0.999)	0.17 (0.999)	3.6	2.9	25.5
2:1	0.55 (0.996)	0.20 (0.996)	2.8	2.1	32.8

[a.] in parentheses - R^2

5.3.2 EtPABA-PVP solid dispersions

5.3.2.1 EtPABA-PVP K15 solid dispersions

The release profiles of EtPABA and PVP K15 from solid dispersions are shown in Figure 5-27 and Figure 5-28. Their release rates and ratios are summarized in Table 5-9. Overall, PVP showed nearly linear dissolution profiles for all the dispersions studied. Most EtPABA dissolution profiles were linear, as well, except for a 4:1 PVP:PABA ester dispersion. At this ratio, EtPABA showed a biphasic dissolution profile (i.e., initially faster then slower). The terminal dissolution profile had a slope of 0.2 $mg/cm^2 \cdot min$ which was equivalent to that of the pure drug. This behavior might indicate that drug precipitated in the first few minutes on the tablet surface during dissolution. Similar to the MePABA-K15 dispersions, EtPABA release also first increased then decreased as drug loading increased. However, the drug release rate never decreased to that of the pure drug as in the MePABA-K15 dispersions. On the contrary, the drug release rate decreased to that of the

pure drug for 4:1, 3:1 and 2:1 PVP:EtPABA dispersions which suggested amorphous EtPABA quickly converted into its crystalline form in those systems during dissolution. A maximum EtPABA release rate was observed at a 10:1 polymer:drug ratio which was different than MePABA:PVP K15 dispersions where the maximum drug release rate was observed at a 6:1 polymer:drug ratio. However, the maximum dissolution rate appearing at different compositions for different drugs with the same carrier is not unique. Dubois et al. reported the dissolution rate of ten different drugs in PEG 6000 dispersions using a rotation disc method. The results showed that the maximum drug dissolution occurred at various drug loadings with the same PEG carrier.[42] It seems that where maximum drug release occurs is related to the drug properties in dispersions.

Polymer release between MePABA and EtPABA systems are very similar. The polymer dissolution rate decreased continuously as EtPABA was incorporated into the dispersion. At a 2:1 ratio (PVP:EtPABA), the polymer dissolution rate dropped to ~15% of that of the pure polymer. Similarly, the polymer dissolution rate also decreased to ~15% of that of the pure polymer for a 2:1 PVP:MePABA dispersion. This might be related to the structure similarity between the two PABA esters.

As shown in Table 5-9, drug dissolved congruently with polymer for 20:1 and 10:1 PVP K15-EtPABA dispersions as with PVP K15-MePABA dispersions. Also similar to the MePABA dispersion systems, the % deviation increased continuously with increasing of drug loading.

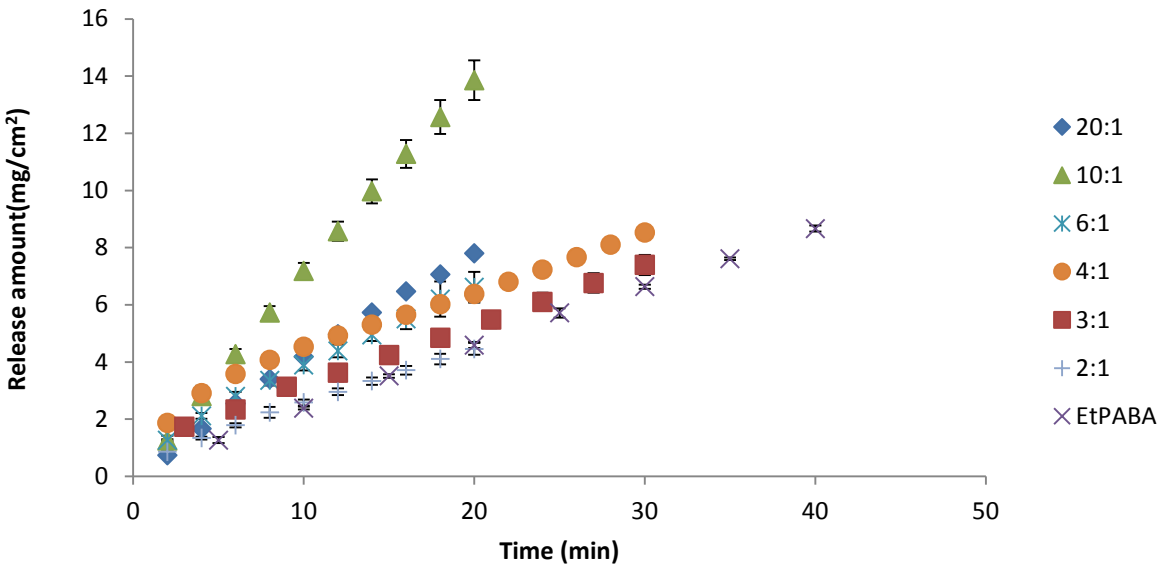

Figure 5-27: Rotating disk intrinsic release profiles of EtPABA from PVP K15-EtPABA dispersions at 37 ºC at 100 rpm (n=3).

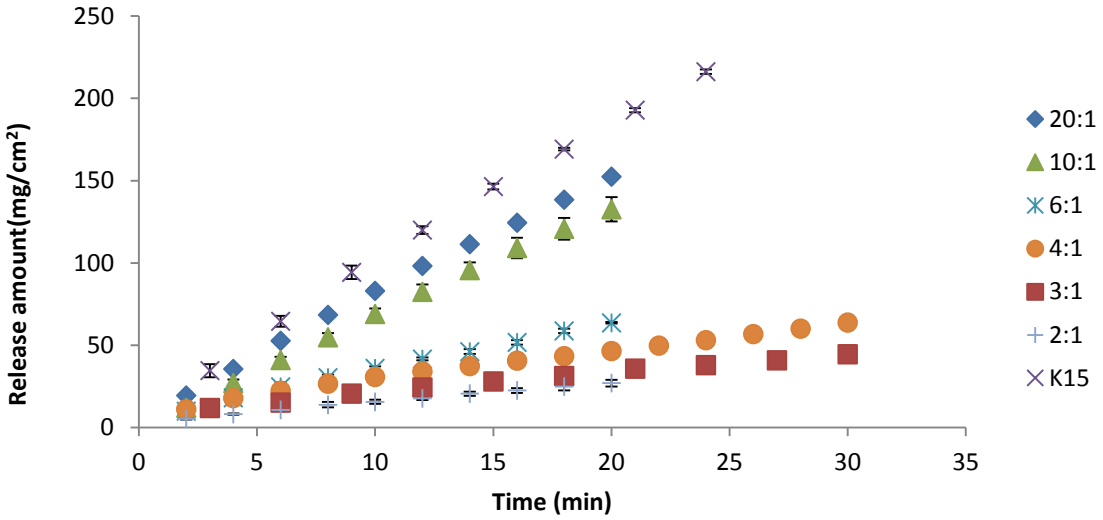

Figure 5-28: Rotating disk intrinsic release profiles of PVP K15 from PVP K15-EtPABA dispersions at 37 ºC at 100 rpm (n=3).

Table 5-9: Rotating disk intrinsic release rates of PVP K15-EtPABA dispersions at 37 ºC at 100 rpm.

Solid nominal ratio	PVP K15[a] release rate ($mg/cm^2 \cdot min$)	EtPABA[a] release rate ($mg/cm^2 \cdot min$)	PVP:PABA ester release rate ratio	Solid dispersion assay ratio	% Deviation
20:1	7.33 (0.998)	0.39 (0.997)	18.8	18.8	0.0
10:1	6.71 (0.999)	0.70 (0.999)	9.6	9.5	0.6
6:1	2.89 (0.997)	0.29 (0.996)	10.0	6.0	66.9
4:1	2.81 (0.988)[c] 1.87 (0.993)[b]	0.43 (0.984)[c] 0.20 (0.998)[b]	7.9	4.0	96.7
3:1	1.21 (0.994)	0.21 (0.9994)	5.8	2.9	99.4
2:1	1.19 (0.998)	0.20 (0.998)	6.0	2.1	183.3

[a.] in parentheses - R^2
[b.] terminal phase slope
[c.] initial phase slope

5.3.2.2 EtPABA-PVP K30 solid dispersions

The release profiles of EtPABA and PVP K30 from solid dispersions are shown in Figure 5-29 and Figure 5-30. Most of the EtPABA release profiles were linear except for a 4:1 PVP:PABA ester dispersion. At this ratio, EtPABA showed a biphasic dissolution profile which was similar to the 4: 1 PVP K15-EtPABA dispersion. The drug terminal dissolution profile also had a slope of 0.2 $mg/cm^2 \cdot min$ which was equivalent to that of the pure drug. Like EtPABA-K15 systems, drug release rate from solid dispersions also first increased then decreased as drug loading increased in K30 solid dispersions. A maximum EtPABA dissolution rate was observed at a 6:1 polymer:drug ratio. Drug dissolution rate decreased to that of the pure drug in 4:1, 3:1 and 2:1 PVP:EtPABA dispersions. This may suggest that EtPABA quickly converted from the amorphous form to its original form during dissolution.

Polymer release between the MePABA systems and the EtPABA systems are very consistent which might be related to the similar structure between these two compounds. PVP showed nearly linear dissolution profiles for all PVP K30 dispersions. PVP release decreased continuously as drug loading increased. For a 2:1 PVP:EtPABA dispersion, the polymer release rate dropped to ~15% of that of the pure polymer.

The release rates and ratios of PVP K30 and EtPABA are summarized in Table 5-10. As shown in the table, drug dissolved congruently with polymer, which occurred to 20:1, 10:1 and 6:1 PVP K30-EtPABA dispersions. Similar to other dispersion systems, the % deviation increased constantly as drug loading increased.

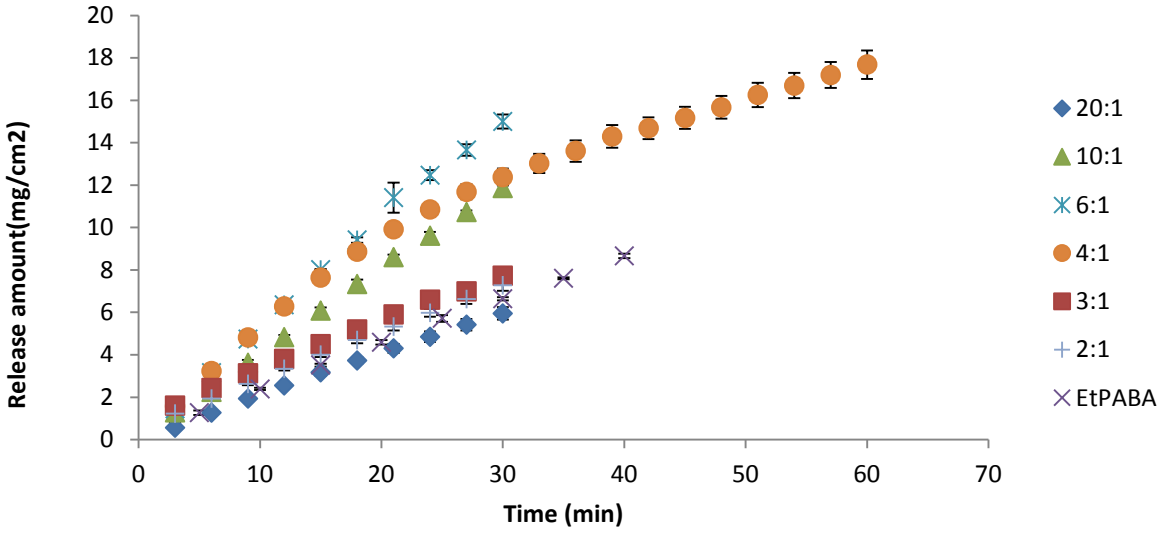

Figure 5-29: Rotating disk intrinsic release profiles of EtPABA from PVP K30-EtPABA dispersions at 37 ºC at 100 rpm (n=3).

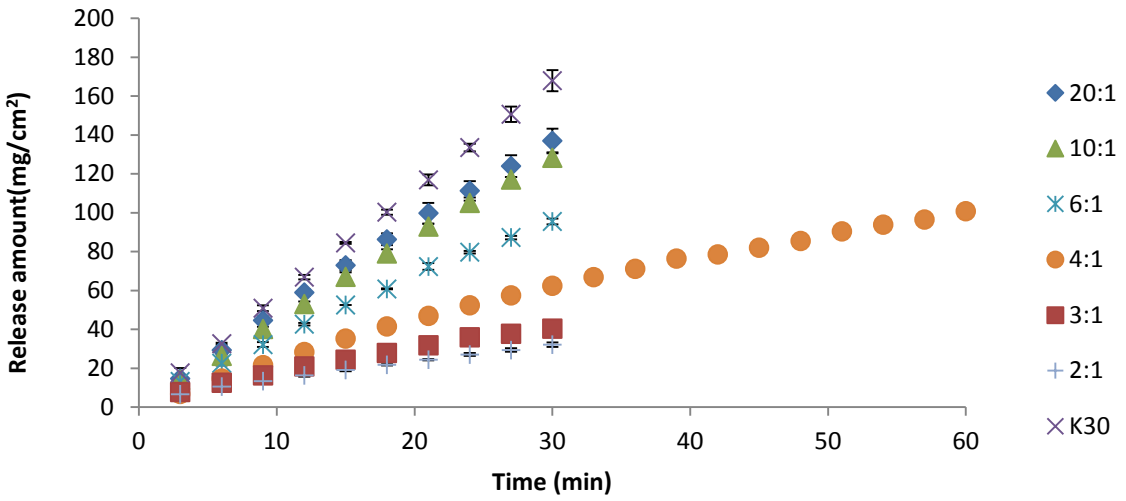

Figure 5-30: Rotating disk intrinsic release profiles of PVP K30 from PVP K30-EtPABA dispersions at 37 ºC at 100 rpm (n=3).

Table 5-10: Rotating disk intrinsic release rates of PVP K30-EtPABA dispersions at 37 ºC at 100 rpm.

Solid nominal ratio	PVP K30[a] Release rate (mg/cm^2·min)	EtPABA[a] release rate (mg/cm^2·min)	PVP:PABA ester release rate ratio	Solid dispersion assay ratio	% Deviation
20:1	4.51 (0.998)	0.20 (0.998)	21.6	20.6	4.4
10:1	4.28 (0.999)	0.40 (0.999)	10.7	10.3	4.0
6:1	3..09 (0.998)	0.51 (0.997)	6.1	6.0	1.5
4:1	2.19 (0.998)[c] 1.26 (0.995)[b]	0.49 (0.997)[c] 0.20 (0.999)[b]	6.3	4.2	50.0
3:1	1.22 (0.992)	0.22 (0.997)	5.6	2.9	91.9
2:1	0.92 (0.999)	0.22 (0.999)	4.2	2.2	93.7

[a] in parentheses - R^2
[b] terminal phase slope
[c] initial phase slope

5.3.2.3 EtPABA-PVP K90 solid dispersions

The release profiles of EtPABA and PVP K90 from EtPABA-PVP K90 solid dispersions are shown in Figure 5-31 and Figure 5-32. Both drug and polymer showed nearly linear release profiles. This is different than EtPABA-K15 and EtPABA-K30 dispersions but similar to MePABA-K90 dispersions. Higher molecular weight PVP might slow drug precipitations during dissolution because of its high viscosity. That would explain why no biphasic release profiles were observed in K90 dispersions. Like other dispersions, a continuous decrease in PVP K90 release was observed as drug loading increased. The decrease in polymer release was not as large in K90 dispersions as in the lower molecular weight dispersions, i.e., PVP K15-EtPABA and K30-EtPABA systems. But it was similar to that of the MePABA-K90 solid dispersions. For example, no obvious decrease in polymer release was observed for 20:1 and 10:1 solid dispersions. For a 2:1 solid dispersion, K90 release rate dropped to ~ 50% of that of the pure polymer.

In both EtPABA-K15 and the EtPABA-K30 dispersions, drug release rate first increased then decreased as drug loading increased. In K90 dispersions, drug release rate increased continuously as drug loading increased. Thus, a maximum drug dissolution rate was observed at a 2:1 PVP K90-EtPABA dispersion. This is similar to PVP K90-MePABA dispersions.

The EtPABA and PVP K90 release rates and ratios are summarized in Table 5-11. For 20:1 10: 1 and 6:1 PVP K90:EtPABA dispersions, drug dissolved congruently with polymer. The % deviation increased constantly as drug loading increased. However, the % deviation was not as large as for EtPABA-PVP K15 and EtPABA-K30 dispersions. For example, a ~30% deviation in K90 system was observed for a 2:1 PVP-EtPABA solid dispersion, which was significant lower than what was observed in K15 and K30 systems for the same ratio. Similar to what occurred to the MePABA–PVP K90 dispersions, the maximum dissolution rate in the EtPABA-PVP K90

dispersion was lower than that of the pure drug. Thus, solid dispersion did not enhance both MePABA and EtPABA intrinsic dissolution rate in K90 dispersions.

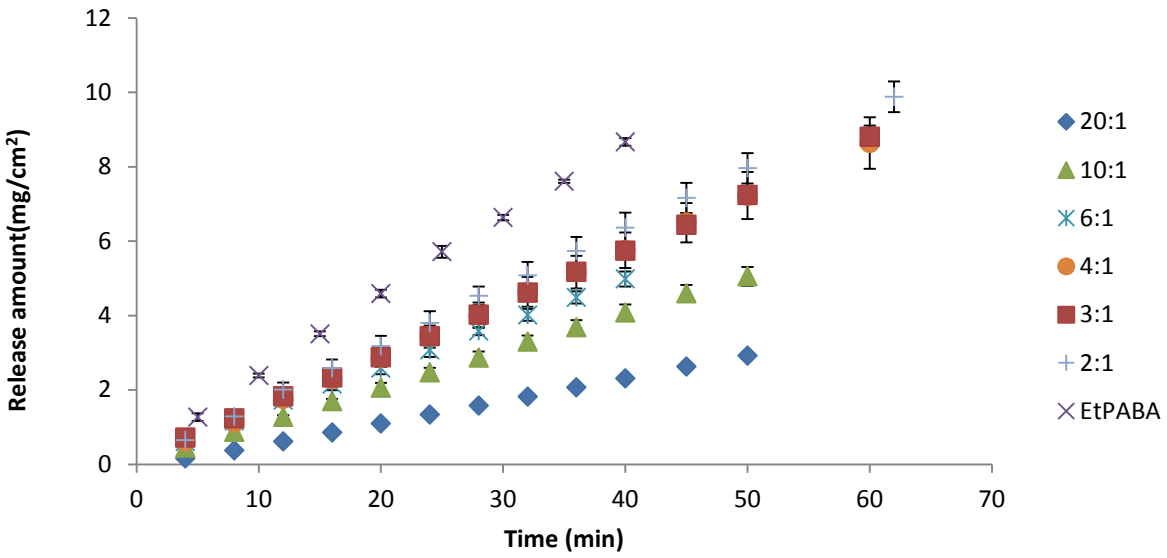

Figure 5-31: Rotating disk intrinsic release profiles of EtPABA from PVP K90-EtPABA dispersions at 37 ºC at 100 rpm (n=3).

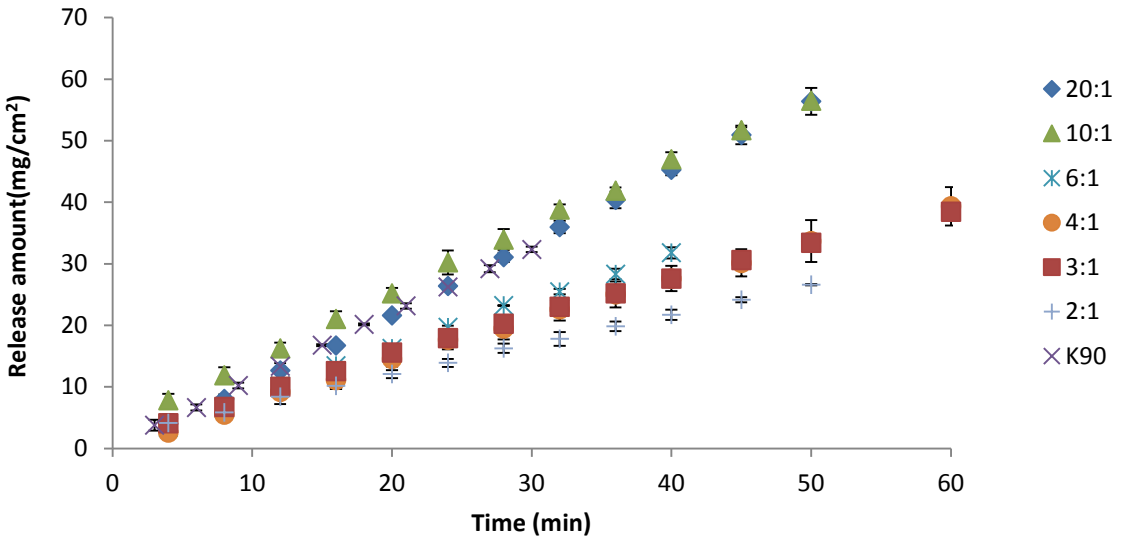

Figure 5-32: Rotating disk intrinsic release profiles of PVP K90 from PVP K90-EtPABA dispersions at 37 ºC at 100 rpm (n=3).

Table 5-11: Rotating disk intrinsic release rates of PVP K90-EtPABA dispersions at 37 ºC at 100 rpm.

Solid nominal ratio	PVP K90[a] release rate (mg/cm^2·min)	EtPABA[a] release rate (mg/cm^2·min)	PVP:PABA ester release rate ratio	Solid dispersion assay ratio	% Deviation
20:1	1.16 (0.999)	0.06 (0.999)	19.3	19.0	1.7
10:1	1.07 (0.999)	0.10 (0.999)	10.7	10.4	2.9
6:1	0.79 (0.998)	0.12 (0.999)	6.6	6.6	0.0
4:1	0.66 (0.997)	0.14 (0.999)	4.7	4.0	18.2
3:1	0.62 (0.999)	0.15 (0.999)	4.1	3.2	29.2
2:1	0.48 (0.999)	0.16 (0.999)	3.0	2.2	38.3

[a] in parentheses - R^2

5.3.3 PrPABA-PVP solid dispersions

5.3.3.1 PrPABA-PVP K15 sold dispersions

The release profiles of PrPABA and PVP K15 from the solid dispersions are shown in Figure 5-33 and Figure 5-34. Their release rates and ratios are summarized in Table 5-12. Overall, the PVP had nearly linear dissolution profiles for all dispersions. Contrastingly, PrPABA dissolution profiles showed non-linearity. Biphasic dissolution profiles were observed for 6:1, 4:1 and 3:1 dispersions which might be related to lower solubility of PrPABA (i.e., lower solubility higher precipitation probability). As seen in Table 5-12, the terminal dissolution profile of the drug in these ratios was closer and closer to that of the pure PrPABA dissolution (0.09 $mg/cm^2 \cdot min$) as drug loading increased. For a 2:1 dispersion, drug dissolution rate was equivalent to that of the pure drug. This might suggest more and more drug precipitated on the tablet surface during dissolution as drug loading increased. Like other PVP K15 systems, the PrPABA release rate from solid dispersions also first increased then decreased as drug loading increased. When drug loading was high enough, the drug dissolution rate decreased to that of the pure drug.

Polymer dissolution behaved consistently among all the dispersions. Like what occurred in the other PVP K15 dispersions, polymer release decreased continuously as drug loading increased. For a 2:1 PVP:PrPABA dispersion, the polymer dissolution rate dropped to ~15% of that of the pure polymer. Similar decrease was observed in a 2:1 PVP K15-MePABA and PVP K15-EtPABA dispersions. This behavior might be related to the structure similarities among all the PABA esters.

As shown in Table 5-12, congruently release only occurred to a 20:1 PVP K15-PrPABA solid dispersions. Elsewhere, the % deviation increased constantly as drug loading increased. The deviations were also significantly higher than that in the PVP K15-MePABA and PVP K15-EtPABA systems. This behavior might be related to PrPABA precipitations.

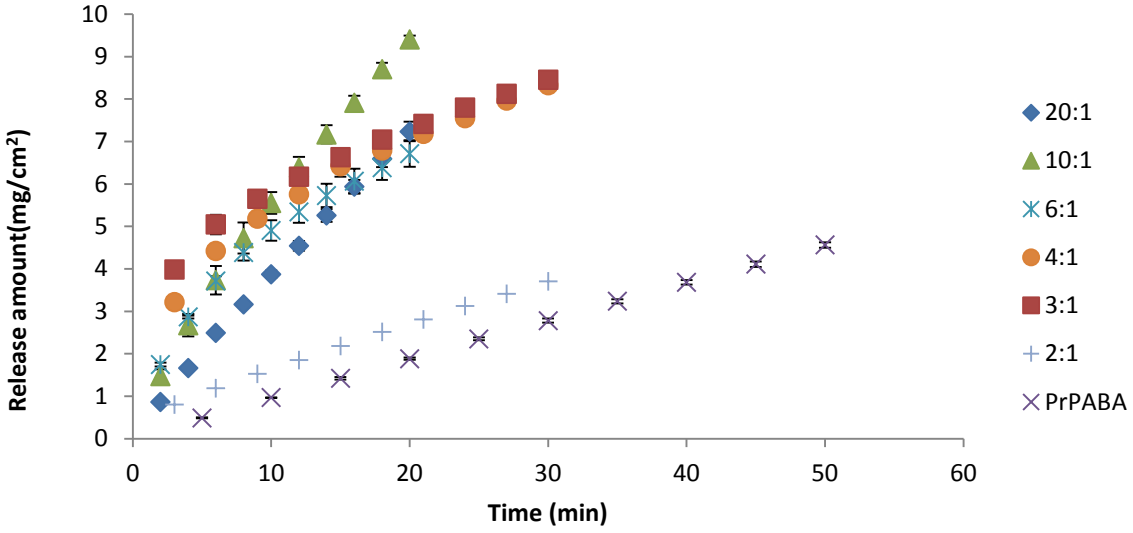

Figure 5-33: Rotating disk intrinsic release profiles of PrPABA from PVP K15-PrPABA dispersions at 37 ºC at 100 rpm (n=3).

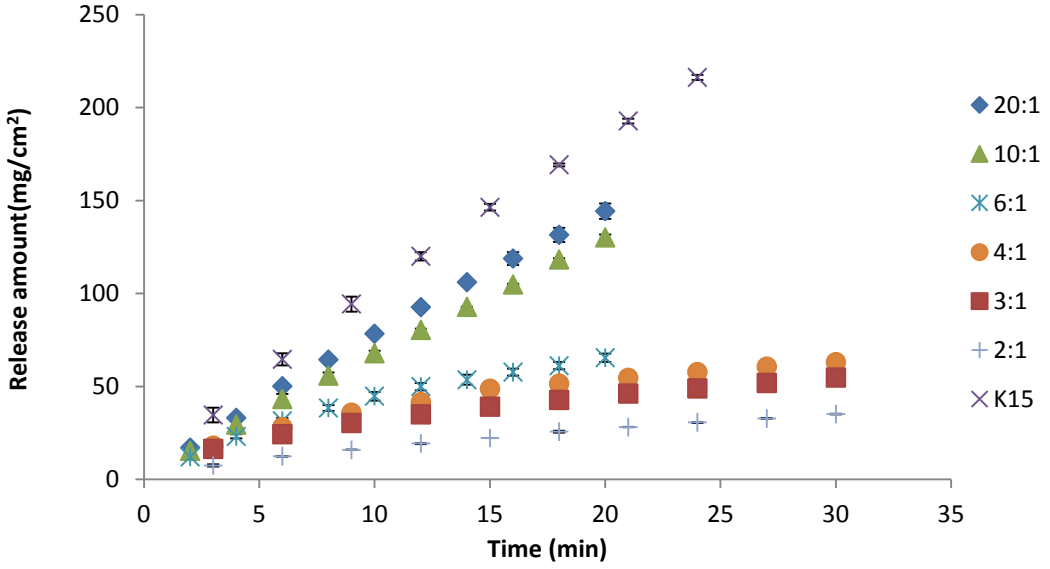

Figure 5-34: Rotating disk intrinsic release profiles of PVP K15 from PVP K15-PrPABA dispersions at 37 ºC at 100 rpm (n=3).

Table 5-12: Rotating disk intrinsic release rates of PVP K15-PrPABA dispersions at 37 ºC at 100 rpm.

Solid nominal ratio	PVP K15[a] release rate ($mg/cm^2 \cdot min$)	PrPABA[a] release rate ($mg/cm^2 \cdot min$)	PVP:PABA ester release rate ratio	Solid dispersion assay ratio	% Deviation
20:1	7.02 (0.998)	0.35 (0.999)	20.1	20.1	0
10:1	6.32 (0.999)	0.43 (0.993)	14.7	9.8	50.0
	4.83 (0.993)[c]	0.49(0.994)[c]			
6:1	1.87(0.999)[b]	0.17 (0.999)[b]	11.0	6.0	83.3
	2.92 (0.995)[c]	0.33 (0.983)[c]			
4:1	0.97 (0.999)[b]	0.13 (0.999)[b]	7.5	3.9	92.3
	2.32 (0.993)[c]	0.28 (0.976)[c]			
3:1	1.03 (0.998)[b]	0.12 (0.999)[b]	8.6	2.9	196.6
2:1	1.19 (0.998)	0.10 (0.999)	12	2.1	471.4

[a] in parentheses - R^2
[b] terminal phase slope
[c] initial phase slope

5.3.3.2 PrPABA-PVP K30 sold dispersions

The release profiles of PrPABA and PVP K30 from the dispersions are shown in

Figure 5-35 and Figure 5-36. Their release rates and ratios are summarized in Table 5-13. Overall, both the PVP and PrPABA showed nearly linear dissolution profiles. Like other dispersion systems, polymer dissolution rate decreased constantly as drug loading increased. On the other hand, drug dissolution first increased then decreased as drug loading increased. A maximum drug release was observed at a 6:1 polymer:drug ratio. When drug loading increased (i.e., 3:1 and 2:1 polymer:drug), PrPABA release was essentially equal to that of the pure drug. This probably implies drug precipitated quickly on the tablet surface. At low drug loadings (20:1 and 10:1 polymer:drug), the deviation was small indicating PVP K30 and PrPABA dissolved congruently. As drug loading increased, the deviation increased as well.

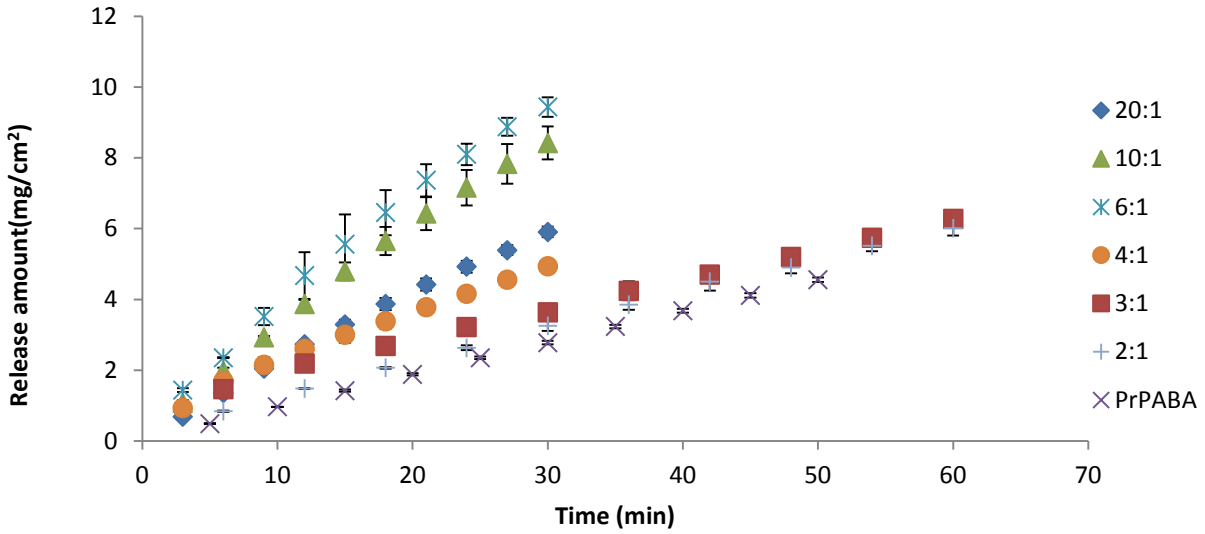

Figure 5-35: Rotating disk intrinsic release profiles of PrPABA from PVP K30-PrPABA dispersions at 37 ºC at 100 rpm (n=3).

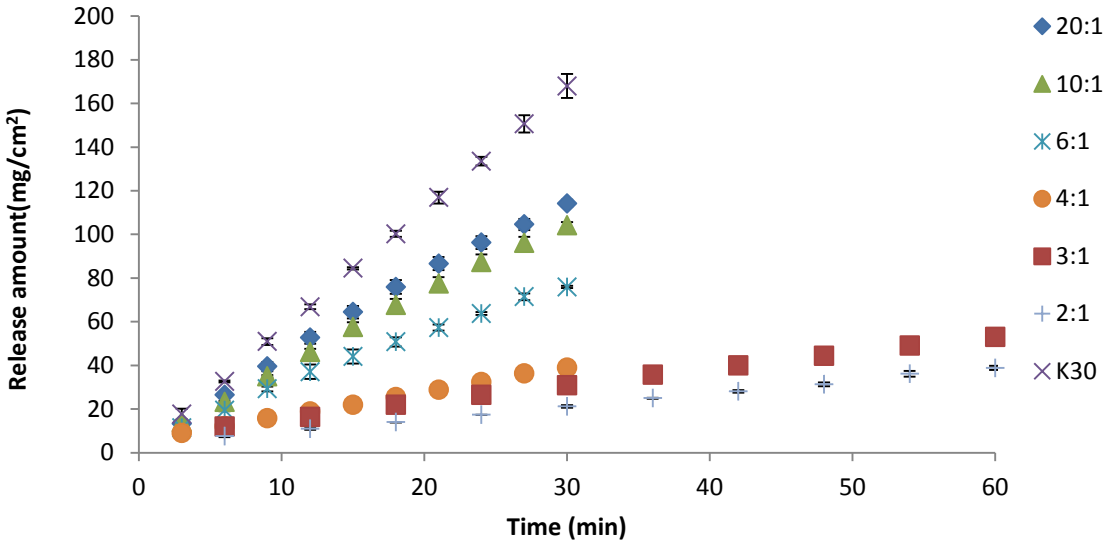

Figure 5-36: Rotating disk intrinsic release profiles PVP K30 from PVP K30-PrPABA dispersions at 37 ºC at 100 rpm (n=3).

Table 5-13: Rotating disk intrinsic release rates of PVP K30-PrPABA dispersions at 37 ºC at 100 rpm.

Solid nominal ratio	PVP K30[a] release rate ($mg/cm^2 \cdot min$)	PrPABA[a] release rate ($mg/cm^2 \cdot min$)	PVP:PABA ester release rate ratio	Solid dispersion assay ratio	% Deviation
20:1	3.74 (0.994)	0.19 (0.996)	19.7	19.6	0.6
10:1	3.41 (0.998)	0.29 (0.995)	11.8	10.7	9.5
6:1	2.40 (0.995)	0.30 (0.992)	8.0	6.3	26.6
4:1	1.11 (0.998)	0.14 (0.991)	7.9	4.3	85.6
3:1	0.76 (0.999)	0.09 (0.999)	8.8	3.1	183.3
2:1	0.59 (0.997)	0.10 (0.999)	6.2	2.1	192.7

[a] in parentheses - R^2

5.3.3.3 PrPABA-PVP K90 sold dispersions

The release profiles of PrPABA and PVP K90 from the dispersion systems are shown in Figure 5-37 and Figure 5-38. Their release rates and ratios are summarized in Table 5-14. The results are very similar to MePABA-K90 and EtPABA-K90 dispersions. Overall, both drug and polymer showed nearly linear dissolution profiles. Like other systems, polymer release decreased continuously as drug loading increased. However, the decrease was not large as what occurred with lower molecular weight polymer dispersions. The drug release increased as drug loading increased. A maximum drug dissolution was equivalent to that of the pure drug. At low drug loading, drug and polymer dissolved congruently and the % deviation was quite small. When drug loading increased, the % deviation increased too.

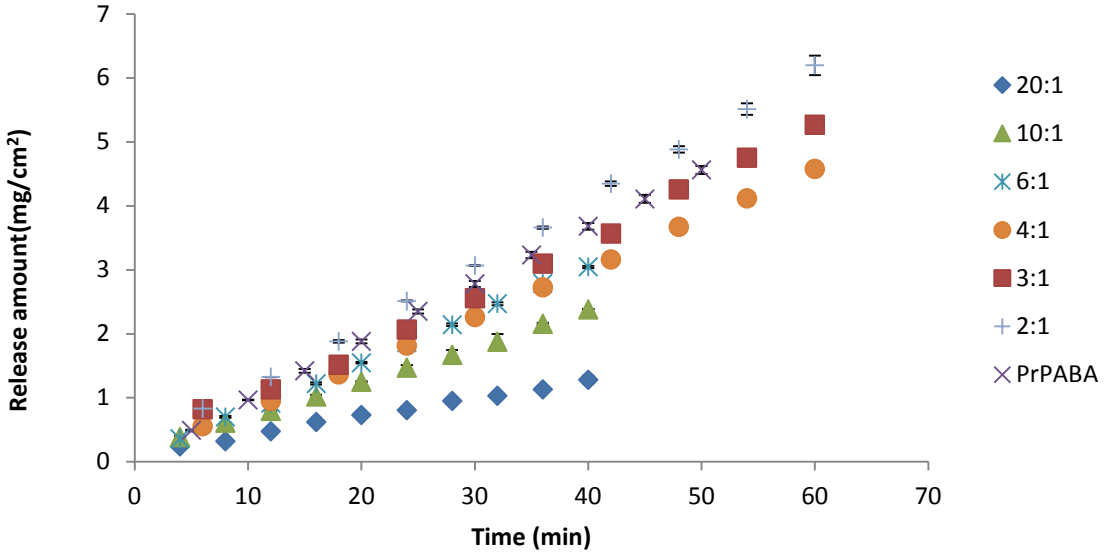

Figure 5-37: Rotating disk intrinsic release profiles of PrPABA from PVP K90-PrPABA dispersions at 37 ºC at 100 rpm (n=3).

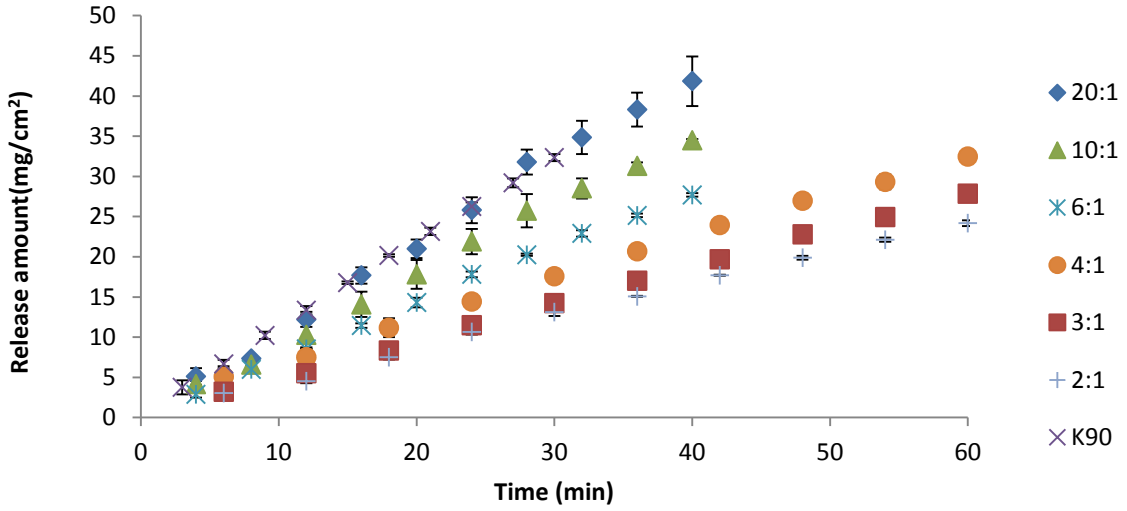

Figure 5-38: Rotating disk intrinsic release profiles of PVP K90 from PVP K90-PrPABA dispersions at 37 ºC at 100 rpm (n=3).

Table 5-14: Rotating disk intrinsic release rates of PVP K90-PrPABA dispersions at 37 ºC at 100 rpm.

Solid nominal ratio	PVP K90[a] release rate ($mg/cm^2 \cdot min$)	PrPABA[a] release rate ($mg/cm^2 \cdot min$)	PVP:PABA ester release rate ratio	Solid dispersion assay ratio	% Deviation
20:1	1.07 (0.995)	0.03 (0.996)	36.9	36.1	2.3
10:1	0.87 (0.997)	0.06 (0.999)	15.8	15.8	0.0
6:1	0.70 (0.998)	0.08 (0.999)	9.3	6.6	41.2
4:1	0.52 (0.999)	0.08 (0.999)	6.9	3.9	78.7
3:1	0.46 (0.999)	0.09 (0.995)	5.4	2.9	85.3
2:1	0.59 (0.997)	0.10 (0.999)	5.9	2.1	177.0

[a] in parentheses - R^2

5.3.4 BuPABA-PVP solid dispersions

5.3.4.1 BuPABA-PVP K15 solid dispersions

Precipitation was observed on the dissolution rotating disc surface for a 4:1 PVP K15:BuPABA dispersion (Figure 5-39). Similar behavior was observed in a rotating disc dissolution study of haloperidol salt forms.[76] The dissolution surface area changes for such formulations which may account for large variations in the dissolution results.

The dissolution profiles of BuPABA and PVP K15 from the dispersions are shown in Figure 5-40 and Figure 5-41. Their dissolution rates are summarized in Table 5-15. For the most part, the BuPABA dispersions were similar like to other PABA ester-PVP K15 dispersions. As drug loading increased, polymer dissolution rate decreased. The drug intrinsic dissolution rate, on the other hand, first increased then decreased as more drug was incorporated into the dispersion. When drug

loading was low, the drug and polymer dissolved simultaneously. As the drug loading increased, deviations from congruent release became larger.

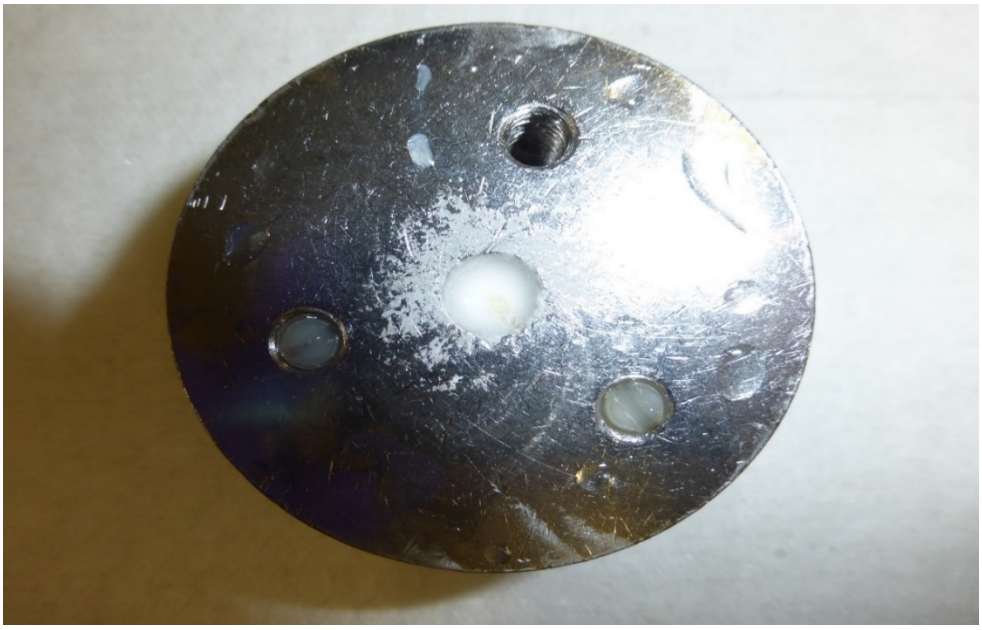

Figure 5-39: Precipitation of BuPABA on rotating disc surface for a 4:1 PVP K15:BuPABA dispersion.

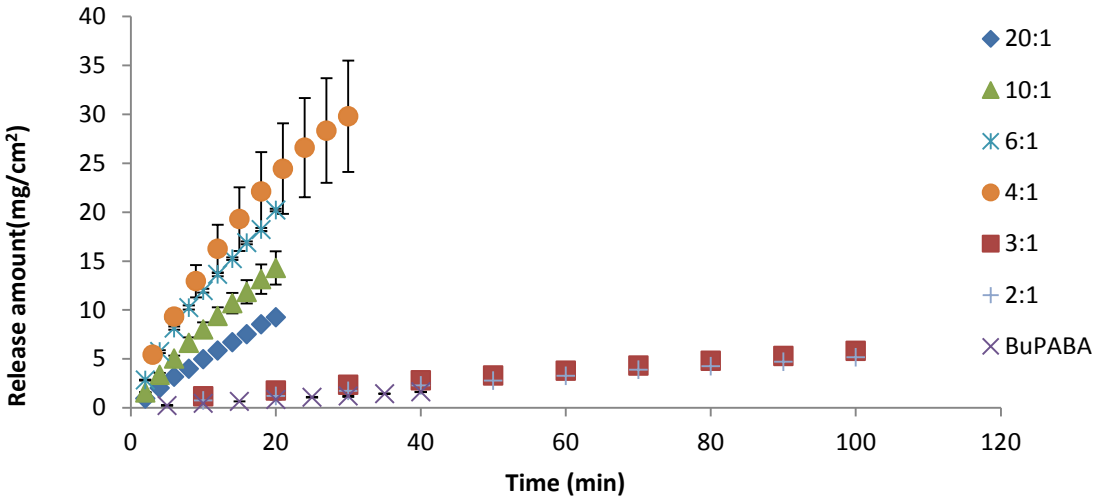

Figure 5-40: Rotating disk intrinsic release profiles of BuPABA from PVP K15-BuPABA dispersions at 37 ºC at 100 rpm (n=3).

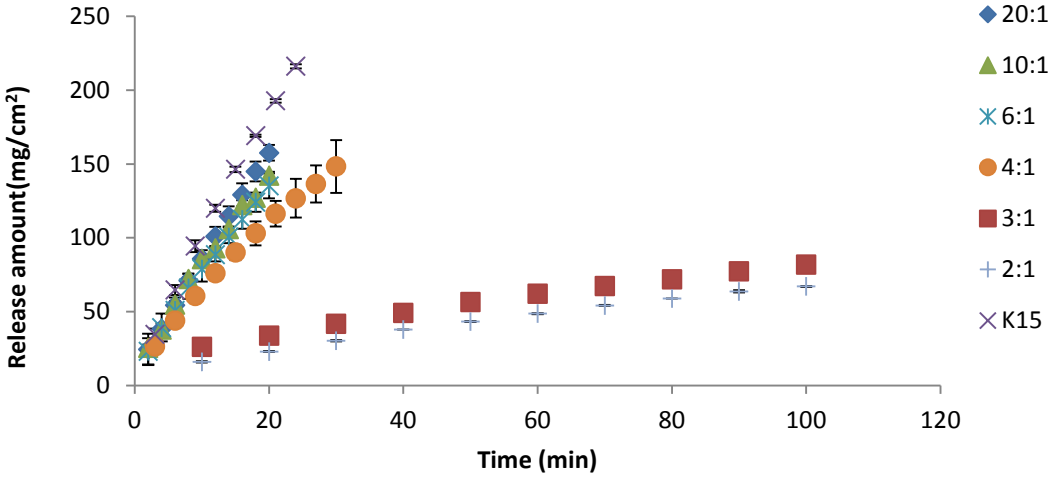

Figure 5-41: Rotating disk intrinsic release profiles of PVP K15 from PVP K15-BuPABA dispersions at 37 ºC at 100 rpm(n=3).

Table 5-15: Rotating disk intrinsic release rates of PVP K15-BuPABA dispersions at 37 ºC at 100 rpm.

Solid nominal ratio	PVP K15[a] release rate ($mg/cm^2 \cdot min$)	BuPABA[a] release rate ($mg/cm^2 \cdot min$)	PVP:PABA ester release rate ratio	Solid dispersion assay ratio	% Deviation
20:1	7.46 (0.999)	0.46 (0.998)	16.2	17.0	4.7
10:1	6.50 (0.997)	0.69 (0.995)	9.4	9.5	1.1
6:1	6.13 (0.992)	0.92 (0.989)	6.7	6.8	2.0
4:1[b]	4.47 (0.991)	0.91 (0.980)	4.9	4.1	21.3
3:1[b]	0.59 (0.989)	0.051 (0.999)	11.6	2.8	307.4
2:1[b]	0.55 (0.989)	0.051 (0.999)	10.8	2.1	413.5

[a.] in parentheses - R^2

[b.] accumulation of precipitate on intrinsic dissolution die observed

5.3.4.2 BuPABA-PVP K30 solid dispersions

The dissolution profiles of BuPABA and PVP K30 from the solid dispersion systems are shown in Figure 5-42 and Figure 5-43. The dissolution rates are summarized in Table 5-16. Precipitation was observed on the disc surface for all dispersions at drug loadings > 10% w/w (i.e., 6:1, 4:1, 3:1 and 2:1 PVP:BuPABA). No precipitation was observed for 20:1 and 10:1 dispersions. For these two ratios, drug and polymer dissolved congruently, which was similar to other low drug loading dispersion systems for other PABA esters.

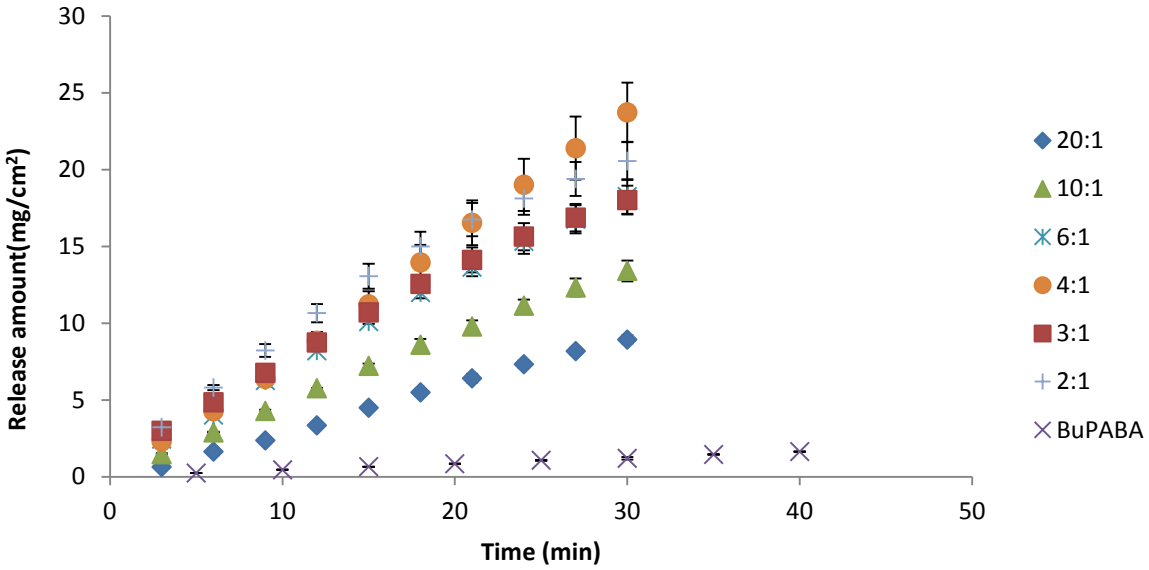

Figure 5-42: Rotating disk intrinsic release profiles of BuPABA from PVP K30-BuPABA dispersions at 37 ºC at 100 rpm (n=3).

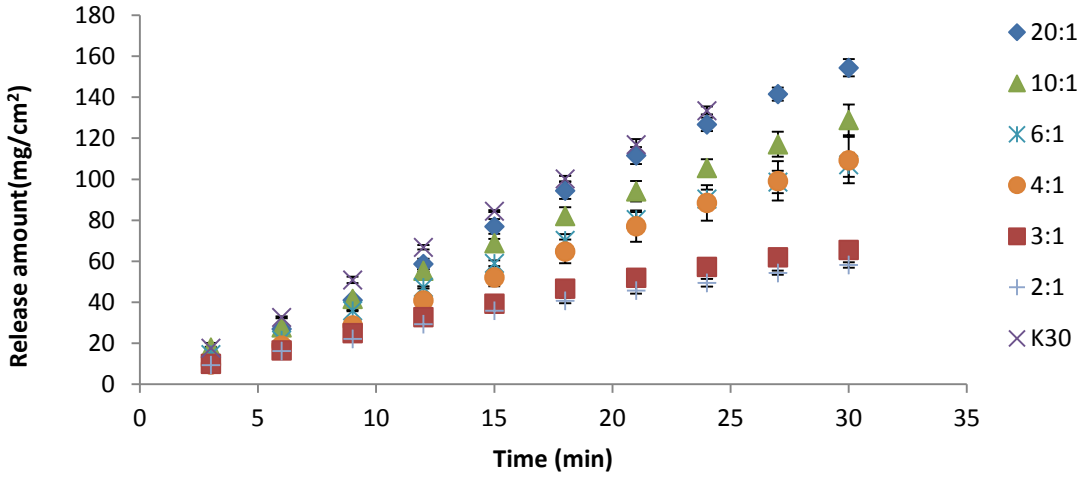

Figure 5-43: Rotating disk intrinsic release profiles of PVP K30 from PVP K30-BuPABA dispersions at 37 ºC at 100 rpm (n=-3).

Table 5-16: Rotating disk intrinsic release rates of PVP K30-BuPABA dispersions at 37 ºC at 100 rpm.

Solid nominal ratio	PVP K30[a] release rate ($mg/cm^2 \cdot min$)	BuPABA[a] release rate ($mg/cm^2 \cdot min$)	PVP:PABA ester release rate ratio	Solid dispersion assay ratio	% Deviation
20:1	5.41 (0.998)	0.31 (0.998)	17.4	17.0	2.2
10:1	4.18 (0.999)	0.45 (0.998)	9.3	10.2	9.3
6:1[b]	3.55 (0.996)	0.65 (0.997)	5.5	7.2	23.6
4:1[b]	3.79 (0.999)	0.81 (0.999)	4.7	3.7	24.8
3:1[b]	2.17 (0.986)	0.57 (0.993)	3.8	3.4	10.4
2:1[b]	1.81 (0.989)	0.65 (0.982)	2.8	2.2	25.4

[a.] in parentheses - R^2

[b.] accumulation of precipitate on intrinsic dissolution die observed

5.3.4.3 BuPABA-PVP K90 solid dispersions

The dissolution profiles of BuPABA and PVP K90 from the solid dispersion systems are shown in Figure 5-44 and Figure5-45. The dissolution rates are summarized in Table 5-17. Precipitation was observed on the disc surface for all dispersions at drug loadings > 10% w/w (i.e., 6:1, 4:1, 3:1 and 2:1 PVP:BuPABA ratios). Similar to K30 dispersions, no precipitation was observed for 20:1 and 10:1 dispersions for K90 dispersions. For these two ratios, drug and polymer dissolved congruently, which was similar to other low drug loading dispersion systems for other PABA esters.

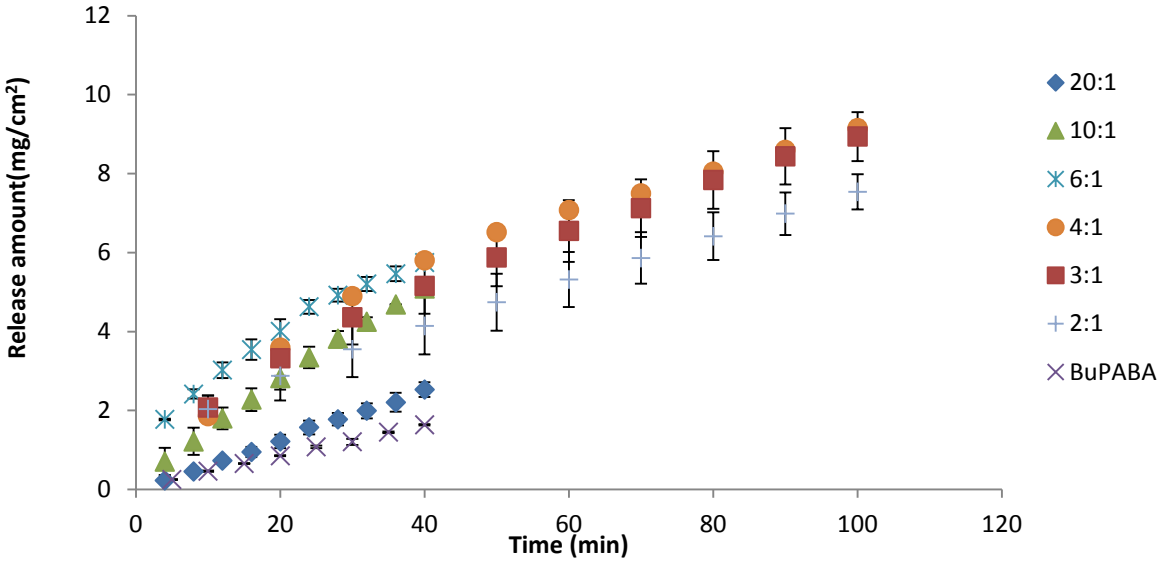

Figure 5-44: Rotating disk intrinsic release profiles of BuPABA from PVP K90-BuPABA dispersions at 37 ºC at 100 rpm (n=3).

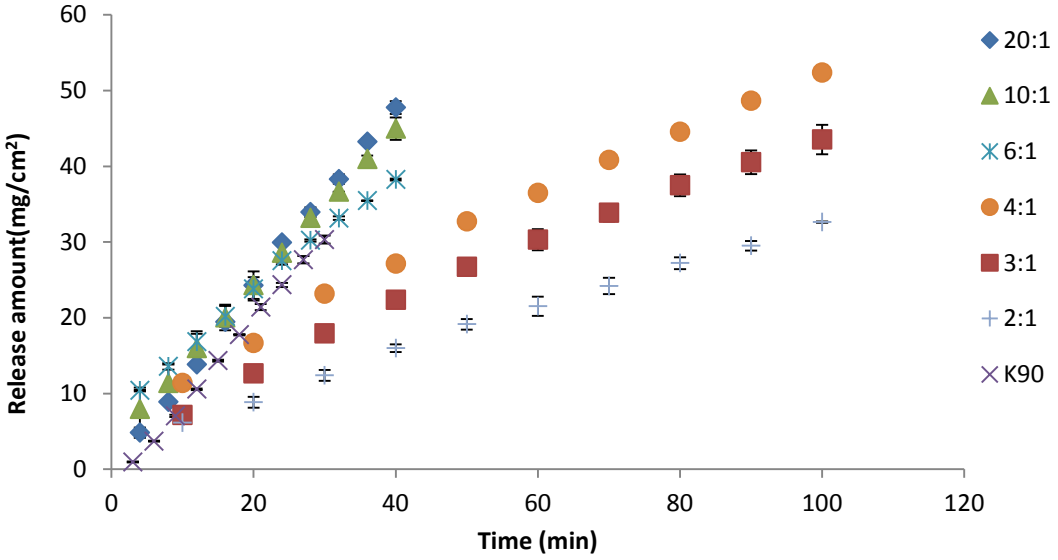

Figure5-45: Rotating disk intrinsic release profiles of PVP K90 from PVP K90-BuPABA dispersions at 37 ºC at 100 rpm (n=3).

Table 5-17: Rotating disk intrinsic release rates of PVP K90-BuPABA dispersions at 37 ºC at 100 rpm.

Solid nominal ratio	PVP K90[a] release rate ($mg/cm^2 \cdot min$)	BuPABA[a] release rate ($mg/cm^2 \cdot min$)	PVP:PABA ester release rate ratio	Solid dispersion assay ratio	% Deviation
20:1	1.21 (0.999)	0.064 (0.998)	18.9	18.6	1.5
10:1	1.04 (0.999)	0.12 (0.998)	8.7	8.8	1.1
6:1[b]	0.79 (0.996)	0.11 (0.975)	7.2	6.3	14.7
4:1[b]	0.46 (0.994)	0.074 (0.944)	6.2	3.8	63.6
3:1[b]	0.40 (0.990)	0.074 (0.984)	5.4	2.9	89.0
2:1[b]	0.29 (0.996)	0.06 (0.997)	4.8	1.9	154.4

[a.] in parentheses - R^2

[b.] accumulation of precipitate on intrinsic dissolution die observed

5.4 Discussion

To characterize the PVP-PABA ester dispersions, both DSC and PXRD analyses were performed. No PABA ester melting peak was not seen in any of the dispersion thermograms, demonstrating that the drug was amorphously dispersed in the polymer matrix. As with the DSC results, all diffraction peaks of PABA esters disappeared from the powder X-ray diffraction patterns for all PVP dispersions, again indicating amorphous systems.

The following observations are applicable to all solid dispersion intrinsic release data:

- The majority of the solid dispersion systems displayed nearly linear dissolution profiles for both PVP and PABA ester. In a few cases, the PABA ester showed a biphasic phase dissolution profile with the initial phase being more rapid and the terminal phase being close to that of the pure ester.

- The PVP dissolution rate decreased as drug loading increased. The decrease was more obvious for the lower molecular weight PVP dispersions (PVP K15 and PVP K30) and less pronounced for the higher molecular weight PVP dispersions (PVP K90).
- PABA ester release rate first increased then decreased as drug loading increased in the PVP K15 and K30 dispersions. In the PVP K90 dispersions, the drug dissolution increased as drug content in the dispersion systems increased. In the K90 systems, no dissolution enhancement was observed in any of the dispersions studied because of the higher viscosity and low intrinsic dissolution rate of the polymer.
- At low drug loadings (PVP:PABA ester ratios of 20:1, 10:1 and 6:1), the polymer and drug dissolved congruently. As the drug loading increased, the deviation from congruency increased.
- Precipitation of BuPABA was observed on the rotating disc surface for many BuPABA-PVP dispersion systems. For this reason, BuPABA release behavior will be of minimal importance in discussing overall dispersion release since its rapid precipitation caused higher variability in the dissolution data.

5.4.1 Pure PVP dissolution

Polymer dissolution has been extensively investigated experimentally and theoratically.[77-86] However, for a very water soluble and fast dissolving polymer like PVP the studies have been quite limited. In the intrinsic dissolution studies by Nogami et al., the authors observed an initial swelling stage of PVP K30 in a 4:1 acetone-water cosolvent followed by dissolution.[74,75] An initial swelling was observed by Corrigan et al. in his studies on PEG indicated by upward curvature of the dissolution profiles.[19] In addition, these authors observed that the curvature increased with PEG

molecular weight.[19] In our work, the three PVPs exhibited nearly linear dissolution files as pure substances. The only significant negative intercept for a dissolution profile was observed for K90 dissolution. This suggested a possible initial curvature in the K90 dissolution rate which implied a possible initial swelling phase before dissolution started. This seems to agree with reported PEG results, where higher MW PEGs exhibited a more pronounced swelling phase.[19] The PVP intrinsic dissolution rates were inversely related to their molecular weight. Similar dissolution behavior has been reported in other polymer systems.[19,77]

The treatment process (i.e., dissolving and re-precipitation) did not change PVP K15 or PVP K90 dissolution rates. However, an increase in dissolution rate was seen for PVP K30 dissolution after re-precipitation from methanol. There have been no such reports of this behavior in literature. This phenomenon could be related to moisture content in the PVP. In general, PVP is very hygroscopic. The dissolving and solvent evaporation process might remove water from PVP. Water can act as a binder and increase interactions between polymer particles. With less water in the polymer, the interaction between polymer particles may be reduced. The dissolution medium can hydrate polymer particles quickly which would leave faster PVP dissolution. This increase did not occur in the low and high molecular weight PVPs (K15 and K90). This could be because this faster hydration did not affect their dissolution process significantly. In other words, K15 might hydrate fast and K90 might hydrate slowly regardless of the treatment.

In PEG studies, large variations in dissolution rates were observed for different lots of PEG of the same molecular weight.[39] In our preliminary study, similar behavior was observed (i.e., as much as 30% variation was observed for PVP K15 dissolution among different batches). In this thesis, all the PVPs used were from the same batch to eliminate lot-to-lot variation.

5.4.2 Pure PABA ester dissolution behavior

PABA ester intrinsic dissolution rates using the rotation disc method can be predicted with the Levich's equation (Equation 5-3).[45] In Levich's equation, J is the flux; D is the diffusion coefficient of a compound; C_s is its solubility; ν is the kinematic viscosity; ω is the rotation speed. The calculated intrinsic dissolution rate as well as the experimental results are presented in (Table 5-18). In this analysis, the diffusion coefficient of EtPABA at 37 ºC was obtained from the literature.[87] Other PABA esters have similar molecular weights as EtPABA. Their diffusion coefficients were assumed to be near that of EtPABA. Due to the relative low solubility of the PABA ester series, water's viscosity at 37 ºC was used in this calculation without further adjustment. As shown in Table 5-18, the calculated dissolution rates are comparable to the experimental values. As indicated in Levich's equation, a compound's intrinsic dissolution rate is determined by its solubility, diffusion coefficient, the viscosity of the medium and rotation speed. PABA esters have similar molecular weight, which gives them similar diffusion coefficients. For this series of compounds, solubility is the main factor in determining its dissolution rate under the same experimental conditions. MePABA was the most soluble compound and had the highest dissolution rate. BuPABA was the least soluble and dissolved the slowest.

$$J = 0.62\, D^{2/3} V^{-1/6} \omega^{1/2} \mathrm{Cs} \qquad \text{Equation 5-3}$$

Table 5-18: Calculated PABA ester intrinsic dissolution rates compared to experimental intrinsic dissolution rates 37 ºC at 100 rpm.

	C_s (mg/cm^3)	D[a] (cm^2/s)	Predicted dissolution rate (mg/cm^2·min)	Experimental dissolution rate (mg/cm^2·min)
MePABA	2.3	1.4 x 10^{-5}	0.35	0.28
EtPABA	1.5	1.4 x 10^{-5}	0.23	0.20
PrPABA	0.72	1.4 x 10^{-5}	0.11	0.095
BuPABA	0.28	1.4 x 10^{-5}	0.042	0.038

[a.] literature value for EtPABA[87]

5.4.3 Polymer dissolution from solid dispersions

For the few studies where the water-soluble carrier release from solid dispersions was monitored, all were similar to that was observed for the PVP-PABA ester dispersions: polymer dissolution decreased as drug loading increased. For example, in the classic sulfathiazole-PVP (MW=10,000) study, PVP's dissolution rate showed a constant decrease as drug loading increased.[20] A ~10% decline in PVP release was observed in 20:1 and 10:1 PVP-sulfathiazole dispersions. The decline was more pronounced as drug content increased in the dispersions. Similar results were observed in the studies by Corrigan et al.[19,39] In one of his studies on PEG 4000-bendrofluazide or -hydroflumethiazide dispersions, the polymer intrinsic dissolution rate decreased as drug loading increased.[19] Even at a 20:1 polymer:drug loading, the reduction in PEG release was observed.[19] In another study, these authors investigated 30:1 and 10:1 PEG 4000:barbituric acid and 30:1 and 50:1 PEG 4000:phenobarbitone dispersions and found out that polymer dissolution decline was obvious in these dispersions even at these extremely low drug loadings (i.e.,30:1 and 50:1).[39] These authors also pointed out that both bendrofluazide and hydroflumethiazide formed a more soluble complex with PEG in the dispersions while

phenobarbitone formed a less soluble complex with PEG and barbituric acid did not form a complex with PEG.[39] These authors suggested that polymer dissolution decrease might be irrelevant to drug-polymer complex formation in the dispersions. In a 2015 study by Ji et al., the authors monitored PVP release from PVP K25-indomethacin and PVP K25-naproxen dispersions (20%, 40%, 60% and 80% w/w drug loading for both indomethacin and naproxen).[51] They observed that PVP release rate from dispersions decreased compared to that of the pure polymer. Moreover, the reduction in PVP release was more pronounced when drug loading increased. These results are also consistent with our observations. As shown in Figure 5-46 to Figure 5-48, PVP release reduction are obvious in almost all dispersions. In these figures, purple lines represent that PVP release is linearly related to its content in the dispersion. Clearly, PVP dissolution retardation does not decrease linearly with PVP content. In most cases, the reduction is non-linear and greater than that of assuming PVP release is linearly related to its content. Also shown in these figures, the PVP release reduction is more pronounced for the lower MW PVPs (i.e., K15 and K30) than the higher MW PVP (i.e., K90).

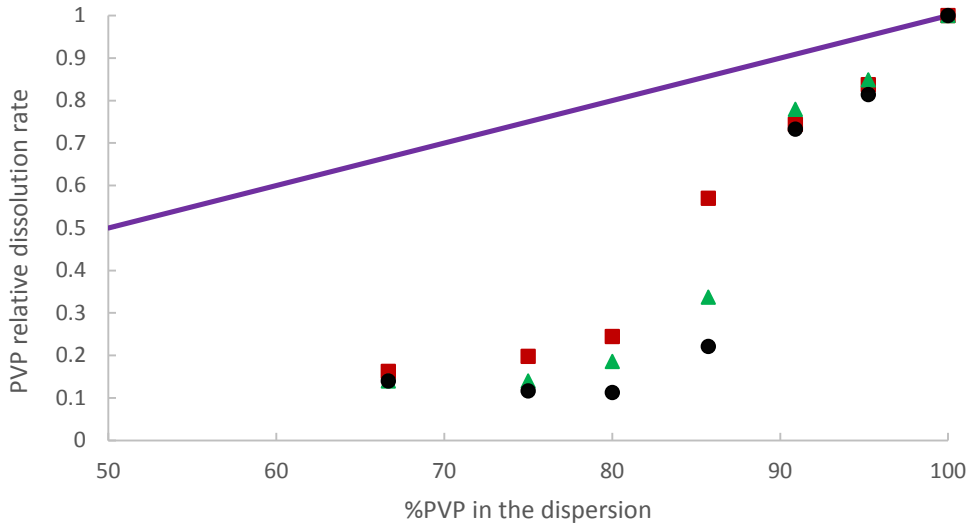

Figure 5-46: PVP K15 relative release rate vs % PVP in the dispersion. Red square: MePABA; green triangle: EtPABA; black dot: PrPABA; purple line: hypothetical PVP release rate assuming it changes linearly with PVP content.

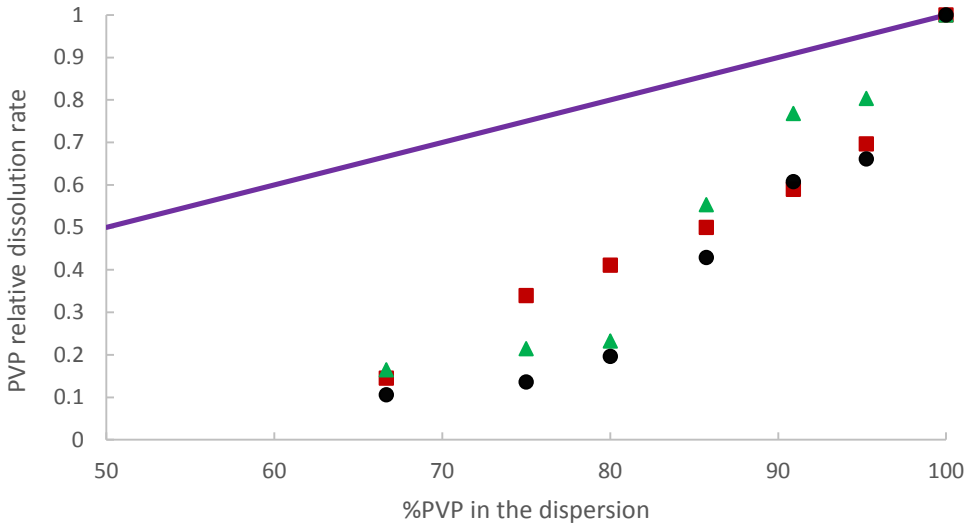

Figure 5-47: PVP K30 relative release rate vs % PVP in the dispersion. Red square: MePABA; green triangle: EtPABA; black dot: PrPABA; purple line: hypothetical PVP release rate assuming it changes linearly with PVP content.

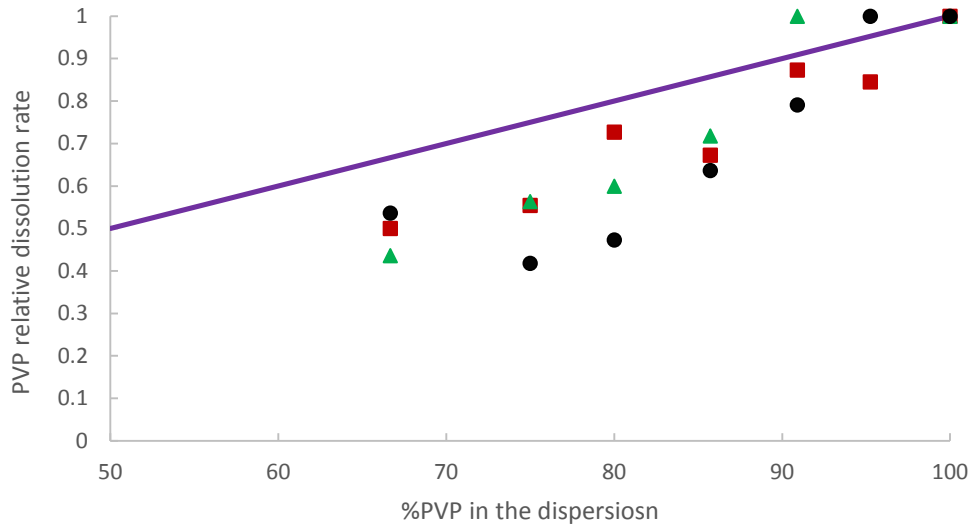

Figure 5-48: PVP K90 relative release rate vs % PVP in the dispersion. Red square: MePABA; green triangle: EtPABA; black dot: PrPABA; purple line: hypothetical PVP release rate assuming it changes linearly with PVP content.

There are two possible explanations for PVP dissolution retardation from dispersion systems. First, the interaction between PABA esters and PVP in the dissolution medium, which was confirmed by complexation studies might reduce PVP's hydration rate and thus its dissolution rate. The PABA esters also may interact between polymer chains holding them together which slows the polymer chain detachment. When PVP molecular weight is high (i.e., K90), chain entanglement is higher and hydration/dissolution is naturally slower independent of the PABA ester. Another possibility for carrier dissolution reduction is when PABA ester precipitation occurs, it forms a physical barrier to slow PVP dissolution since its boundary recedes more rapidly into the tablet. When PVP molecular weight is high and dissolves slower compared to other PVPs,

the physical barrier for the high molecular weight polymer may be less important to its overall release rate compared to its generally lower intrinsic dissolution behavior.

To further explore PVP release rate reductions from solid dispersions, an intrinsic dissolution study of physical mixtures of PVP and PABA ester was performed with monitoring of polymer release rates. The goal of this study was to examine how drug-polymer interactions in the solid phase and/or physical drug barrier formation causes polymer release reduction. In physical mixtures, there is assumed to be no complex formation or interaction in the solid-state, so if similar PVP release reductions are observed, most likely the reduction is from a drug-polymer interaction in solution and/or excess drug as a physical barrier.

Only EtPABA was selected for this study, and since polymer dissolution reduction was more pronounced for the PVP K15 and K30 dispersions only these two grades were chosen to prepare physical mixtures with EtPABA. Like solid dispersions, PVP release from physical mixtures displayed nearly linear dissolution behavior (APPENDIX G). PVP relative dissolution rates from physical mixtures and dispersions are shown in Figure 5-49. PVP release rates from physical mixtures and dispersions are compared in Table 5-18 and Table 5-20. Clearly, polymer dissolution retardation was observed in both physical mixtures and in dispersions. In both cases, a more pronounced reduction was observed than assuming PVP release being linearly related to its content. Even at very low drug loadings (20:1) a decrease of 20-25% in both PVP K15 and K30 dissolution was observed. The polymer release reduction increased as drug loading increased in the mixture systems. For a 2:1 drug loading, > 80% decrease and > 60% decrease were observed for PVP K15 and PVP K30, respectively. Thus, it appears that complex formation in the solid dispersions is not the primary cause of polymer dissolution reduction in the dispersions.

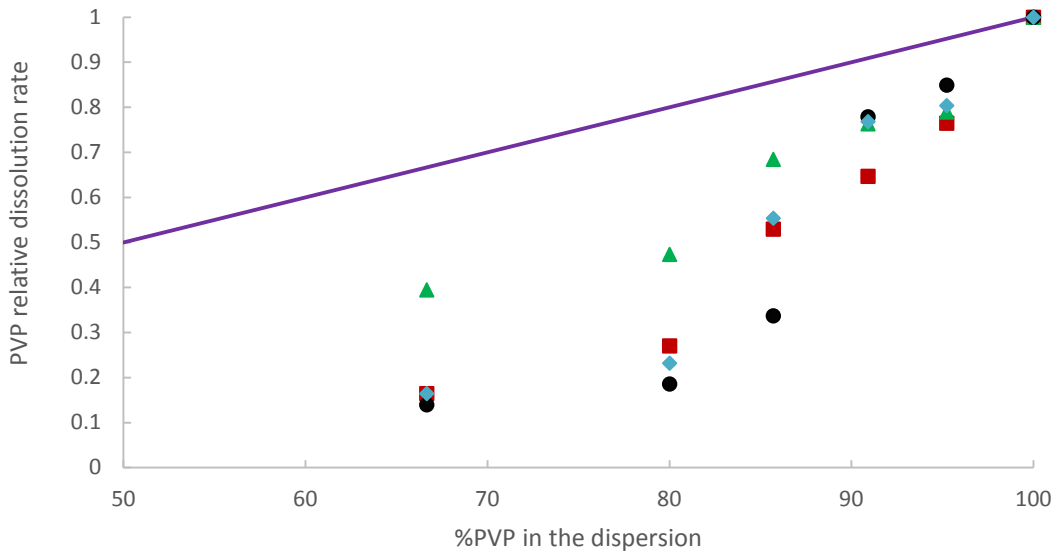

Figure 5-49: PVP relative release rate vs % PVP. Red square: K15-EtPABA physical mixture; green triangle: K30-EtPABA physical mixture; black dot: K15-EtPABA dispersion; blue diamond**:** K30-EtPABA dispersion; purple line: hypothetical PVP release rate assuming it changes linearly with PVP content.

Table 5-19: Intrinsic release rate of PVP K15 from K15-EtPABA physical mixtures and solid dispersions at 37 ºC at 100 rpm.

PVP K15:EtPABA ratios	K15 release rate from mixture ($mg/cm^2 \cdot min$)	K15 release rate from dispersion ($mg/cm^2 \cdot min$)
Pure PVP K15	8.6	8.6
20:1	6.5	7.3
10:1	5.5	6.7
6:1	4.5	2.9
4:1	2.3	1.6
2:1	1.4	1.2

Table 5-20: Intrinsic release rate of PVP K30 from K30-EtPABA physical mixtures and solid dispersions at 37 ºC at 100 rpm.

PVP K30:EtPABA ratios	K30 release rate from mixture ($mg/cm^2 \cdot min$)	K30 release rate from dispersion ($mg/cm^2 \cdot min$)
Pure PVP K30	3.8	5.6
20:1	3.0	4.5
10:1	2.9	4.3
6:1	2.6	3.4
4:1	1.8	1.3
2:1	1.5	0.92

The possibility of a drug barrier at high drug loadings in mixtures was investigated. A disintegrating dissolving surface should be observed from falling particles during dissolution study.[19,20,39,40,46,47] This behavior was not seen for the EtPABA-PVP physical mixtures. No particles falling for any physical mixtures led to a different approach. In this approach, side-by-side intrinsic dissolution studies on physical mixtures were performed: in one study, the dissolution medium was water and in the other, a saturated EtPABA solution. The study was carried out for an extended time period (>2-3 hours) to exaggerate any visible differences in the tablet surfaces. The tablets were examined and compared at the end. If there was not enough EtPABA in the mixture to hold an intact surface together during dissolution, no difference would be observed between the two tests (i.e., tablets dissolved regardless of which medium was used). However, if there was enough EtPABA in the mixture to hold an intact surface together during dissolution, a difference would be expected in the two tests. When the dissolution medium was water, the tablet

would still dissolve and show visual surface loss. When the medium was saturated EtPABA solution, an intact drug layer on the surface would prevent any obvious surface loss.

For a 6:1 physical mixture (Figure G-1), the small fraction (~14%) of drug could not hold the surface intact because it disintegrated as PVP dissolved away. As expected, a receding surface was observed in both water and a saturated EtPABA medium indicating EtPABA disappeared from the tablet sample into water and a saturated EtPABA solution. For a 2:1 mixture (Figure G-2), there was sufficient EtPABA in the mixture to hold an intact surface together as evidenced by the receding surface was only observed in water while no surface loss appeared in saturated EtPABA. The surface integrity studies were performed on five PVP-EtPABA mixture ratios (20:1, 10:1, 6:1, 4:1 and 2:1) and the results are summarized in Table G-1. For both K15 and K30, an intact surface without receding was observed only for a 2:1 ratio. At this ratio, a significant reduction in polymer dissolution was observed, which might be due to a combination of drug-polymer interaction in solution and drug acting as a physical barrier to polymer release. If drug precipitates on the tablet surface during dissolution, the actual drug compositions on the surface might be much greater than what existed in the solid dispersions. Thus, the barrier effect might begin with drug loading < than 2:1 ratio. Another important aspect of these results is estimating how much drug is actually needed to generate an intact drug surface.

5.4.4 PABA ester dissolution from solid dispersions

All the PABA ester-PVP K15 and PABA ester-PVP K30 dispersions displayed similar results: the drug intrinsic dissolution rate first increased then decreased to that of the pure drug as drug loading increased. However, the specific change of intrinsic dissolution rate with solid dispersion composition varied with each PABA ester and PVP combination. Similar results were observed in

other intrinsic dissolution studies on solid dispersion systems.[20,46,47] Reported results showed that the drug intrinsic dissolution rate first increased then decreased to that of the pure drug as drug loading increased as found in this work. Moreover, the maximum drug dissolution rate occurred at different drug loadings depending on the specific PABA ester and PVP type. For example, for PVP K15, the maximum drug dissolution rate was observed at a 6:1, 10:1 and 10:1 ratios for MePABA, EtPABA or PrPABA, respectively. When the carrier was PVP K30, the maximum drug dissolution rate was observed at a 3:1, 6:1 or 6:1 ratios for MePABA, EtPABA or PrPABA, respectively. The maximum drug dissolution varied with drug loadings: 25% sulfathiazole, 20% CI-987 and 40% furosemide with various carriers.[20,46,47] Biphasic dissolution behavior was observed for EtPABA and PrPABA solid dispersions. This behavior also occurred at intermediate drug loadings for furosemide and sulfathiazole dispersions as well.[20,47]

Overall PABA ester-PVP K15 and PABA ester-PVP K30 systems behaved consistently with the previous reported studies. In the region where drug dissolution increased with drug loading, all agree that this region is the "carrier-controlled" region.[20,46,47] Drug dissolution rate in this region is solely dependent on the carrier dissolution rate (i.e., PVP or polymer) and the drug loading. This conclusion is also supported by Dubois's work where different drugs and the same carrier offered almost identical dissolution rates when drug loading was the same for several drugs with different physicochemical properties.[42] In some studies conducted by Corrigan et al., the results showed that congruent release between various drugs and one carrier occurred at high carrier content (i.e., low drug loading).[19,39,40] Their studies support the carrier-controlled theory. Furthermore, for nortriptyline HCl, drug dissolution rate increased linearly with drug loading (when drug loading < 20%).[44] This also reinforces the "carrier-controlled" theory at low drug loadings. The PABA ester-PVP results have supported the "carrier-controlled" concept at low drug loading. When there is

little drug in the dispersions (often <15%), PVP and PABA esters release simultaneously from the solid dispersions in proportion to their ratios in the dispersion.

In the region where drug dissolution is equivalent to or nearly equivalent to that of the pure drug, this is the "drug-controlled" region.[20,46,47] There are two possible reasons that can be suggested for this dissolution behavior. One is crystalline drug becoming present in the dispersions when drug loading is very high. High drug loading solid dispersions of furosemide and CI-987 are examples of this possibility.[46,47] The other possibility is that precipitation of amorphous drug during the dissolution process produces a surface layer of crystalline drug. Examples of this possibility include sulfathiazole, Cyclosporine A, bendrofluazide, hydroflumethiazide, phenobarbitone and barbituric acid dispersion systems.[19,20,39-41] Biphasic release profiles for furosemide and CI-987 dispersions with the end phase release rates were close to that of the pure drug also supported the precipitation possibility.[46,47] For PABA ester -PVP systems, amorphous solids were obtained for the dispersions prepared as confirmed by the PXRD and DSC results. PABA ester dissolution rates from solid dispersion with higher drug loading were generally equivalent to that of the pure PABA ester, which suggested drug crystallization. The terminal phase release profiles observed for EtPABA and PrPABA dispersions were equivalent to those of the pure ester.

Between "carrier-controlled" region and the "drug-controlled" region, drug dissolution is no longer solely controlled by carrier release and drug loading nor is it equivalent to that of the pure drug. Drug in the dispersions possessed partial amorphous form and partial crystalline form in the furosemide and CI-987 systems. This observation was qualitatively linked to this dissolution behavior.[46,47] On the other hand, completely amorphous sulfathiazole was obtained in this drug loading region. Simonelli et al. proposed a quantitative approach (SMH) with good success but it

only applied to one drug and one type of PVP.[20] Previous problems in utilizing this model include: the lack of a general expression and the difficulty in estimating some parameters such as polymer diffusion coefficient, diffusion layer thickness, etc. In Chapter 3, a general expression was developed based on the concepts in the traditional approach (SMH) where the relative dissolution rate (ratio between of drug intrinsic dissolution rate from dispersion and that of the pure drug) can be calculated without parameters that are difficult to obtain or predict. Simulation results showed that dissolution rate underestimation can occur when drug solubility was low (i.e., $W_2 < 0.01$, Chapter 3). Predictions, as well as the experimental results, for the PABA esters are shown in Figure 5-50 to Figure 5-53. When PVP content is > 80%, predictions deviate from experimental results for all PABA ester systems making it less useful for modeling these dispersions. The deviations are particularly apparent for BuPABA dispersions (Figure 5-53).

PABA ester-PVP K90 dispersions (except BuPABA dispersions) exhibited a different trend from the other two PVPs because drug dissolution rate increased constantly to that of the pure drug as drug loading increased. In fact, drug release rates were lower than that of the pure drug in all K90 dispersion systems since K90 solutions are much more viscous than K15 or K30 solutions. This observation has not been reported previously. Like other PVPs, it can be seen that the SMH model gives reasonable predictions when PVP K90 is less than 80% in the dispersion system. However, disagreement is observed when drug loading is lower.

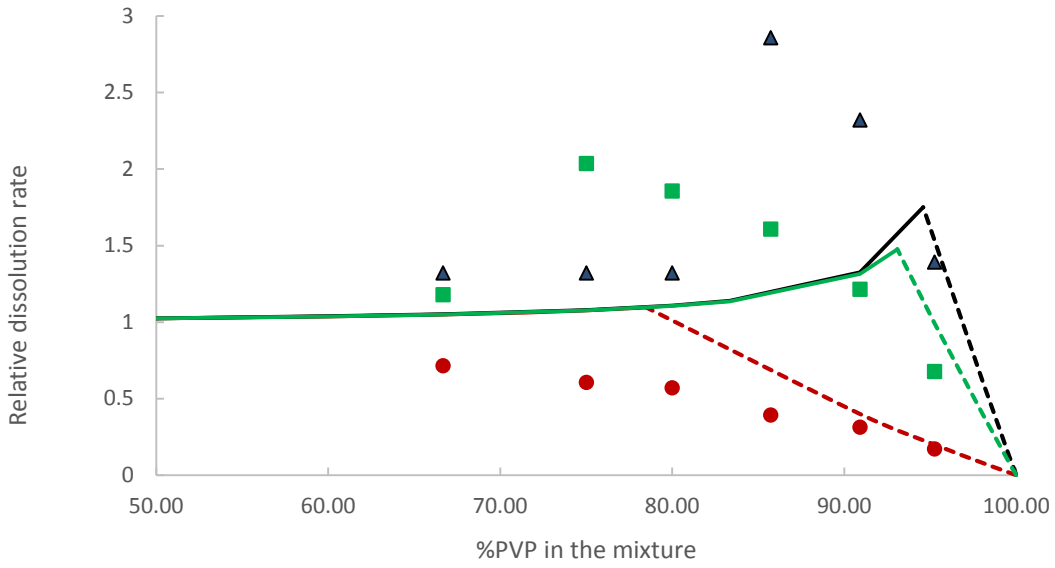

Figure 5-50: MePABA relative dissolution rates vs %PVP in the mixture compared to SMH model predictions. The points are experimental results and lines (curves) are SMH predictions (dashed lines represent the regions where PVP is the front substance while solid lines (curves) represent the regions where MePABA is in front). Black triangle: MePABA-PVP K15; green square: MePABA-PVP K30; red dot: MePABA-PVP K90.

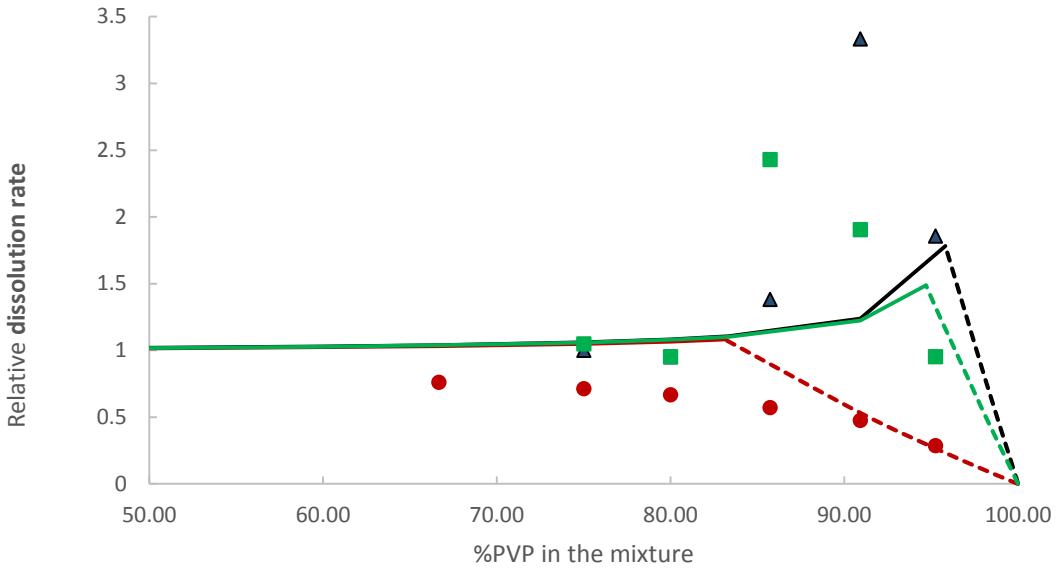

Figure 5-51: EtPABA relative dissolution rates vs %PVP in the mixture compared to SMH model predictions. The points are experimental results and lines (curves) are SMH predictions (dashed lines represent the regions where PVP is the front substance while solid lines (curves) represent the regions where EtPABA is in front). Black triangle: EtPABA-PVP K15; green square: EtPABA-PVP K30; red dot: EtPABA-PVP K90.

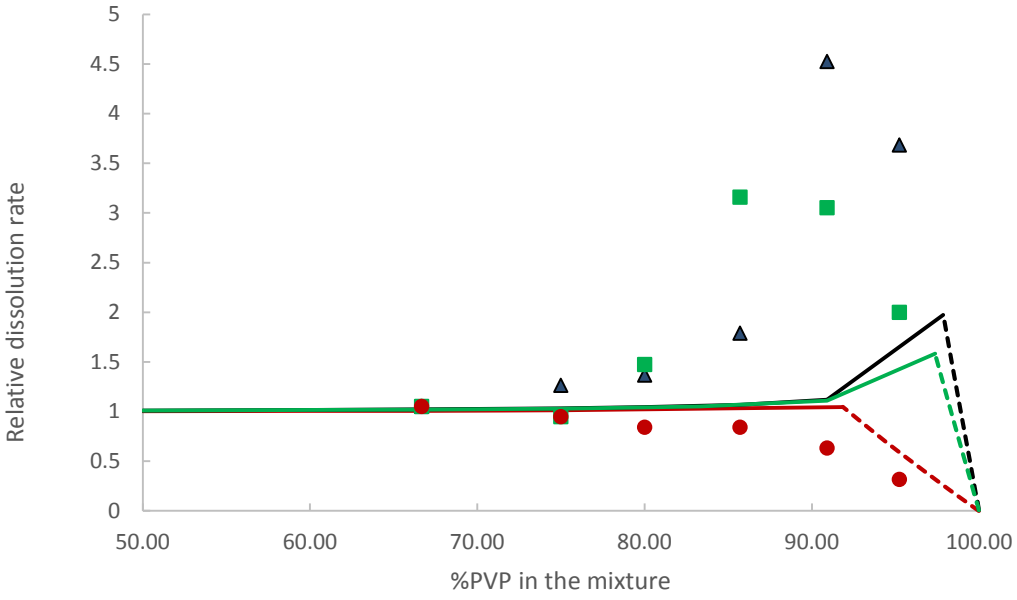

Figure 5-52: PrPABA relative dissolution rates vs %PVP in the mixture compared to SMH model predictions. The points are experimental results and lines (curves) are SMH predictions (dashed lines represent the regions where PVP is the front substance while solid lines (curves) represent the region where PrPABA is in front). Black triangle: PrPABA-PVP K15; green square: PrPABA-PVP K30; red dot: PrPABA-PVP K90.

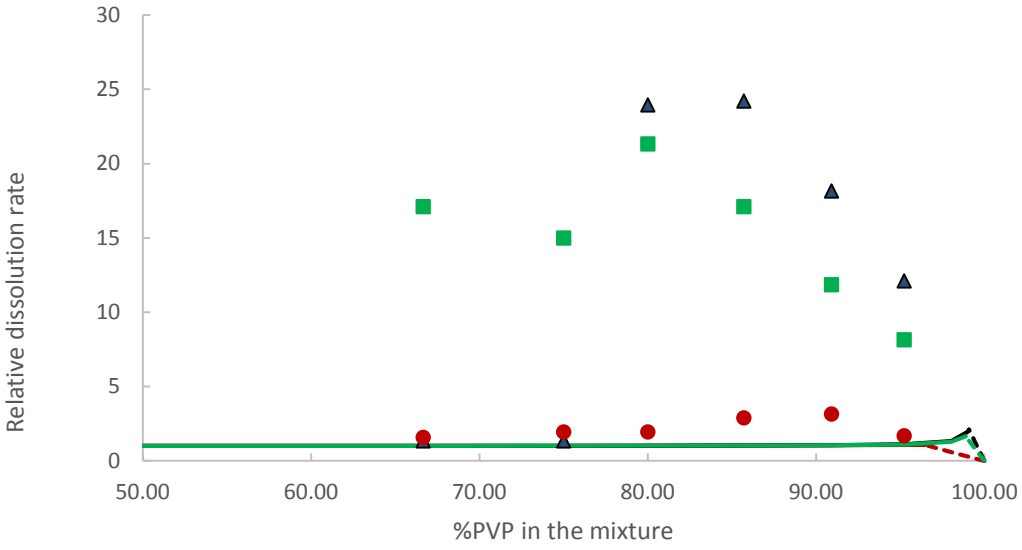

Figure 5-53: BuPABA relative dissolution rates vs %PVP in the mixture compared to SMH model predictions. The points are experimental results and lines (curves) are SMH predictions (dashed lines represent the regions where PVP is the front substance while solid lines (curves) represent the region where BuPABA is in front). Black triangle: BuPABA-PVP K15; green square: BuPABA-PVP K30; red dot: BuPABA-PVP K90.

5.4.5 Proposed model

As drug loading increases, the PABA ester release rate in PVP K15 and K30 dispersions first increases then decreases to that of the pure drug. Similar behavior has been observed in other dispersion dissolution studies.[19,20,39,40,43,46,47] Simonelli et al. proposed a traditional approach (SMH) to account for their results.[20] Other researchers have shown that their results on similar systems could only qualitatively correlate with this traditional approach.[19,39,40,43,46,47] One of the challenges with applying this approach (SMH) is the difficulty in estimating some of the required parameters (i.e., polymer diffusion coefficient or diffusion layer thickness). However, in this thesis it has been shown that those parameters are unnecessary if relative dissolution rates are used rather

than absolute dissolution rates. As in other studies, only qualitative agreement between the experimental results and the predictions are observed for the PABA ester-PVP systems (Figure 5-50 to Figure 5-53).[19,39,40,43,46,47] Secondly, it also has been shown in this work that the prediction underestimates dissolution rates when drug solubility is low (Chapter 3). Finally, the traditional approach (SMH) proposes that dissolution can be divided into two regions: "drug in front" (solid lines) and "polymer in front" (dashed lines). One of the assumptions is that the dissolving surface remains intact at all drug loadings. However, as indicated in Figure 5-50 to Figure 5-53, the "drug in front" region for PABA ester-PVP systems starts at > 90% polymer content or < 10% drug loading. Our physical mixture dissolution results (APPENDIX G) show that it is difficult (or impossible) to maintain an intact dissolution surface at such low drug loadings.

Corrigan et al. claimed that the SMH model is essentially a modification of two-component small molecule dissolution model of Higuchi.[39,40] One would expect the polymer dissolution rate in the "polymer in front" region to be equal to or greater than that of the pure polymer. This expectation is contrary to Corrigan's PEG dispersion results: PEG's dissolution rates from dispersions were always lower than that of pure PEG.[19,39,40] In our PABA ester-PVP systems, similar results were obtained: PVP dissolution rates from dispersions were always lower than that of pure PVP. That was true for all PVP grades investigated.

As drug loading increased, the PABA ester intrinsic dissolution rates from the PVP K90 dispersions increased constantly approaching to that of the pure PABA ester. This behavior has not been reported in other studies but PVP K90 is unique because of its high MW and slower intrinsic dissolution behavior. PVP K90 dissolves must slower than the other two PVPs which basically inhibit PABA ester dissolution at all compositions except as K90 is reduced to low levels (<75%).

Many authors suggest that drug precipitation is unavoidable during dissolution if supersaturation in the boundary layer is high.[1,3,11,13,14,17,88,89] In addition to supersaturation, water acts as a plasticizer to facilitate drug recrystallization. Previously, researchers believed that if drug particles were released into the dissolution medium (assuming an intact surface was not maintained) as the carrier dissolved, a non–linear dissolution profile would be expected.[19,39,40,46,47] However, in this work EtPABA-PVP physical mixtures (APPENDIX G) showed that linear dissolution profiles were achieved even when drug particles were assumed to be released into the dissolution medium as the faster dissolving PVP released from the dissolving surface. Thus, linear dissolution profiles are not necessarily a good measure of whether drug particles are released from a dissolving mixture or dispersion.

An alternate proposal for depicting drug intrinsic release vs PVP content for dispersions is shown in Figure 5-54. In this model, the dissolution of PABA ester (small molecule) can be divided into two general regions: A and B. In the region A (dashed line, Equation 5-4) where polymer controls release drug (small molecule) dissolves rapidly as polymer dissolves.

$$G_A{}^T = \frac{N_B}{N_A} G_B \qquad \text{Equation 5-4}$$

In the region B (solid line, Equation 5-5), pure drug dissolution controls release. In region B crystalline drug forms because of quick precipitation or crystallization during dissolution. As a consequence, the drug dissolution rate in the region B is equivalent to or close to that of the pure drug. There is no continuity between regions A and B (i.e., a discontinuity of relative dissolution rates is observed in between these two regions).

$$G_A{}^T = G_A{}^0 \qquad \text{Equation 5-5}$$

In region A, a number of possible conditions could occur: 1) drug does not precipitate/crystallize during dissolution; 2) if precipitation occurs, drug particles formed are released into the dissolution medium as PVP dissolves; 3) if precipitation occurs , a partial coverage is formed on the tablet surface. In this region, congruent release of both drug and polymer occurs initially for all the ratios. However, as drug loading increases or time goes, the drug dissolution no longer keeps up with the polymer release due to precipitation. Larger deviations from congruent release behavior are then observed. Overall there are several competing factors affecting the drug release: 1) increasing drug loading in the dispersion increases drug release because as polymer dissolves more drug will be released when drug loading is higher; 2) polymer release rates decrease as drug loading increases leading to a decrease in drug release; 3) drug precipitation on to the tablet surface leads to a decrease in drug release. Thus, by increasing drug loading there can be an increase in drug release (region A1) and then to a decrease (region A2). The maximum release rate is a balance of these three factors. Alternatively, if the polymer dissolution is very slow (i.e., PVP K90), a constant increase in the drug dissolution rate may be observed as drug loading increases (region A3).

Comparisons of the predicted results of this model and experimental results are plotted in Figure 5-55 to Figure 5-58. The dashed curves are the PVP-controlled region. PVP release rate was measured. The PABA ester release rates were calculated with the measured PVP release rate and a congruent relationship between PVP and PABA ester release rates assumed. The solid line is the PABA ester-controlled region. In this region, rapid precipitation and/or recrystallization is assumed. Therefore, it is estimated that the PABA ester's dissolution rate is equivalent to that of the pure PABA ester. It can be seen that good agreement between the experimental results and predictions is achieved in most cases. Large deviations are observed in BuPABA when drug

loading is > 20%. Significant precipitations on the disc surface during dissolution occurred for BuPABA dispersions when drug loading was > 20%. Such behavior may account for the large discrepancy between the predicted results and the experimental results.

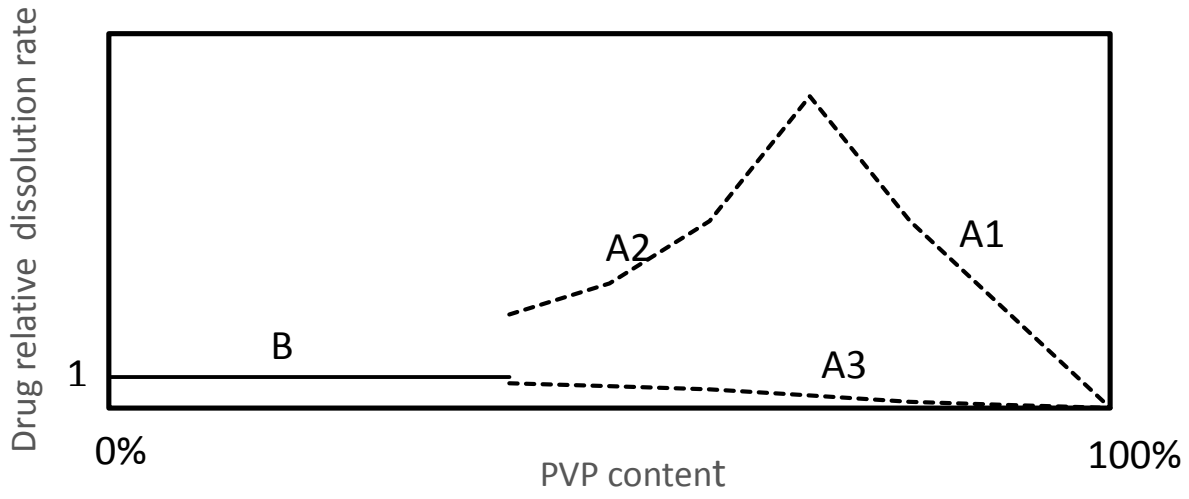

Figure 5-54: General profile of PABA ester relative dissolution vs solid dispersion composition for PABA ester-PVP systems based on the new model.

This alternative model better explains the dispersion dissolution results for PABA esters with PVP. One new consideration in this model is addressing the observation that polymer dissolution rate decreases as drug loading increases. As shown in the PABA ester-PVP systems, as well as a few drug-PEG systems in the literature, there is a constant decrease in polymer dissolution rates from solid dispersions.[19,39,40] With this correction, an improvement in model prediction is achieved than the traditional approach (constant polymer dissolution is assumed) especially when polymer dissolution rate decreases are significant. Another improvement is the division between polymer-controlled and drug-controlled regions. In Figure 5-50 to Figure 5-53, the drug-controlled region

begins as early as < 5% drug loading. In this modified model, the change from polymer-controlled behavior to drug-controlled behavior occurs in the 25%-33% drug loading range. Since precipitation/recrystallization can occur during dissolution, this division is closer to reality than in the traditional approach.

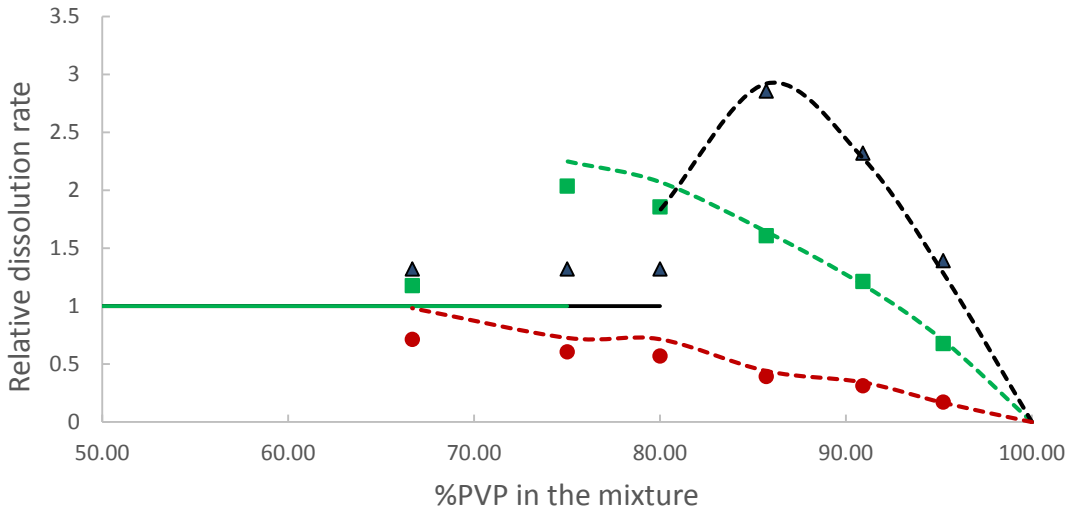

Figure 5-55: MePABA relative dissolution rate vs %PVP in the dispersion compared to the new model predictions. The points are experimental results and lines are predictions (dashed lines represent polymer- controlled region and solid lines represent drug-controlled region). Black triangle: MePABA-PVP K15; green square: MePABA-PVP K30; red dot: MePABA-PVP K90. (Assuming drug-controlled region starts at 4:1, 3:1 and 2:1 polymer:MePABA ratios for PVP K15, K30 and K90, respectively).

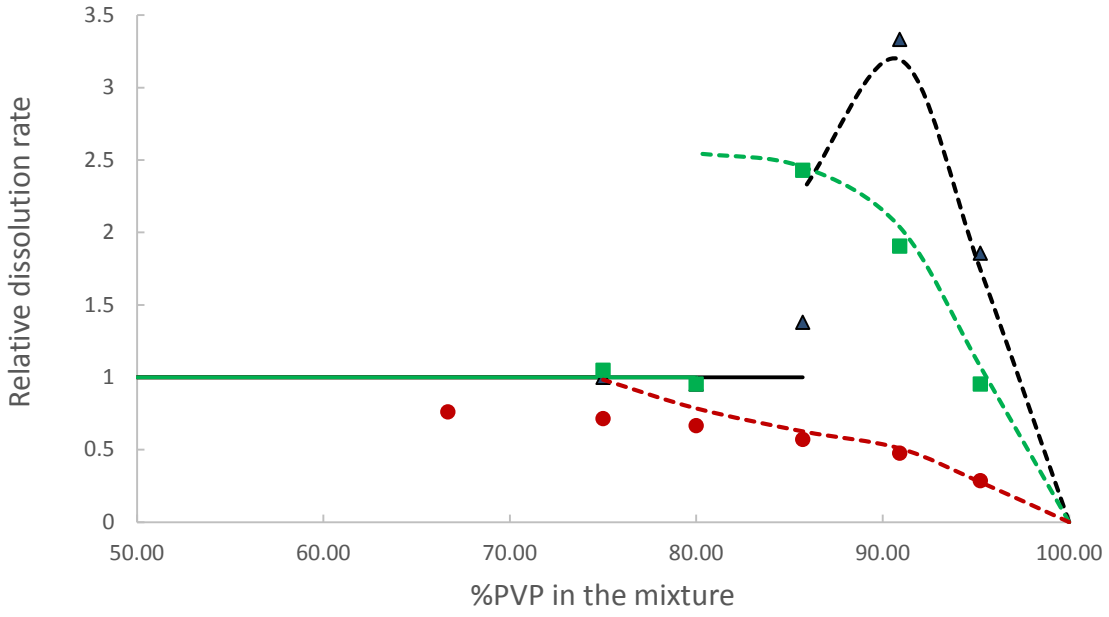

Figure 5-56: EtPABA relative dissolution rate vs %PVP in the dispersion compared to the new model predictions. The points are experimental results and lines are predictions (dashed lines represent polymer- controlled region and solid lines represent drug-controlled region). Black triangle: EtPABA-PVP K15; green square: EtPABA-PVP K30; red dot: EtPABA-PVP K90. (Assuming drug-controlled region starts at 6:1, 4:1 and 3:1 polymer:EtPABA ratios for PVPK15, K30 and K90, respectively).

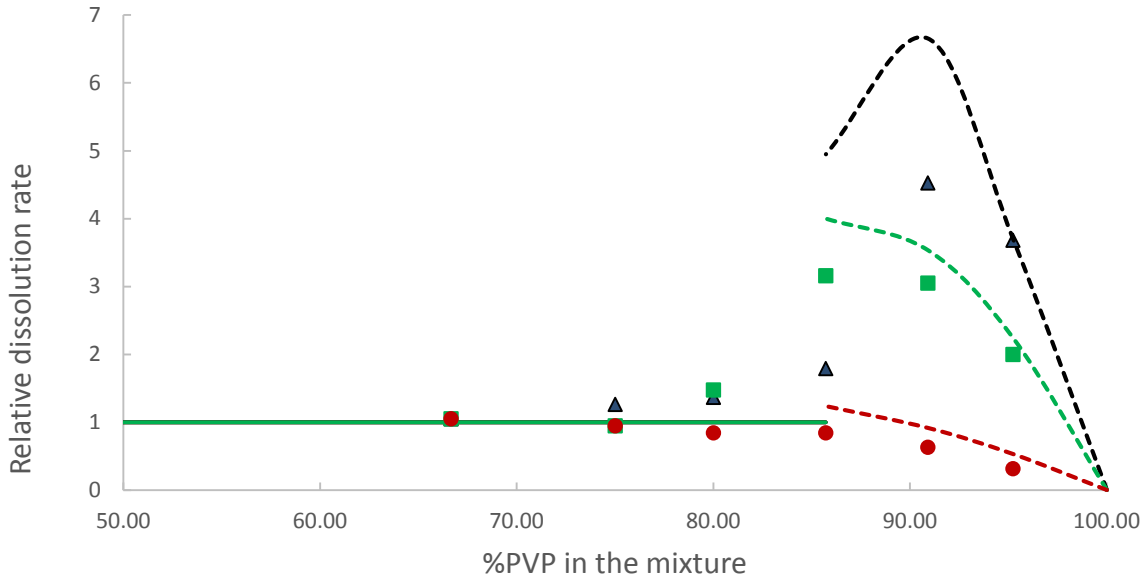

Figure 5-57: PrPABA relative dissolution rate vs %PVP in the dispersion compared to the new model predictions. The points are experimental results and lines are predictions (dashed lines represent polymer- controlled region and solid lines represent drug-controlled region). Black triangle: PrPABA-PVP K15; green square: PrPABA-PVP K30; red dot: PrPABA-PVP K90. (It is assumed drug controlling region starts at 6:1 polymer:PrPABA ratios for all PVPs).

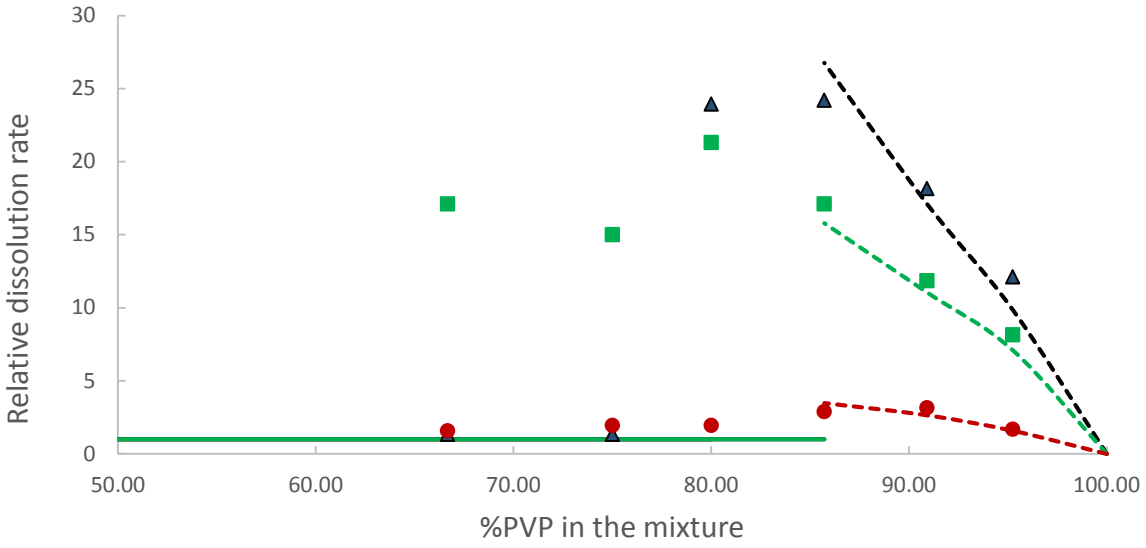

Figure 5-58: BuPABA relative dissolution rate vs %PVP in the dispersion compared to the new model predictions. The points are experimental results and lines are predictions (dashed lines represent polymer- controlled region and solid lines represent drug-controlled region). Black triangle: BuPABA-PVP K15; green square: BuPABA-PVP K30; red dot: BuPABA-PVP K90. (It is assumed drug controlling region starts at 6:1 polymer:BuPABA ratios for all PVPs).

5.5 Summary and Conclusions

The unique contributions and conclusions arising from this work on PABA ester-PVP dispersions can be summarized b**y:**

1) The lack of a general mathematical expression for the traditional approach for polymer-drug dispersion dissolution behavior limited other scientists from integrating this approach into their research. This work developed a model based on the concepts in the traditional approach to demonstrate the effects of drug intrinsic dissolution rate, carrier intrinsic dissolution rate, drug-

carrier interaction (K_{ass}) and dispersion composition on relative dissolution rates. Simulations of this model showed that for a general profile of relative dissolution rate vs carrier composition that relative dissolution rate first increases then decreases to eventually reach unity as drug loading increases. However, this model significantly underestimates the release behavior of poorly soluble compounds (i.e., $W_2 < 0.01$, Chapter 3) indicating poor predictability with this model.

2) The new model developed in this thesis was based on a solid dispersion consisting of two components (drug and carrier) and two phases (a continuous carrier phase and a discontinuous drug phase). With this assumption, a congruency of release occurs in the carrier-controlled region and pure drug release dominates in the drug-controlled region. In the carrier-controlled region, carrier dissolution rate, drug loading and drug precipitation can cause deviations from congruent release behavior and affect overall drug release rates. Whether the dispersion is in the carrier-controlled region or in the drug-controlled region is determined by both the dispersion composition and the precipitation tendency of the drug.

3) The traditional dispersion model is based on that assumption the dispersion acts as a physical mixture of drug and carrier. Because of this assumption dispersions are assumed to consist of two components (drug and carrier) and two discontinuous phases (i.e., carrier and drug phases). Therefore, this model assumes that the dispersion acts as a mixture of two small molecules combined with an empirical observation that drug and carrier release congruently in a particular composition region. Thus, release behavior is either in the empirical region (i.e., high carrier content) or in the mixture region and the two regions are characterized by separate mathematical expressions.

4) The new model developed in this work showed better correlations between PABA ester-PVP dispersion dissolution data than did the previous model. This is mainly due to the new model being based on a different view of a solid dispersion structure rather than the assumed physical mixture structure in the traditional approach. Secondly, the transition from carrier-controlled region to drug-controlled region is determined by both the dispersion compositions as well as drug precipitation. In the traditional approach these two regions are artificially connected. Finally, the carrier release reduction from a dispersion is addressed directly rather than assuming that carrier release remains constant as in the traditional approach.
5) A homologous series of small molecules (i.e., PABA esters) were used to blend with various molecular weight PVPs. This allowed examination of solid dispersion dissolution behavior in a systematic fashion for compounds of differing solubility but similar structure and to study PVP molecular weight effects on dispersion dissolution behavior. The results indicated that almost identical dispersion release behavior was achieved for this homologous series with the same MW carrier and same dispersion composition. Thus, the lower the intrinsic solubility/dissolution rate of the small molecule, the higher the relative dissolution rate obtained. This work also showed that the lower the intrinsic solubility/dissolution rate of the small molecule the more likely precipitation occurred during dissolution for a particular carrier and carrier:drug ratio. Thus, a drug with lower solubility moved from being carrier-controlled to drug-controlled at a higher carrier:drug ratio.
6) Using different molecular weights carriers (PVP K15, K30 and K90) showed that the higher the carrier dissolution rate, the higher dispersion release rates. Thus, the polymeric carriers' dissolution behavior affected dissolution rates of their dispersions to such an extent that the highest molecular weight carrier (K90) caused a reduction in dissolution rate of the small

molecule at all ratios rather than an increase seen with the two lower MW carriers (K15 and K30). This work also indicated that higher MW carriers inhibited drug precipitation more effectively during dissolution primarily due to a viscosity effect.

7) By monitoring both PABA ester and polymer (PVP) dissolution rates from dispersions a comparison of both components release behavior provided a picture of overall dispersion dissolution behavior. The simultaneous measurement of small molecule and carrier is unique in this work since most other reported studies only monitored the release of the small molecule (i.e., drug).
8) This work provides a more fundamental basis for estimating maximum dispersion release rates (or relative release rates) if intrinsic dissolution rates of carrier and drug are known and their degree of interaction. Before significant drug precipitation occurs, estimated maximum drug release rates can be calculated from intrinsic dissolution rates and dispersion compositions. Estimated maximum drug release rates are dependent on two parameters - one is the carrier release rate reduction due to the small molecule and the other is deviation from observed congruency of drug and carrier dissolution.
9) The complexation between carrier and drug (K_{ass}) in the new model is incorporated as a reduction in deviation from dissolution congruency. Thus, stronger interaction between carrier and drug reduces drug precipitation which reduces deviation from congruency. Similarly, the carrier viscosity effect in the new model is incorporated in the new model as an interaction effect. High carrier viscosity reduces drug precipitation which maintains congruency of drug and carrier but at the same time may reduce overall drug release rates regardless of dispersion composition.

APPENDIX A CALIBRATION CURVES

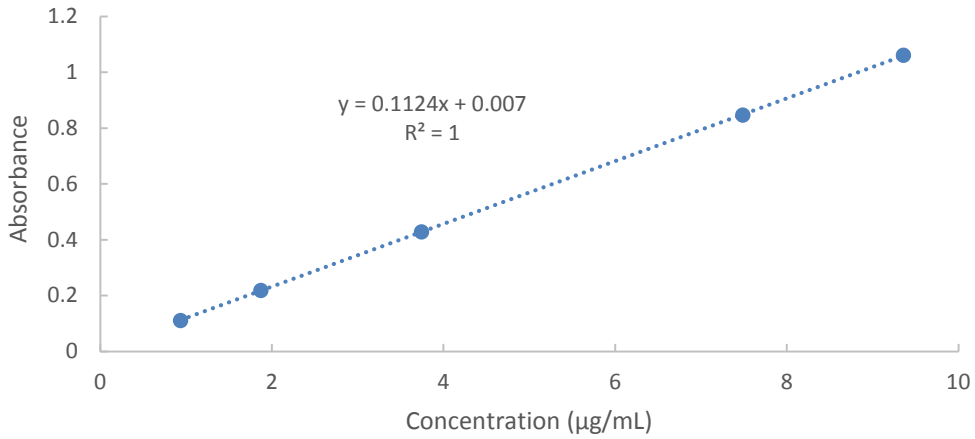

Figure A-1: UV calibration curve for MePABA at 285 nm.

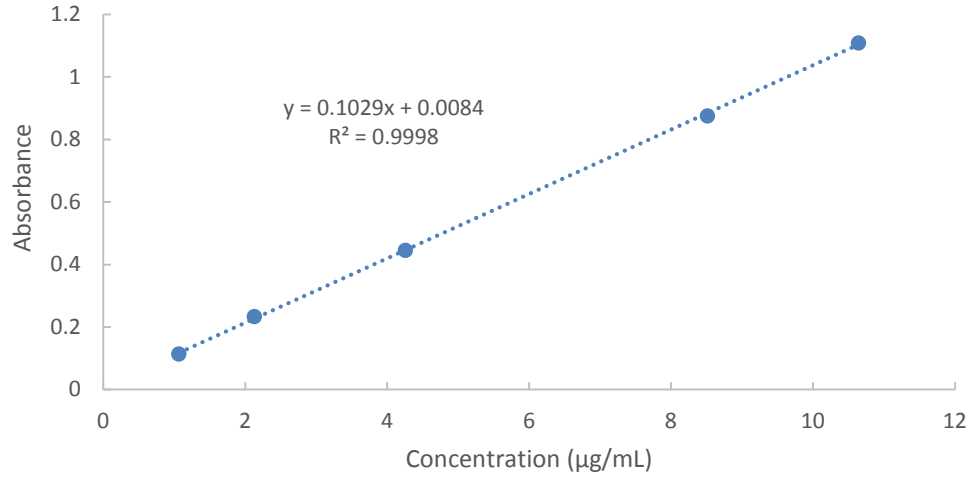

Figure A-2: UV calibration curve for EtPABA at 285nm.

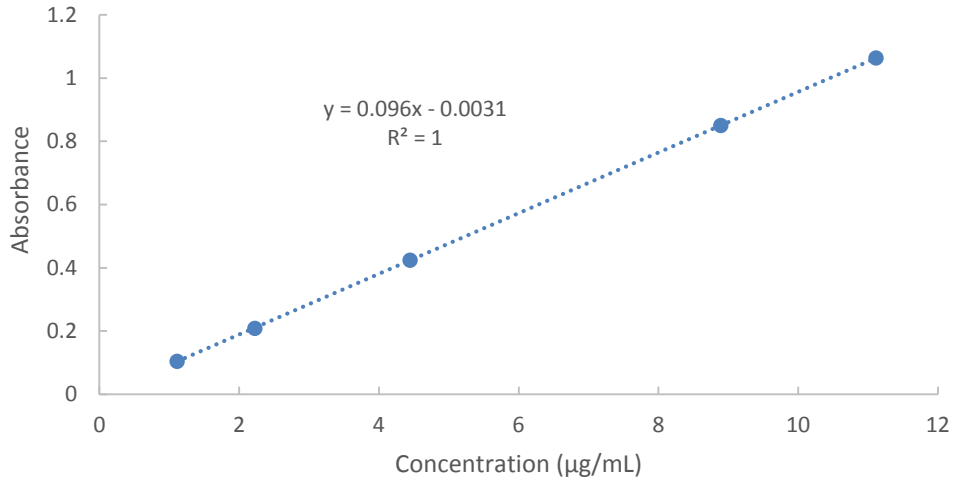

Figure A-3: UV calibration curve for PrPABA at 285nm.

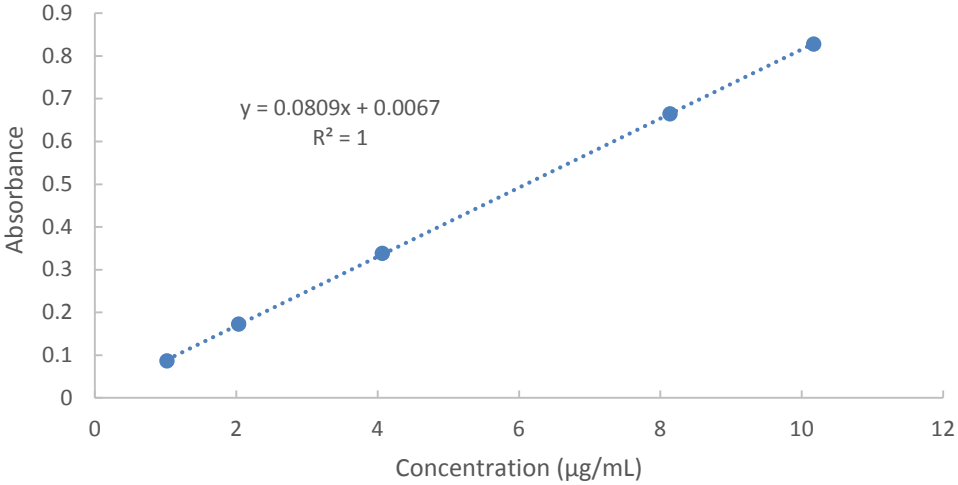

Figure A-4: UV calibration curve for BuPABA at 285nm.

APPENDIX B PVP UV SPECTRA

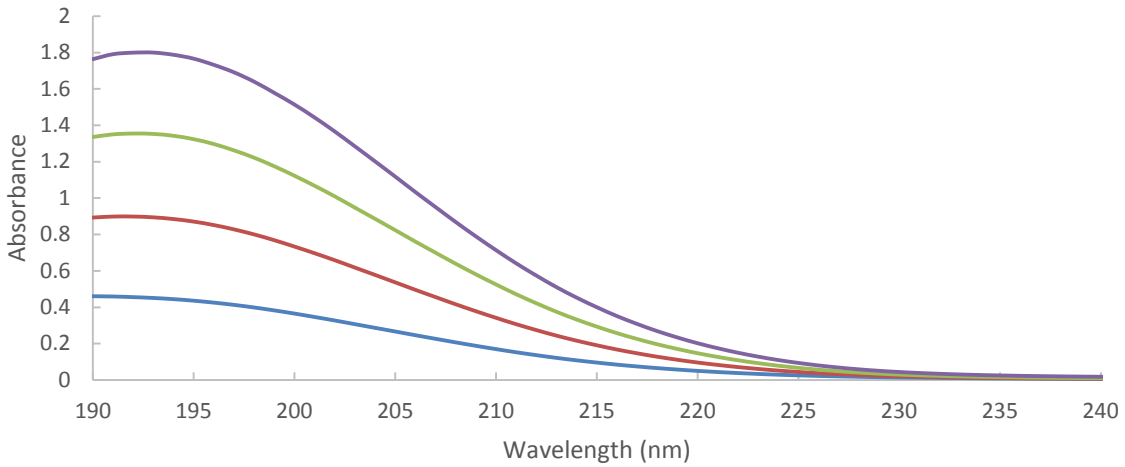

Figure B-1: UV spectra of PVP K15 standard solutions. From bottom to top: blue-40.52 µg/mL, red-81.04 µg/mL, green-121.56 µg/mL and purple-162.08 µg/mL.

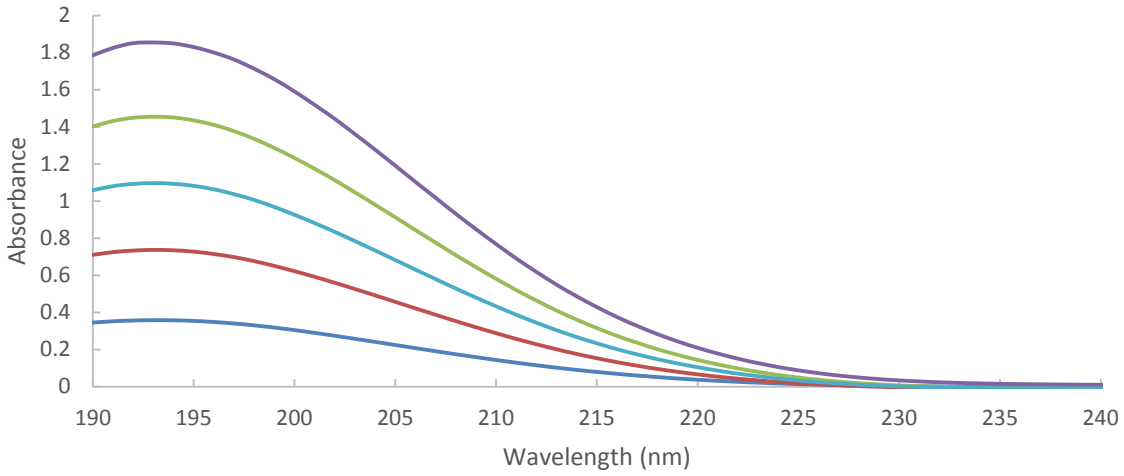

Figure B-2: UV spectra of PVP K30 standard solutions. From bottom to top: blue-38.95 µg/mL, red-71.81 µg/mL, green-107.72 µg/mL, purple-143.62 µg/mL and light blue-179.53 µg/mL.

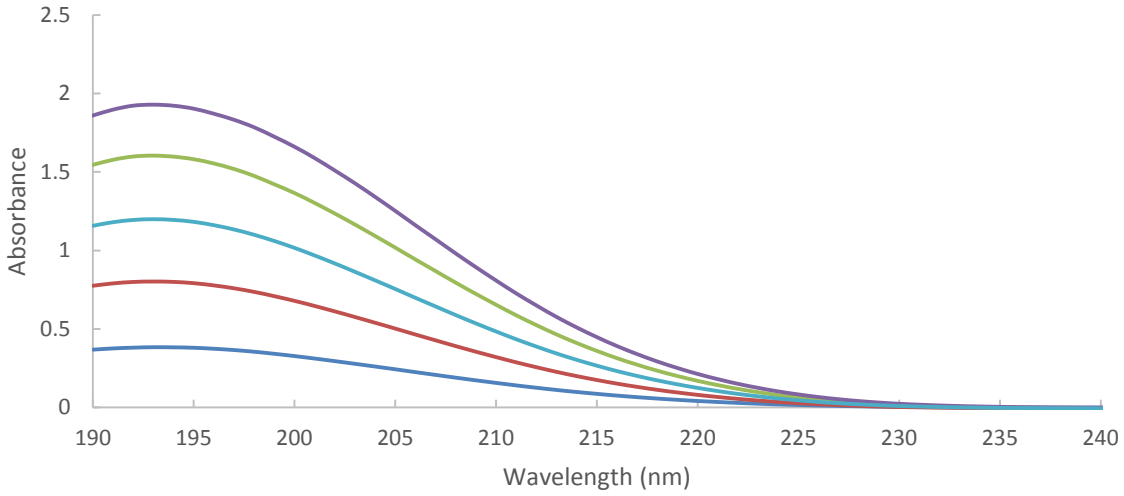

Figure B-3: UV spectra of PVP K90 standard solutions. From bottom to top: blue-30.02 µg/mL, red-76.03 µg/mL, green-114.05 µg/mL, purple-152.06 µg/mL and light blue-190.08 µg/mL.

APPENDIX C PABA ESTER-PVP ASSAY VALIDATIONS

Table C-1: Multi-component UV validation results for PVP K15/MePABA mixtures in water (195-325 nm; linear regression algorithm).

Prepared conc. (µg/mL)		Determined conc. (µg/mL)	
PVP K15	MePABA	PVP K15	MePABA
103.0	5.4	102.5	5.6
40.1	6.7	43.6	6.4
41.5	10.4	42.1	10.7
22.3	11.2	22.5	10.6

Table C-2: Multi-component UV validation results for PVP K30/MePABA mixtures in water (195-325 nm; linear regression algorithm).

Prepared conc. (µg/mL)		Determined conc. (µg/mL)	
PVP K30	MePABA	PVP K30	MePABA
88.3	4.4	83.4	4.5
89.1	8.9	88.8	8.9
55.2	9.2	63.1	9.4
44.8	11.2	49.1	11.0
29.4	14.7	27.8	14.5

Table C-3: Multi-component UV validation results for PVP K90/MePABA mixtures in water (195-325 nm; linear regression algorithm).

Prepared conc. (µg/mL)		Determined conc. (µg/mL)	
PVP K90	MePABA	PVP K90	MePABA
104.3	5.2	102.9	5.0
152.8	15.3	147.1	14.9
63.4	10.6	66.9	10.6
36.3	12.1	36.1	12.6
33.8	16.9	34.6	16.8

Table C-4: Multi-component UV validation results for PVP K15/EtPABA mixtures in water (195-325 nm; linear regression algorithm).

Prepared conc. (µg/mL)		Determined conc. (µg/mL)	
PVP K15	EtPABA	PVP K15	EtPABA
108.3	5.4	104.5	5.6
109.3	10.9	101.2	10.5
57.8	9.6	57.0	9.5
40.2	10.0	40.4	10.1
33.2	16.6	34.4	16.4

Table C-5: Multi-component UV validation results for PVP K30/EtPABA mixtures in water (195-325 nm; linear regression algorithm).

Prepared conc. (µg/mL)		Determined conc. (µg/mL)	
PVP K30	EtPABA	PVP K30	EtPABA
125.1	6.3	118.8	5.8
105.4	10.5	108.0	10.5
58.3	9.7	59.2	9.8
35.4	8.8	37.7	8.9
30.0	15.0	32.9	15.2

Table C-6: Multi-component UV validation results for PVP K90/EtPABA mixtures in water (195-325 nm; linear regression algorithm).

Prepared conc. (µg/mL)		Determined conc. (µg/mL)	
PVP K90	EtPABA	PVP K90	EtPABA
87.8	4.4	92.6	4.9
102.9	10.3	107.4	10.7
46.5	7.7	51.2	7.8
46.4	11.6	48.0	12.0
36.0	12.0	36.3	11.4

Table C-7: Multi-component UV validation results for PVP K15/PrPABA mixtures in water (195-325 nm; linear regression algorithm).

Prepared conc. (µg/mL)		Determined conc. (µg/mL)	
PVP K15	PrPABA	PVP K15	PrPABA
93.3	4.7	93.0	4.6
95.9	9.6	95.1	9.7
45.4	7.6	47.0	7.8
41.2	10.3	40.8	10.4
39.5	19.8	39.1	19.5

Table C-8: Multi-component UV validation results for PVP K30/PrPABA mixtures in water (195-325 nm; linear regression algorithm).

Prepared conc. (µg/mL)		Determined conc. (µg/mL)	
PVP K30	PrPABA	PVP K30	PrPABA
125.1	6.3	131.0	6.7
54.5	9.1	57.2	9.0
40.0	10.0	41.9	9.8
36.6	12.2	37.8	12.2
30.5	15.2	31.7	15.1

Table C-9: Multi-component UV validation results for PVP K90/PrPABA mixtures in water (195-325 nm; linear regression algorithm).

Prepared conc. (µg/mL)		Determined conc. (µg/mL)	
PVP K90	PrPABA	PVP K90	PrPABA
51.9	8.6	55.4	8.4
32.4	8.1	32.9	8.5
25.3	8.5	25.8	8.8
30.7	15.4	32.3	15.2

Table C-10: Multi-component UV validation results for PVP K15/BuPABA mixtures in water (195-325 nm; linear regression algorithm).

Prepared conc. (µg/mL)		Determined conc. (µg/mL)	
PVP K15	BuPABA	PVP K15	BuPABA
88.3	4.4	89.2	4.1
89.1	8.9	87.8	9.0
35.1	11.7	36.0	11.0
29.4	14.7	29.4	15.7

Table C-11: Multi-component UV validation results for PVP K30/BuPABA mixtures in water (195-325 nm; linear regression algorithm).

Prepared conc. (µg/mL)		Determined conc. (µg/mL)	
PVP K30	BuPABA	PVP K30	BuPABA
178.1	8.9	182.4	9.1
122.4	12.2	123.2	11.8
37.4	9.4	38.6	10.3
28.1	9.4	31.6	9.2
22.8	11.4	23.0	11.4

Table C-12: Multi-component UV validation results for PVP K90/BuPABA mixtures in water (195-325 nm; linear regression algorithm).

Prepared conc. (µg/mL)		Determined conc. (µg/mL)	
PVP K90	BuPABA	PVP K90	BuPABA
121.7	6.1	123.3	6.6
68.0	11.3	67.5	10.8
35.2	8.8	35.2	9.3
24.8	8.3	24.7	8.6
34.4	17.2	34.3	17.0

APPENDIX D DSC THERMOGRAMS

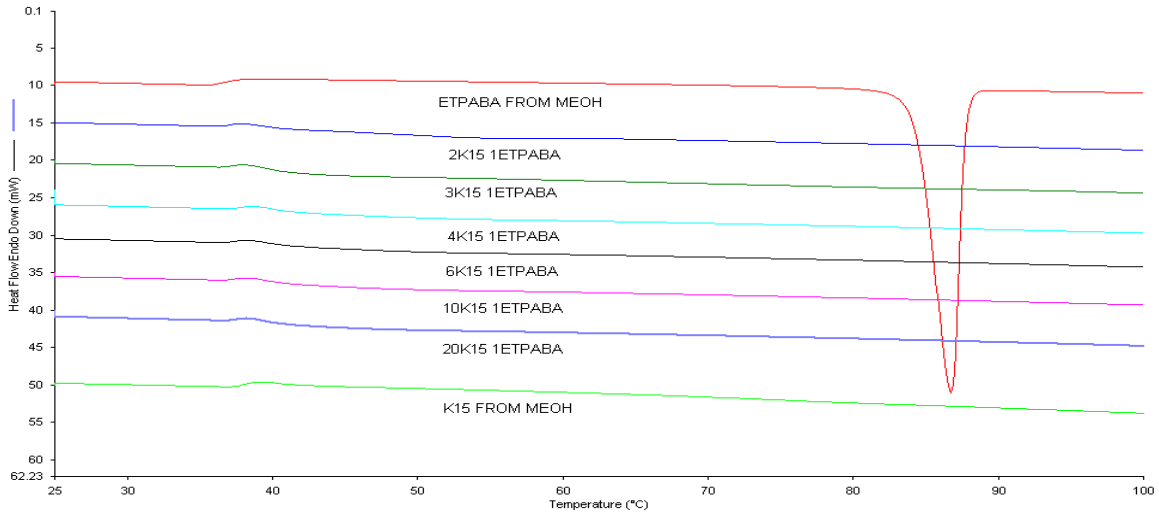

Figure D-1: DSC thermograms of EtPABA-K15 solid dispersions. From top to bottom: EtPABA (treated), PVP K15:EtPABA 2:1, PVP K15:EtPABA 3:1, PVP K15:EtPABA 4:1, PVP K15:EtPABA 6:1, PVP K15:EtPABA 10:1, PVP K15:EtPABA 20:1 and PVP K15 (treated).

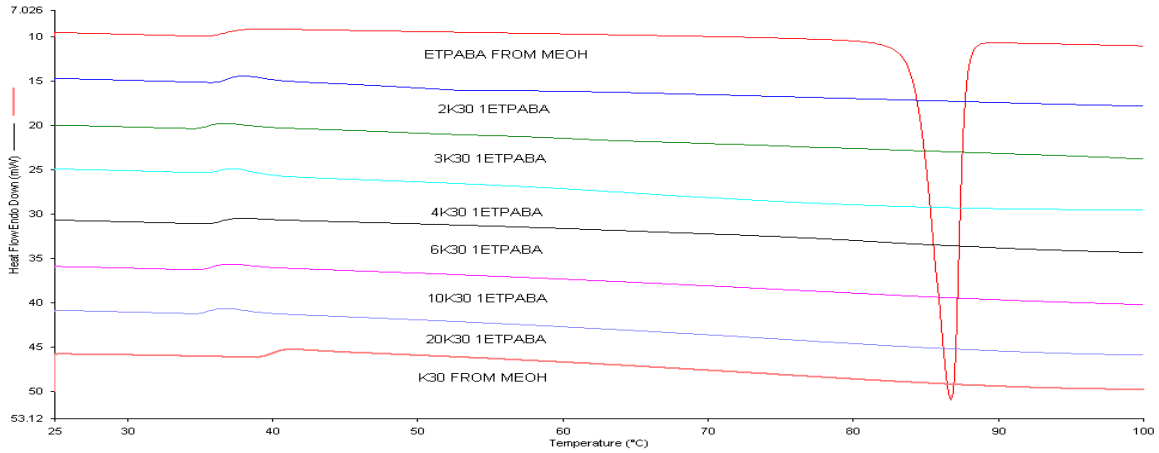

Figure D-2: DSC thermograms of EtPABA-K30 solid dispersions. From top to bottom: EtPABA (treated), PVP K30:EtPABA 2:1, PVP K30:EtPABA 3:1, PVP K30:EtPABA 4:1, PVP K30:EtPABA 6:1, PVP K30:EtPABA 10:1, PVP K30:EtPABA 20:1 and PVP K30 (treated).

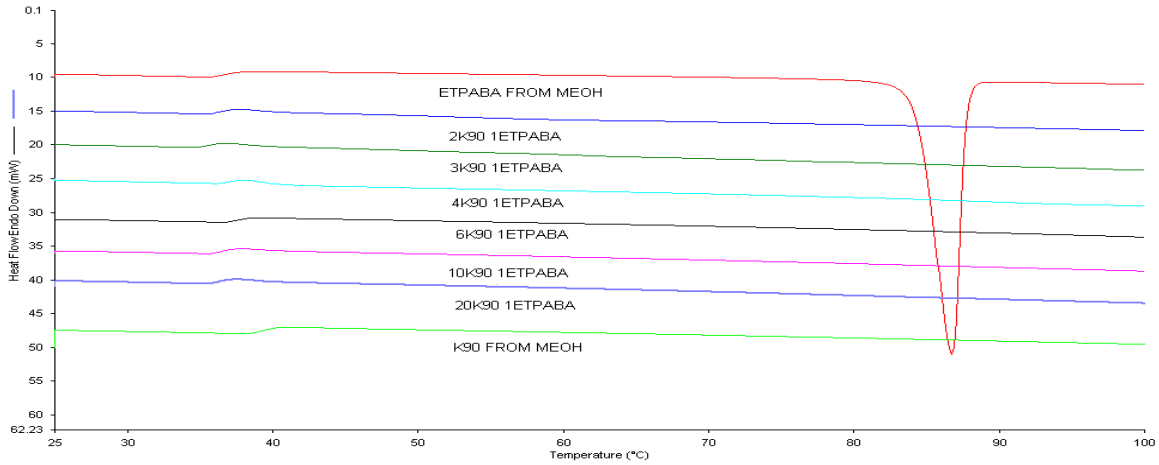

Figure D-3: DSC thermograms of EtPABA-K90 solid dispersions. From top to bottom: EtPABA (treated), PVP K90:EtPABA 2:1, PVP K90:EtPABA 3:1, PVP K90:EtPABA 4:1, PVP K90:EtPABA 6:1, PVP K90:EtPABA 10:1, PVP K90:EtPABA 20:1 and PVP K90 (treated).

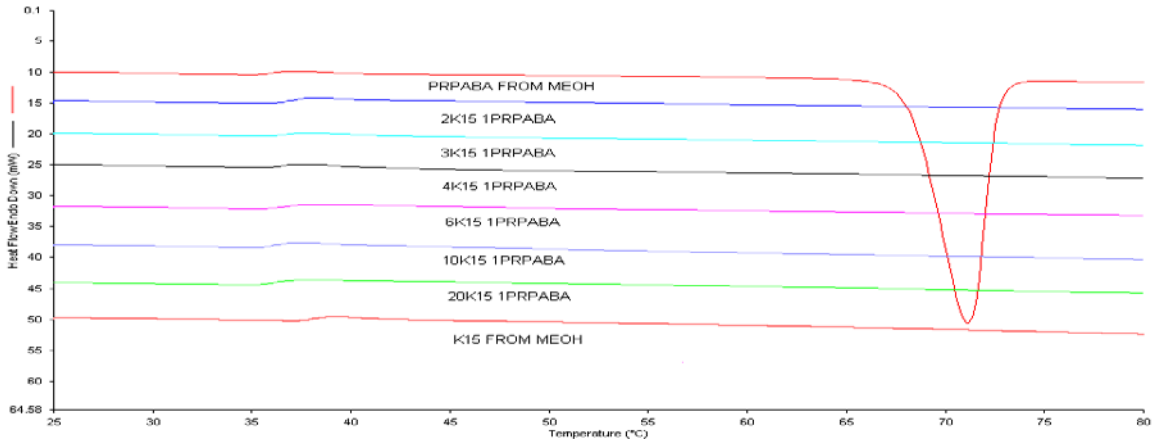

Figure D-4: DSC thermograms of PrPABA-K15 solid dispersions. From top to bottom: PrPABA (treated), PVP K15:PrPABA 2:1, PVP K15:PrPABA 3:1, PVP K15:PrPABA 4:1, PVP K15:PrPABA 6:1, PVP K15:PrPABA 10:1, PVP K15:PrPABA 20:1 and PVP K15 (treated).

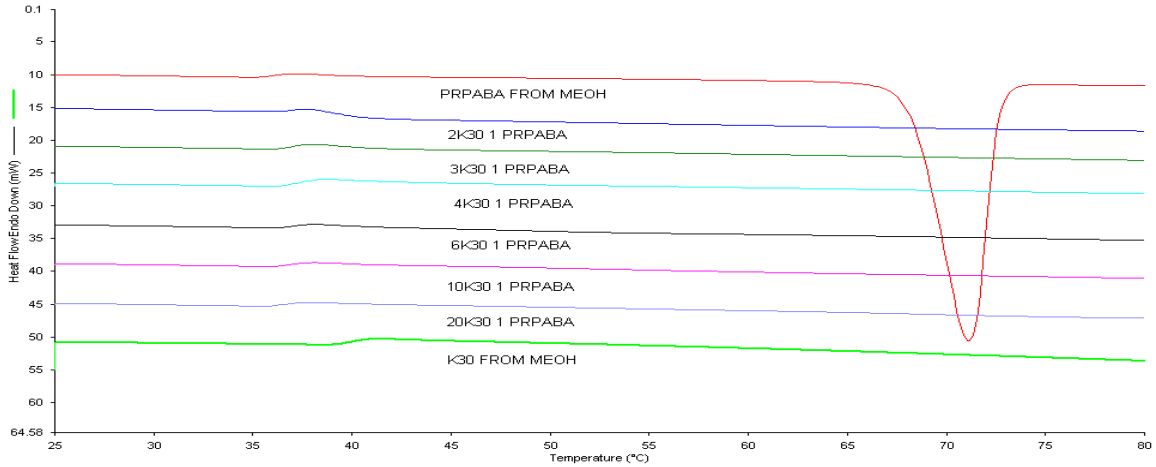

Figure D-5: DSC thermograms of PrPABA-K30 solid dispersions. From top to bottom: PrPABA (treated), PVP K30:PrPABA 2:1, PVP K30:PrPABA 3:1, PVP K30:PrPABA 4:1, PVP K30:PrPABA 6:1, PVP K30:PrPABA 10:1, PVP K30:PrPABA 20:1 and PVP K30 (treated).

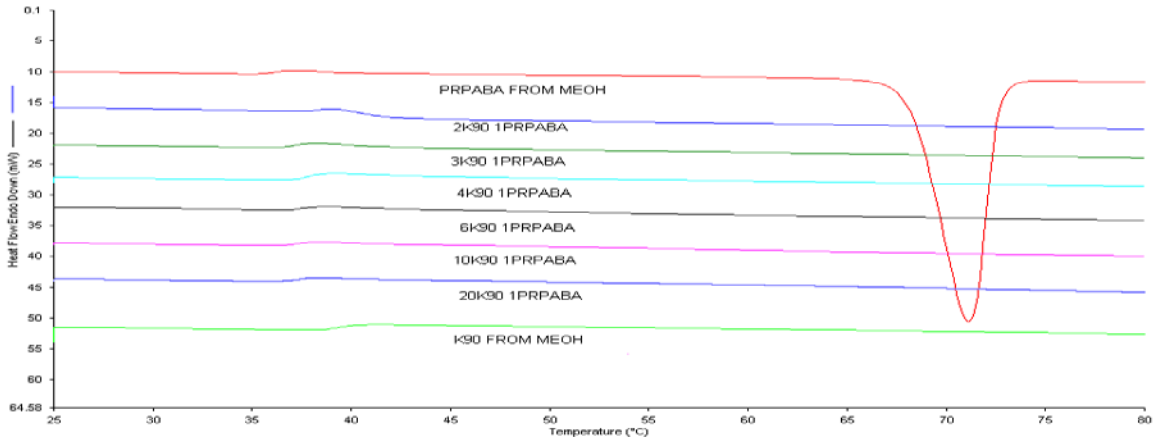

Figure D-6: DSC thermograms of PrPABA-K90 solid dispersions. From top to bottom: PrPABA (treated), PVP K90:PrPABA 2:1, PVP K90:PrPABA 3:1, PVP K90:PrPABA 4:1, PVP K90:PrPABA 6:1, PVP K90:PrPABA 10:1, PVP K90:PrPABA 20:1 and PVP K90 (treated).

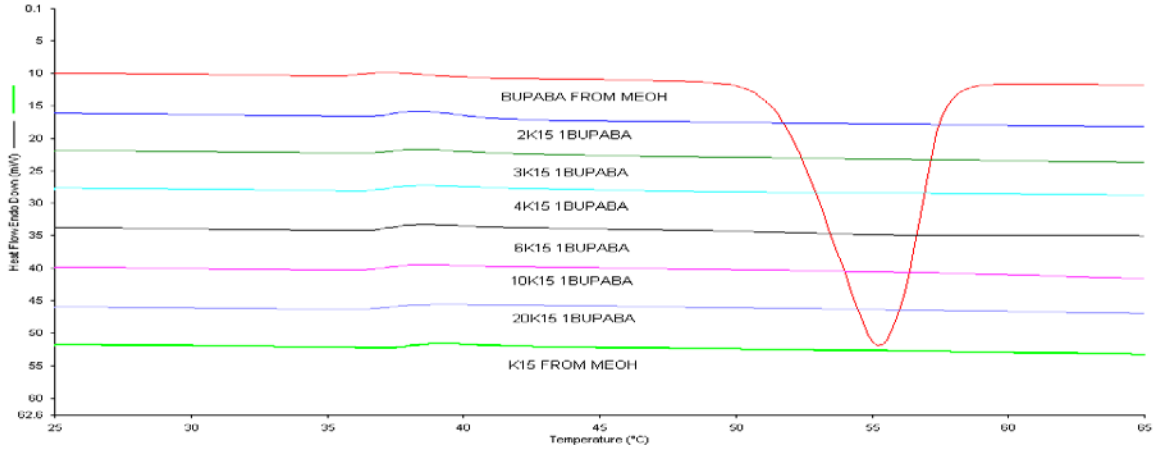

Figure D-7: DSC thermograms of BuPABA-K15 solid dispersions. From top to bottom: BuPABA (treated), PVP K15:BuPABA 2:1, PVP K15:BuPABA 3:1, PVP K15:BuPABA 4:1, PVP K15:BuPABA 6:1, PVP K15:BuPABA 10:1, PVP K15:BuPABA 20:1 and PVP K15 (treated).

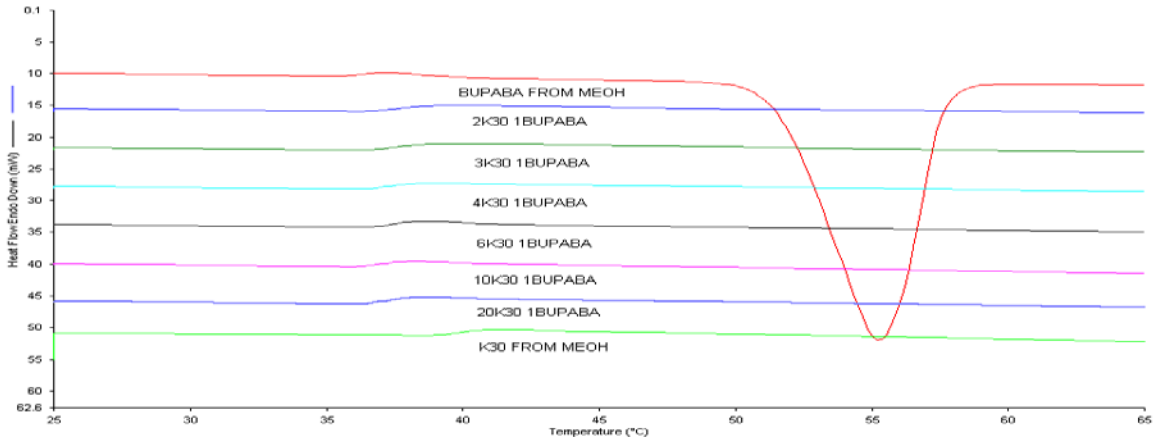

Figure D-8: DSC thermograms of BuPABA-K30 solid dispersions. From top to bottom: BuPABA (treated), PVP K30:BuPABA 2:1, PVP K30:BuPABA 3:1, PVP K30:BuPABA 4:1, PVP K30:BuPABA 6:1, PVP K30:BuPABA 10:1, PVP K30:BuPABA 20:1 and PVP K30 (treated).

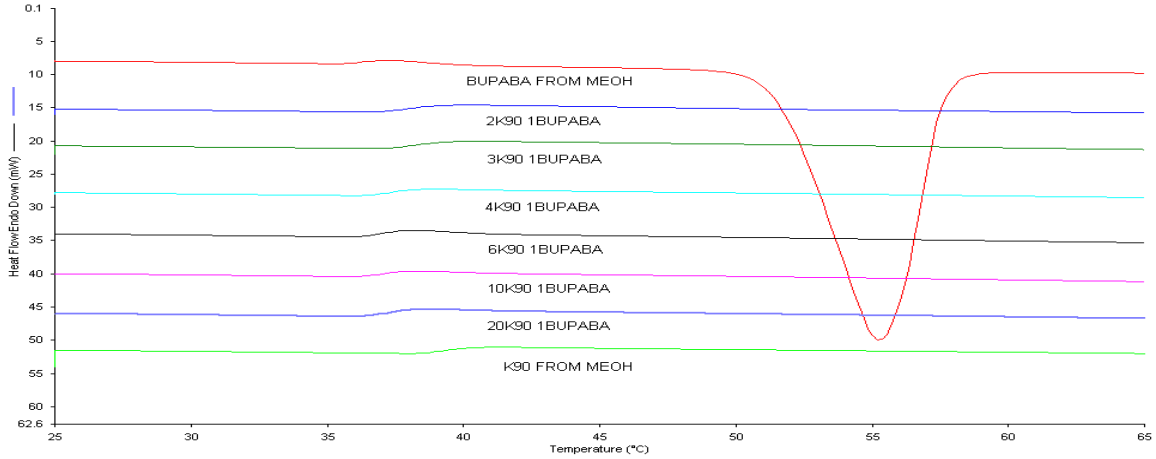

Figure D-9: DSC thermograms of BuPABA-K90 solid dispersions. From top to bottom: BuPABA (treated), PVP K90:BuPABA 2:1, PVP K90:BuPABA 3:1, PVP K90:BuPABA 4:1, PVP K90:BuPABA 6:1, PVP K90:BuPABA 10:1, PVP K90:BuPABA 20:1 and PVP K90 (treated).

APPENDIX E PXRD DIFFRACTOGRAMS

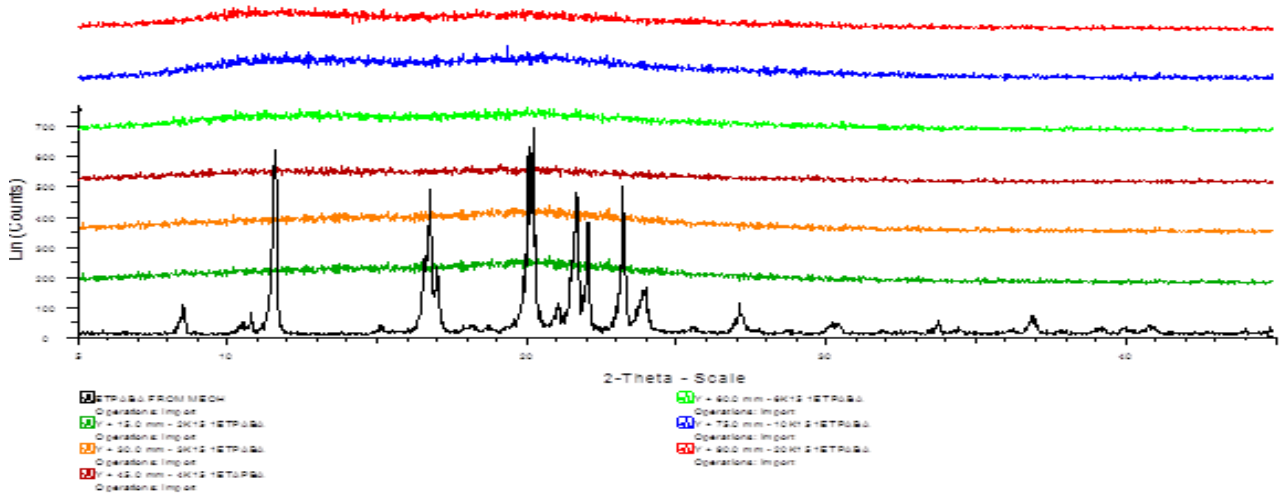

Figure E-1: X-ray diffractograms of EtPABA-K15 solid dispersions. From top to bottom: PVP K15:EtPABA 20:1, PVP K15:EtPABA 10:1, PVP K15:EtPABA 6:1, PVP K15:EtPABA 4:1, PVP K15:EtPABA 3:1, PVP K15:EtPABA 2:1 and EtPABA (treated).

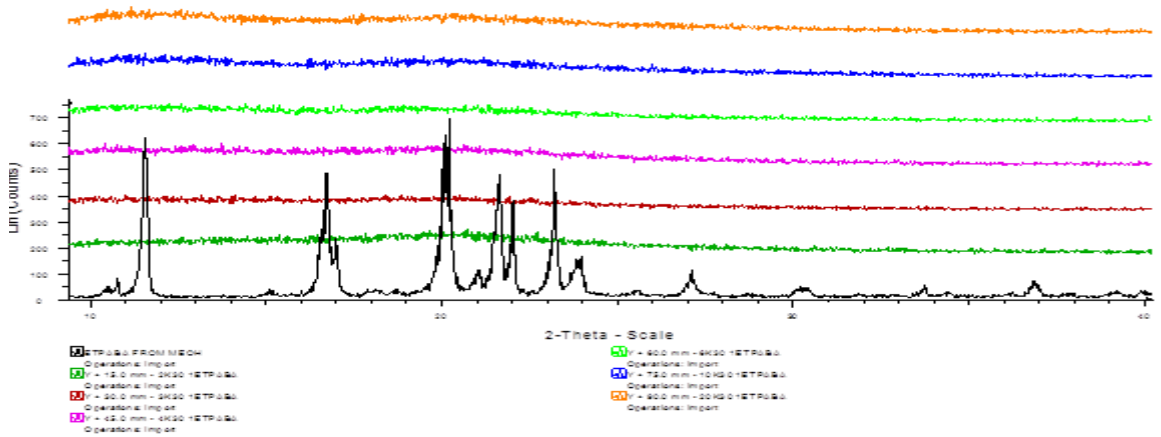

Figure E-2: X-ray diffractograms of EtPABA-K30 solid dispersions. From top to bottom: PVP K30:EtPABA 20:1, PVP K30:EtPABA 10:1, PVP K30:EtPABA 6:1, PVP K30:EtPABA 4:1, PVP K30:EtPABA 3:1, PVP K30:EtPABA 2:1 and EtPABA (treated).

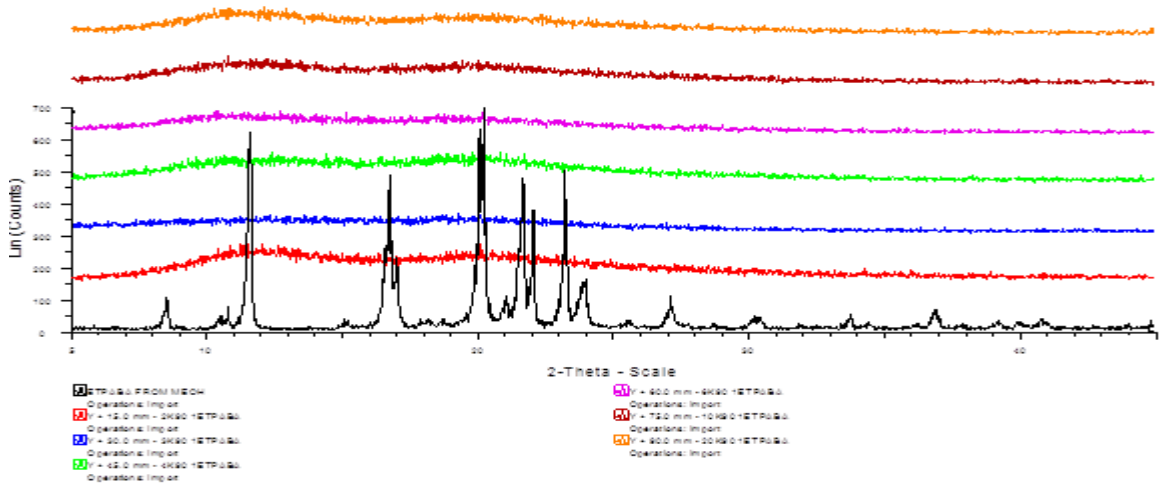

Figure E-3: X-ray diffractograms of EtPABA-K90 solid dispersions. From top to bottom: PVP K90:EtPABA 20:1, PVP K90:EtPABA 10:1, PVP K90:EtPABA 6:1, PVP K90:EtPABA 4:1, PVP K90:EtPABA 3:1, PVP K90:EtPABA 2:1 and EtPABA (treated).

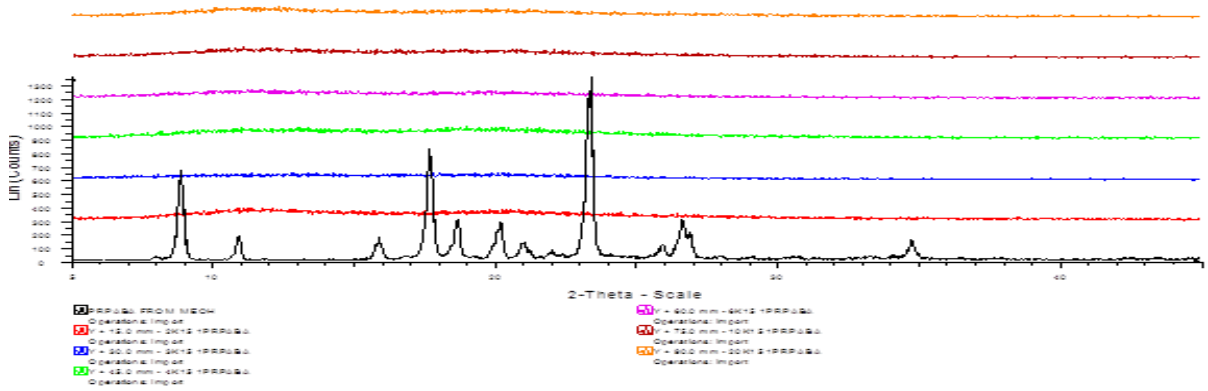

Figure E-4: X-ray diffractograms of PrPABA-K15 solid dispersions. From top to bottom: PVP K15:PrPABA 20:1, PVP K15:PrPABA 10:1, PVP K15:PrPABA 6:1, PVP K15:PrPABA 4:1, PVP K15:PrPABA 3:1, PVP K15:PrPABA 2:1 and PrPABA (treated).

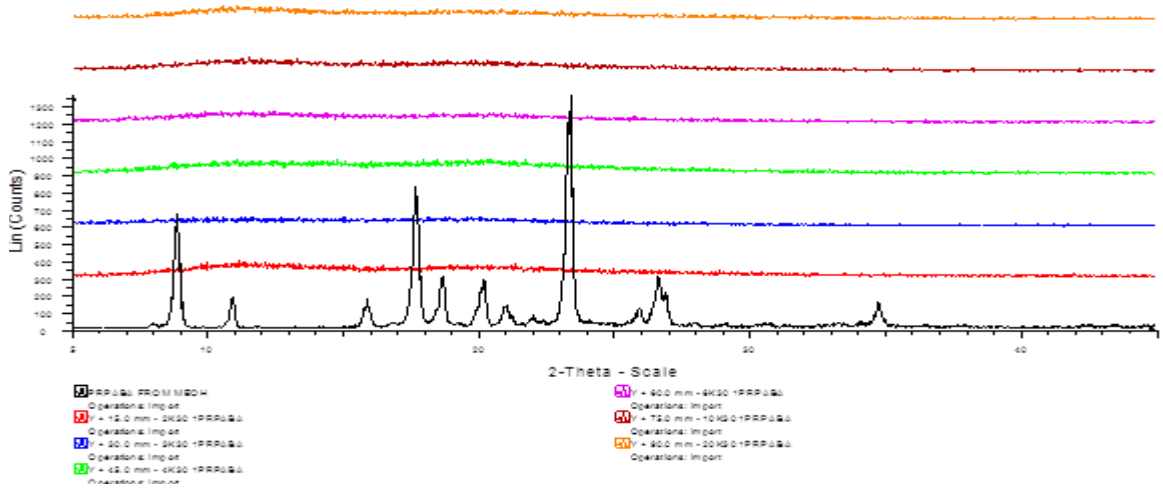

Figure E-5: X-ray diffractograms of PrPABA-K30 solid dispersions. From top to bottom: PVP K30:PrPABA 20:1, PVP K30:PrPABA 10:1, PVP K30:PrPABA 6:1, PVP K30:PrPABA 4:1, PVP K30:PrPABA 3:1, PVP K30:PrPABA 2:1 and PrPABA (treated).

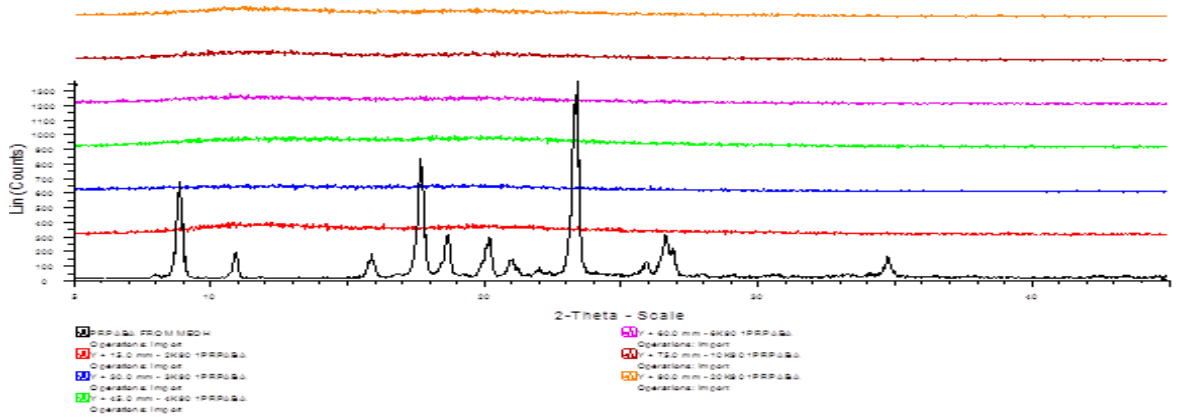

Figure E-6: X-ray diffractograms of PrPABA-K90 solid dispersions. From top to bottom: PVP K90:PrPABA 20:1, PVP K90:PrPABA 10:1, PVP K90:PrPABA 6:1, PVP K90:PrPABA 4:1, PVP K90:PrPABA 3:1, PVP K90:PrPABA 2:1 and PrPABA (treated).

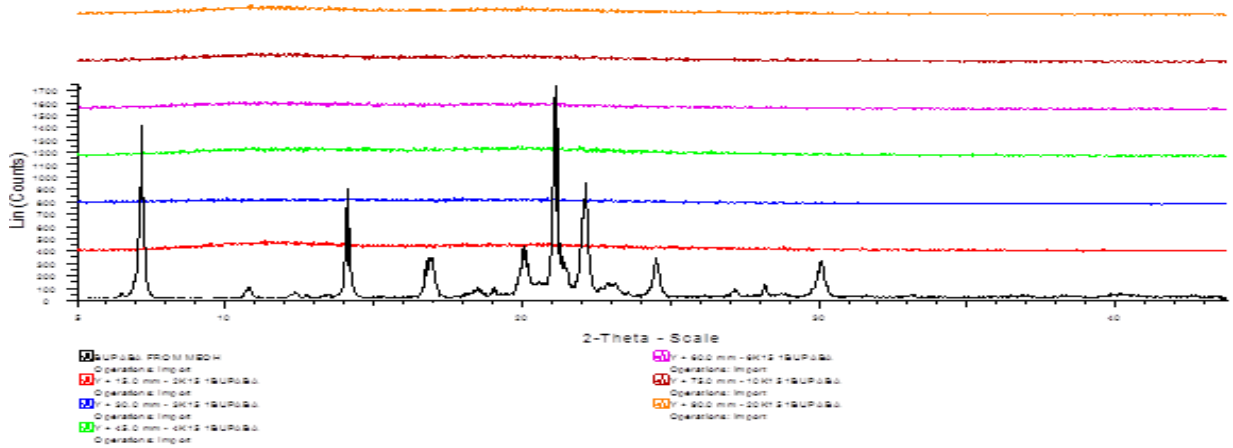

Figure E-7: X-ray diffractograms of BuPABA-K15 solid dispersions. From top to bottom: PVP K15:BuPABA 20:1, PVP K15:BuPABA 10:1, PVP K15:BuPABA 6:1, PVP K15:BuPABA 4:1, PVP K15:BuPABA 3:1, PVP K15:BuPABA 2:1 and BuPABA (treated).

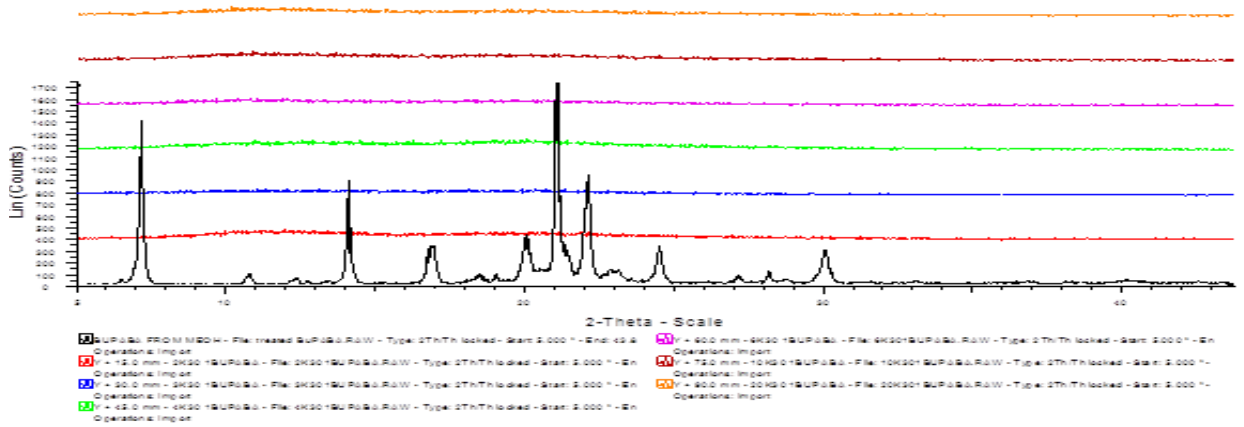

Figure E-8: X-ray diffractograms of BuPABA-K30 solid dispersions. From top to bottom: PVP K30:BuPABA 20:1, PVP K30:BuPABA 10:1, PVP K30:BuPABA 6:1, PVP K30:BuPABA 4:1, PVP K30:BuPABA 3:1, PVP K30:BuPABA 2:1 and BuPABA (treated).

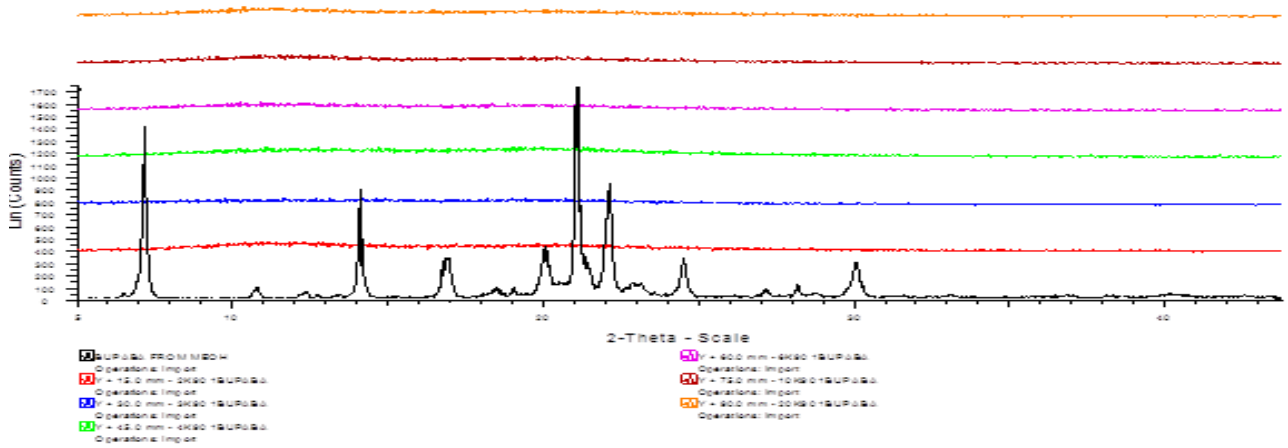

Figure E-9: X-ray diffractograms of BuPABA-K90 solid dispersions. From top to bottom: PVP K90:BuPABA 20:1, PVP K90:BuPABA 10:1, PVP K90:BuPABA 6:1, PVP K90:BuPABA 4:1, PVP K90:BuPABA 3:1, PVP K90:BuPABA 2:1 and BuPABA (treated).

APPENDIX F TREATED COMPONENT DISSOLUTION PROFILES

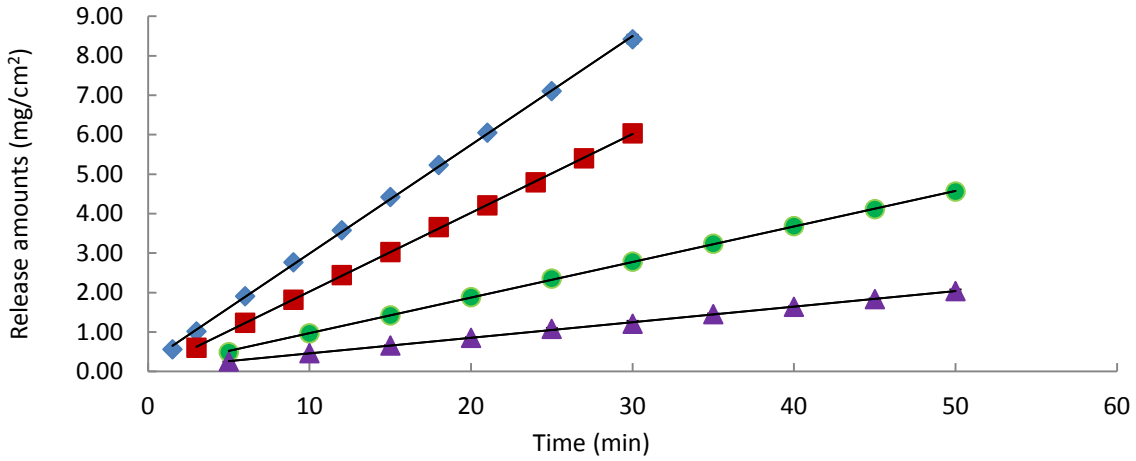

Figure F-1: Rotating disk intrinsic release profiles of treated PABA esters (n=3) at 37 °C at 100 rpm. The data are represented as: blue diamond-MePABA, red square-EtPABA, green dot-PrPABA and purple triangle-BuPABA.

Table F-1: Rotating disk intrinsic release rates of treated PABA esters (n=3) at 37 ºC at 100 rpm.

	Slope (mg/cm^2·min)	Intercept (mg/cm^2)	R^2
MePABA	0.28	0.23	0.9996
EtPABA	0.20	0.026	0.9999
PrPABA	0.09	0.067	0.9999
BuPABA	0.039	0.063	0.9992

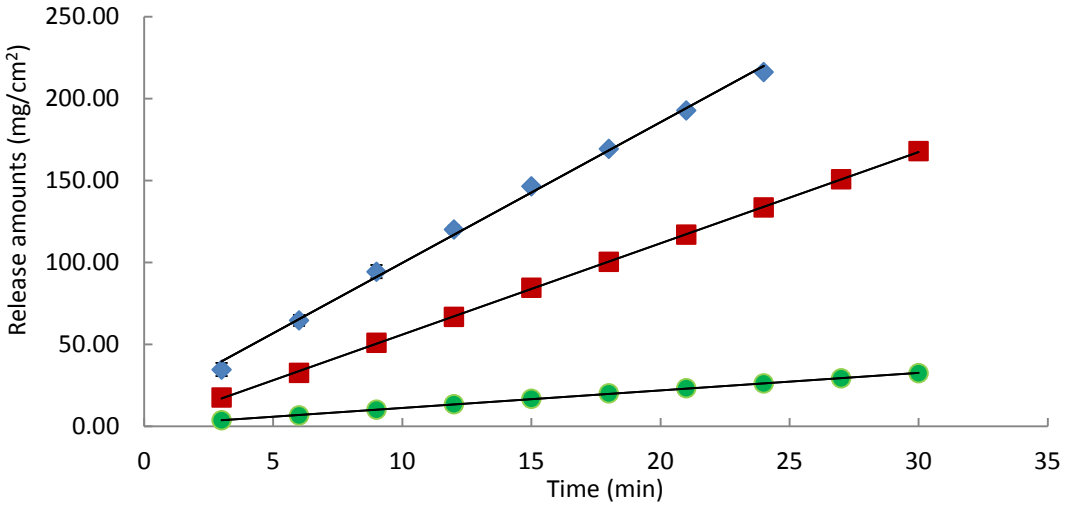

Figure F-2: Rotating disk intrinsic release profiles of treated PABA esters (n=3) at 37 °C at 100 rpm. The data are represented as: blue diamond-PVP K15, red square-PVP K30 and green dot-PVP K90.

Table F-2: Rotating disk intrinsic release rates of treated PVPs (n=3) at 37 ºC at 100 rpm.

	Slope (mg/cm^2·min)	Intercept (mg/cm^2)	R^2
PVP K15	8.6	13.93	0.9973
PVP K30	5.6	0.24	0.9999
PVP K90	1.1	0.59	0.9995

APPENDIX G PHYSICAL MIXTURE DISSOLUTION BEHAVIOR

Figure G-1: Pictures of 6:1 physical mixtures (PVP K15: EtPABA) after release in water (left) or saturated EtPABA solution (right). Both surfaces have receded equally into the disc.

Figure G-2: Pictures of 2:1 physical mixtures (PVP K15: EtPABA) after release in water (left) or saturated EtPABA solution (right). Left surface has receded into the disc while the left surface shows no receding.

Table G-1: Surface integrity results of PVP-EtPABA mixtures after release in water and saturated EtPABA solution at 37 ºC.

Physical mixture	PVP K15-EtPABA (in water)	PVP K15-EtPABA (in saturated EtPABA solution)	PVP K30-EtPABA (in water)	PVP K30-EtPABA (in saturated EtPABA solution)
20:1	recede	recede	recede	recede
10:1	recede	recede	recede	recede
6:1	recede	recede	recede	recede
4:1	recede	recede	recede	recede
2:1	recede	not receded	recede	not receded

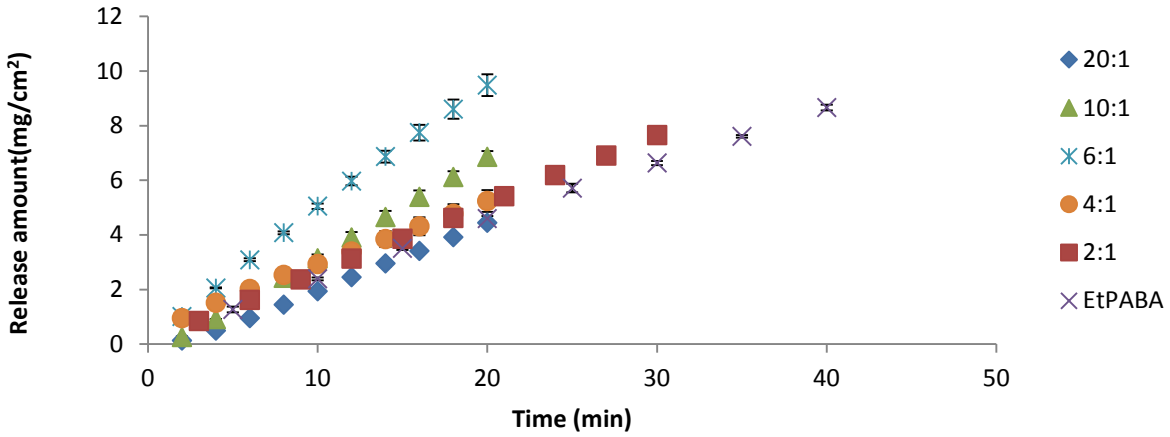

Figure G-3: Rotating disk intrinsic release profiles of EtPABA from PVP K15-EtPABA physical mixtures at 37 ºC at 100 rpm (n=3).

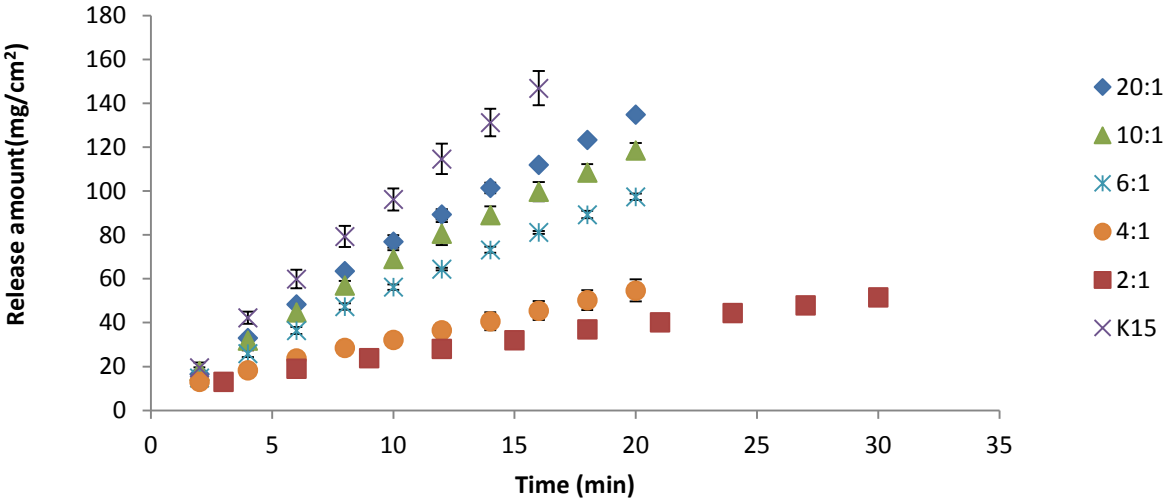

Figure G-4: Rotating disk intrinsic release profiles of PVP K15 from PVP K15-EtPABA physical mixtures at 37 ºC at 100 rpm (n=3).

Table G-2: Rotating disk intrinsic release rates of PVP K15-EtPABA physical mixtures at 37 ºC at 100 rpm.

Solid nominal ratio	PVP K15[a] release rate (mg/cm^2·min)	EtPABA[a] release rate (mg/cm^2·min)	PVP:PABA ester release rate ratio	Physical mixture assay ratio	% Deviation
20:1	6.49 (0.994)	0.24 (0.999)	27.4	22.2	21.8
10:1	5.53 (0.995)	0.37 (0.999)	15.0	11.8	35.9
6:1	4.52 (0.996)	0.47 (0.999)	9.6	7.1	34.9
4:1	2.27 (0.998)	0.23 (0.999)	9.9	4.0	149.2
2:1	1.40 (0.995)	0.25 (0.999)	5.6	2.0	173.2

[a] in parentheses - R^2

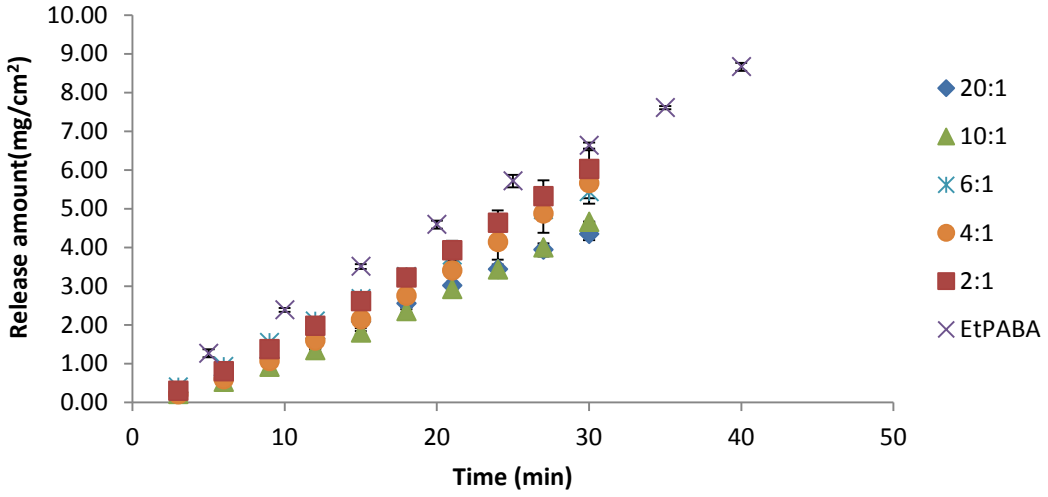

Figure G-5: Rotating disk intrinsic release profiles of EtPABA from PVP K30-EtPABA physical mixtures at 37 ºC at 100 rpm (n=3).

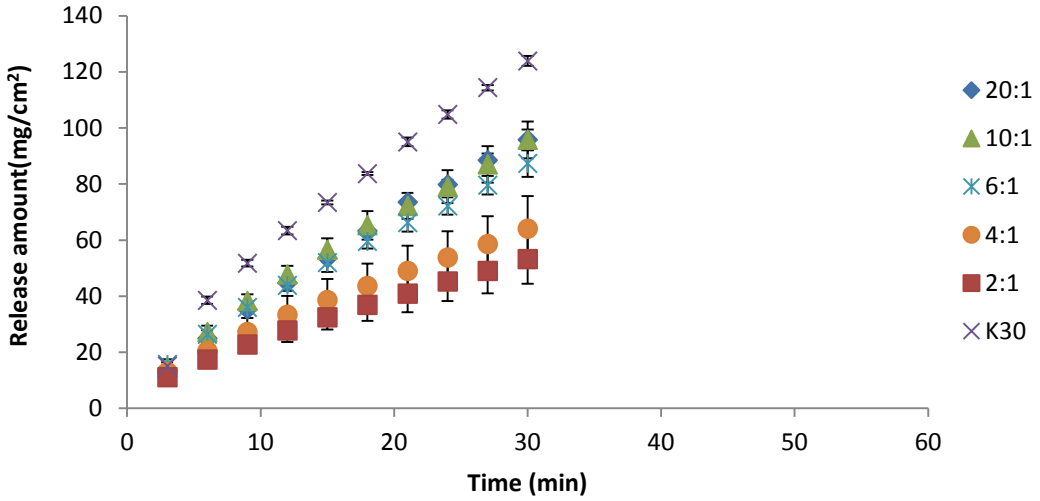

Figure G-6: Rotating disk intrinsic release profiles of PVP K30 from PVP K30-EtPABA physical mixtures at 37 ºC at 100 rpm (n=3).

Table G-3: Rotating disk intrinsic release rates of PVP K30-EtPABA physical mixtures at 37 ºC a 100 rpm.

Solid nominal ratio	PVP K30[a] release rate ($mg/cm^2 \cdot min$)	EtPABA[a] release rate ($mg/cm^2 \cdot min$)	PVP:PABA ester release rate ratio	Physical mixture assay ratio	% Deviation
20:1	3.04 (0.996)	0.15 (0.999)	20.3	22.8	11.3
10:1	2.90 (0.991)	0.19 (0.999)	15.3	15.3	0.0
6:1	2.57 (0.994)	0.17 (0.991)	15.1	6.8	121
4:1	1.84 (0.995)	0.2 (0.990)	9.2	5.0	83.3
2:1	1.53 (0.997)	0.21 (0.998)	7.3	2.7	169.8

[a] in parentheses - R^2

REFERENCES

1. Williams HD, Trevaskis NL, Charman SA, Shanker RM, Charman WN, Pouton CW, Porter CJ 2013. Strategies to address low drug solubility in discovery and development. Pharmacol Rev 65(1):315-499.
2. Rumondor AC, Ivanisevic I, Bates S, Alonzo DE, Taylor LS 2009. Evaluation of drug-polymer miscibility in amorphous solid dispersion systems. Pharm Res 26(11):2523-2534.
3. Vo CL, Park C, Lee BJ 2013. Current trends and future perspectives of solid dispersions containing poorly water-soluble drugs. Eur J Pharm Biopharm 85(3 Pt B):799-813.
4. Kawabata Y, Wada K, Nakatani M, Yamada S, Onoue S 2011. Formulation design for poorly water-soluble drugs based on biopharmaceutics classification system: basic approaches and practical applications. Int J Pharm 420(1):1-10.
5. Berge SM, Bighley LD, Monkhouse DC 1977. Pharmaceutical salts. J Pharm Sci 66(1):1-19.
6. Rautio J, Kumpulainen H, Heimbach T, Oliyai R, Oh D, Jarvinen T, Savolainen J 2008. Prodrugs: design and clinical applications. Nat Rev Drug Discov 7(3):255-270.
7. Loftsson T, Duchene D 2007. Cyclodextrins and their pharmaceutical applications. Int J Pharm 329(1-2):1-11.
8. Rodriguez-Spong B, Price CP, Jayasankar A, Matzger AJ, Rodriguez-Hornedo N 2004. General principles of pharmaceutical solid polymorphism: a supramolecular perspective. Adv Drug Deliv Rev 56(3):241-274.
9. Mosharraf M, Nystrom C 1995. The effect of particle-size and shape on the surface specific dissolution rate of microsized practically insoluble drugs. Int J Pharm 122(1-2):35-47.
10. Chiou WL, Riegelman S 1971. Pharmaceutical applications of solid dispersion systems. J Pharm Sci 60(9):1281-1302.
11. Chokshi RJ, Zia H, Sandhu HK, Shah NH, Malick WA 2007. Improving the dissolution rate of poorly water soluble drug by solid dispersion and solid solution: pros and cons. Drug delivery 14(1):33-45.
12. Ford JL 1986. The current status of solid dispersions. Pharm Acta Helv 61(3):69-88.
13. Janssens S, Van den Mooter G 2009. Review: physical chemistry of solid dispersions. J Pharm Pharmacol 61(12):1571-1586.
14. Serajuddin AT 1999. Solid dispersion of poorly water-soluble drugs: early promises, subsequent problems, and recent breakthroughs. J Pharm Sci 88(10):1058-1066.
15. Vasconcelos T, Sarmento B, Costa P 2007. Solid dispersions as strategy to improve oral bioavailability of poor water soluble drugs. Drug Discov Today 12(23-24):1068-1075.
16. Sekiguchi K, Obi N 1961. Studies on absorption of eutectic mixture .1. comparison of behavior of eutectic mixture of sulfathiazole and that of ordinary sulfathiazole in man. Chem Pharm Bull 9(11):866-872.
17. Leuner C, Dressman J 2000. Improving drug solubility for oral delivery using solid dispersions. Eur J Pharm Biopharm 50(1):47-60.
18. Allen LV, Jr., Yanchick VA, Maness DD 1977. Dissolution rates of corticosteroids utilizing sugar glass dispersions. J Pharm Sci 66(4):494-497.
19. Corrigan OI, Murphy CA, Timoney RF 1979. Dissolution properties of polyethylene glycols and polyethylene glycol drug systems. Int J Pharm 4(1):67-74.
20. Simonell.Ap, Mehta SC, Higuchi WI 1969. Dissolution rates of high energy polyvinylpyrrolidone (PVP)-sulfathiazole coprecipitates. J Pharm Sci 58(5):538-549.
21. Okimoto K, Miyake M, Ibuki R, Yasumura M, Ohnishi N, Nakai T 1997. Dissolution mechanism and rate of solid dispersion particles of nilvadipine with hydroxypropylmethylcellulose. Int J Pharm 159(1):85-93.
22. Mosquera-Giraldo LI, Trasi NS, Taylor LS 2014. Impact of surfactants on the crystal growth of amorphous celecoxib. Int J Pharm 461(1-2):251-257.

23. He Y, Liu H, Xie Z, Liao Q, Lai X, Du Z 2014. PVP and surfactant combined carrier as an effective absorption enhancer of poorly soluble astilbin in vitro and in vivo. Drug Dev Ind Pharm 40(2):237-243.
24. Tran PH, Tran TT, Park JB, Lee BJ 2011. Controlled release systems containing solid dispersions: strategies and mechanisms. Pharm Res 28(10):2353-2378.
25. Ohara T, Kitamura S, Kitagawa T, Terada K 2005. Dissolution mechanism of poorly water-soluble drug from extended release solid dispersion system with ethylcellulose and hydroxypropylmethylcellulose. Int J Pharm 302(1-2):95-102.
26. Tanaka N, Imai K, Okimoto K, Ueda S, Tokunaga Y, Ibuki R, Higaki K, Kimura T 2006. Development of novel sustained-release system, disintegration-controlled matrix tablet (DCMT) with solid dispersion granules of nilvadipine (II): in vivo evaluation. J Control Release 112(1):51-56.
27. Huang J, Wigent RJ, Bentzley CM, Schwartz JB 2006. Nifedipine solid dispersion in microparticles of ammonio methacrylate copolymer and ethylcellulose binary blend for controlled drug delivery. Effect of drug loading on release kinetics. Int J Pharm 319(1-2):44-54.
28. Huang J, Wigent RJ, Schwartz JB 2006. Nifedipine molecular dispersion in microparticles of ammonio methacrylate copolymer and ethylcellulose binary blends for controlled drug delivery: effect of matrix composition. Drug Dev Ind Pharm 32(10):1185-1197.
29. Perioli L, Ambrogi V, Pagano C, Massetti E, Rossi C 2011. New solid mucoadhesive systems for benzydamine vaginal administration. Colloids and surfaces B, Biointerfaces 84(2):413-420.
30. Sun Y, Tao J, Zhang GG, Yu L 2010. Solubilities of crystalline drugs in polymers: an improved analytical method and comparison of solubilities of indomethacin and nifedipine in PVP, PVP/VA, and PVAc. J Pharm Sci 99(9):4023-4031.
31. Tao J, Sun Y, Zhang GG, Yu L 2009. Solubility of small-molecule crystals in polymers: D-mannitol in PVP, indomethacin in PVP/VA, and nifedipine in PVP/VA. Pharm Res 26(4):855-864.
32. Newman A, Knipp G, Zografi G 2012. Assessing the performance of amorphous solid dispersions. J Pharm Sci 101(4):1355-1377.
33. Baird JA, Taylor LS 2012. Evaluation of amorphous solid dispersion properties using thermal analysis techniques. Adv Drug Deliv Rev 64(5):396-421.
34. Shah B, Kakumanu VK, Bansal AK 2006. Analytical techniques for quantification of amorphous/crystalline phases in pharmaceutical solids. J Pharm Sci 95(8):1641-1665.
35. Newman A, Engers D, Bates S, Ivanisevic I, Kelly RC, Zografi G 2008. Characterization of amorphous API:Polymer mixtures using X-ray powder diffraction. J Pharm Sci 97(11):4840-4856.
36. Taylor LS, Zografi G 1997. Spectroscopic characterization of interactions between PVP and indomethacin in amorphous molecular dispersions. Pharmaceut Res 14(12):1691-1698.
37. Craig DQ 2002. The mechanisms of drug release from solid dispersions in water-soluble polymers. Int J Pharm 231(2):131-144.
38. Craig DQM 1990. Polyethyelene glycols and drug release. Drug Dev Ind Pharm 16(17):2501-2526.
39. Corrigan OI 1986. Retardation of polymeric carrier dissolution by dispersed drugs: factors influencing the dissolution of solid dispersions containing polyethlene glycols. Drug Dev Ind Pharm 12(11-13):1777-1793.
40. Corrigan OI 1985. Mechanisms of dissolution of fast release solid dispersions. Drug Dev Ind Pharm 11(2-3):697-724.
41. Zhou Y. 2000. Cyclosporine A: Solubilization, solid dispersion and solid -state transformation. Ph.D thesis: Purdue University. pp 30-51.
42. Dubois JL, Ford JL 1985. Similarities in the release rates of different drugs from polyethylene glycol 6000 solid dispersions. J Pharm Pharmacol 37(7):494-495.

43. Saers ES, Craig DQM 1992. An investigation into the mechanisms of dissolution of alkyl paraaminobenzoates from polyethylene-glycol solid dispersions. Int J Pharm 83(1-3):211-219.
44. Craig DQM, Newton JM 1992. The dissolution of nortriptyline hcl from polyethylene-glycol solid dispersions. Int J Pharm 78(2-3):175-182.
45. Levich VG. 1962. Physicochemical hydrodynamics. ed., Englewood cliffs, NJ: Prentice-Hall. p 60-72.
46. Kearney AS, Gabriel DL, Mehta SC, Radebaugh GW 1994. Effect of polyvinylpyrrolidone on the crystallinity and dissolution rate of solid dispersions of the antiinflammatory CI-987. Int J Pharm 104(2):169-174.
47. Doherty C, York P 1987. Mechanisms of dissolution of frusemide pvp solid dispersions. Int J Pharm 34(3):197-205.
48. Collett JH, Kesteven G 1978. Influence of polyvinylpyrrolidone on the dissolution of allopurinol. Drug Dev Ind Pharm 4(6):569-584.
49. Dave RH. 2006. A thermodynamic model to explain increased drug solubility and dissolution from drug-polymer solid dosage forms. Ph.D thesis: Long Island University. pp 93-206.
50. Iqbal Z. 2010. Effects of drug-carrier interactions on drug dissolution from binary and ternary matrices. Ph.D thesis: Long Island University. p 79-173.
51. Ji YH, Paus R, Prudic A, Lubbert C, Sadowski G 2015. A novel approach for analyzing the dissolution mechanism of solid dispersions. Pharm Res 32:(8):2559–2578.
52. Higuchi WI, Mir NA, Desai SJ 1965. Dissolution rates of polyphase mixtures. J Pharm Sci 54(10):1405-1410.
53. Carmichael GR, Shah SA, Parrott EL 1981. General-model for dissolution rates of normal-component, non-disintegrating spheres. J Pharm Sci 70(12):1331-1338.
54. Parrott EL, Simpson M, Flanagan DR 1983. Dissolution kinetics of a 3-component solid .2. benzoic-acid, salicylic-acid, and salicylamide. J Pharm Sci 72(7):765-768.
55. Shah SA, Parrott EL 1976. Dissolution of 2-component solids. J Pharm Sci 65(12):1784-1790.
56. Simpson M, Parrott EL 1983. Dissolution kinetics of a 3-component Solid .1. ethylparaben, phenacetin, and salicylamide. J Pharm Sci 72(7):757-764.
57. Yalkowsky SH, Amidon GL, Flynn GL 1972. Solubility of nonelectrolytes in polar solvents. J Pharm Sci 61(6):983-984.
58. Yalkowsky SH, Amidon GL, Zografi G, Flynn GL 1975. Solubility of nonelectrolytes in polar-solvents .3. alkyl para-aminobenzoates in polar and mixed solvents. J Pharm Sci 64(1):48-52.
59. Yalkowsky SH, Valvani SC, Amidon GL 1976. Solubility of nonelectrolytes in polar solvents IV: nonpolar drugs in mixed solvents. J Pharm Sci 65(10):1488-1494.
60. Bühler V. 2005. Polyvinylpyrrolidone excipients for pharmaceuticals: povidone, crospovidone and copovidone. Berlin, Germany: Springer. p 1-254.
61. Chow CK. 1997. Permeability of n-alkyl-p-aminobenzoates and ionic compounds through membranes prepared from an aqueous-based silicone elastomer dispersion. PhD thesis: University of Iowa. p 92-295.
62. Muller K 1968. Demonstration and determination of polyvinylpyrrolidone (pvp) and determination of effective substances in drug preparations containing pvp. Pharm Acta Helv 43(2):107-122.
63. Riedhammer TM 1979. Colorimetric determination of poly(N-vinyl-2-pyrrolidone) in contact lens solutions. J Assoc Off Anal Chem 62(1):52-55.
64. Yu L, Liu Z, Hu X, Kong L, Liu S 2010. Fluorescence quenching reaction of polyvinylpyrrolidone-eosin Y system for the determination of polyvinylpyrrolidone. J Fluoresc 20(3):733-738.
65. Yu LH, Liu ZF, Liu SP, Hu XL, Liu LF 2009. Fading spectrophotometric method for the determination of polyvinylpyrrolidone with eosin Y. Chinese J Chem 27(8):1505-1509.

66. Hsiao CH, Rhodes HJ, Blake MI 1977. Fluorescent probe study of sulfonamide binding to povidone. J Pharm Sci 66(8):1157-1159.
67. Tavlarakis P, Urban JJ, Snow N 2011. Determination of total polyvinylpyrrolidone (PVP) in ophthalmic solutions by size exclusion chromatography with ultraviolet-visible detection. J Chromatogr Sci 49(6):457-462.
68. Zeng XM, Martin GP, Marriott C 2001. Effects of molecular weight of polyvinylpyrrolidone on the glass transition and crystallization of co-lyophilized sucrose. Int J Pharm 218(1-2):63-73.
69. Horikoshi S, Hidaka H, Serpone N 2001. Photocatalyzed degradation of polymers in aqueous semiconductor suspensions V. Photomineralization of lactam ring-pendant polyvinylpyrrolidone at titania/water interfaces. J Photochem Photobiol A 138(1):69-77.
70. Jones SA, Martin GP, Brown MB 2004. Determination of polyvinylpyrrolidone using high-performance liquid chromatography. J Pharm Biomed Anal 35(3):621-624.
71. Pedersen G, Kristensen HG 1999. Quantitative analysis of povidone (PVP) in drug-PVP matrix using multicomponent analysis. Drug Dev Ind Pharm 25(1):69-74.
72. Yalkowsk.Sh, Slunick TG, Flynn GL 1972. Importance of chain-length on physicochemical and crystalline properties of organic homologs. J Pharm Sci 61(6):852-857.
73. Oh YK. 2003. Permeability properties of zein-based systems. Ph.D thesis: Univerisity of Iowa. pp 43-45.
74. Nogami H, Nagai T, Kondo A 1970. Dissolution kinetics of polyvinylpyrrolidone. Chem Pharm Bull 18(6):1185-1190.
75. Nogami H, Nagai T, Kondo A 1970. Physico-chemical approach to biopharmaceutical phenomena .14. dissolution kinetics of polyvinylpyrrolidone of various molecular weights. Chem Pharm Bull 18(11):2290-2296.
76. Greco K, McNamara DP, Bogner R 2011. Solution-mediated phase transformation of salts during dissolution: investigation using haloperidol as a model drug. J Pharm Sci 100(7):2755-2768.
77. Miller-Chou BA, Koenig JL 2003. A review of polymer dissolution. Prog Polym Sci 28(8):1223-1270.
78. Narasimhan B 2001. Mathematical models describing polymer dissolution: consequences for drug delivery. Adv Drug Deliv Rev 48(2-3):195-210.
79. Narasimhan B, Peppas NA 1997. Molecular analysis of drug delivery systems controlled by dissolution of the polymer carrier. J Pharm Sci 86(3):297-304.
80. Ahuja N, Katare OP, Singh B 2007. Studies on dissolution enhancement and mathematical modeling of drug release of a poorly water-soluble drug using water-soluble carriers. Eur J Pharm Biopharm 65(1):26-38.
81. Harland RS, Gazzaniga A, Sangalli ME, Colombo P, Peppas NA 1988. Drug/polymer matrix swelling and dissolution. Pharm Res 5(8):488-494.
82. Mallapragada SK, Peppas NA 1997. Crystal unfolding and chain disentanglement during semicrystalline polymer dissolution. AlChE J 43(4):870-876.
83. Peppas NA, Wu JC, Vonmeerwall ED 1994. Mathematical-modeling and experimental characterization of polymer dissolution. Macromolecules 27(20):5626-5638.
84. Ju RT, Nixon PR, Patel MV 1997. Diffusion coefficients of polymer chains in the diffusion layer adjacent to a swollen hydrophilic matrix. J Pharm Sci 86(11):1293-1298.
85. Ju RT, Nixon PR, Patel MV 1995. Drug release from hydrophilic matrices. 1. New scaling laws for predicting polymer and drug release based on the polymer disentanglement concentration and the diffusion layer. J Pharm Sci 84(12):1455-1463.
86. Ju RT, Nixon PR, Patel MV, Tong DM 1995. Drug release from hydrophilic matrices. 2. A mathematical model based on the polymer disentanglement concentration and the diffusion layer. J Pharm Sci 84(12):1464-1477.
87. Wang J, Flanagan DR 2002. General solution for diffusion-controlled dissolution of spherical particles. 2. Evaluation of experimental data. J Pharm Sci 91(2):534-542.

88. Alonzo DE, Zhang GG, Zhou D, Gao Y, Taylor LS 2010. Understanding the behavior of amorphous pharmaceutical systems during dissolution. Pharm Res 27(4):608-618.
89. Langham ZA, Booth J, Hughes LP, Reynolds GK, Wren SA 2012. Mechanistic insights into the dissolution of spray-dried amorphous solid dispersions. J Pharm Sci 101(8):2798-2810.